LUND UNIVERSITY

STRENGTH ANALYSIS OF REBUILT WINDOWS IN HISTORICAL BUILDINGS BY THE FE-METHOD

ZUHA ALSHAAR

Structural Mechanics

Master's Dissertation

DEPARTMENT OF CONSTRUCTION SCIENCES

DIVISION OF STRUCTURAL MECHANICS

ISRN LUTVDG/TVSM--26/5267--SE (1-87) | ISSN 0281-6679

MASTER'S DISSERTATION

STRENGTH ANALYSIS OF REBUILT WINDOWS IN HISTORICAL BUILDINGS BY THE FE-METHOD

ZUHA ALSHAAR

Supervisor: **KENT PERSSON**, Professor, Division of Structural Mechanics, LTH.

Examiner: **SUSANNE HEYDEN**, Associate Professor, Division of Structural Mechanics, LTH.

Printed by V-husets tryckeri LTH, Lund, Sweden, March 2026 *(Pl)*.

For information, address:
Division of Structural Mechanics,
Faculty of Engineering LTH, Lund University, Box 118, SE-221 00 Lund, Sweden.
Homepage: www.byggmek.lth.se

Abstract

The Machine and Assembly Hall in Varvsstaden (Malmö, Sweden) is a heritage industrial building currently being refurbished into office space. As part of the renovation, the historic cast-iron framed windows will be complemented by an inner insulating window installed approximately 500 mm inside the existing line, creating an air cavity and altering the mechanical loading conditions of the original system. This thesis evaluates whether the historic windows can withstand the modified load situation while meeting preservation requirements.

Finite element analyses were performed in Abaqus using measured window geometries and material properties from literature. Wind loading, thermally induced cavity pressure, and atmospheric pressure variations were analyzed individually and in combination for outdoor temperatures between −20 °C and +34 °C. Responses were compared for small and large windows before and after retrofit, supported by mesh convergence studies.

After renovation, the inner window increased stiffness and reduced wind-induced deflection, but the assumed sealed cavity introduced pressure-driven load cases that became critical under cold outdoor conditions. The small window developed higher local glass stresses near supported edges and corners, while the large window showed greater global deflection due to its larger span. Frame stresses remained below conservative reference values for cast iron, whereas glass stresses in most post-retrofit combinations exceeded the adopted screening threshold.

Overall, the retrofit improves serviceability under wind loading but may increase the risk of glass distress in cold scenarios due to cavity-pressure effects. Controlled cavity pressure equalization (ventilation) is therefore recommended to reduce pressure-induced demand on the historic glazing.

Sammanfattning

Maskin och monteringsverkstaden i Varvsstaden i Malmö är en kulturhistoriskt värdefull industribyggnad som för närvarande byggs om till kontorslokaler. Som en del av renoveringen kompletteras de historiska gjutjärnsfönstren med ett nytt invändigt isolerfönster placerat cirka 500 mm innanför det befintliga, vilket skapar en luftspalt och förändrar fönstrens mekaniska belastningsförhållanden. Syftet med detta arbete är att undersöka om de ursprungliga fönstren kan motstå den förändrade lastsituationen samtidigt som byggnadens kulturhistoriska värden bevaras.

Numeriska analyser genomfördes med finita elementmetoden i Abaqus, baserat på uppmätta fönstergeometrier och materialdata hämtade från litteraturen. Vindlast, termiskt inducerat kavitetstryck och variationer i atmosfärstryck analyserades var för sig och i kombination för utomhustemperaturer mellan −20 °C och +34 °C. Spännings- och deformationsrespons jämfördes för små och stora fönster före och efter renovering, och konvergensstudier användes för att säkerställa tillförlitliga resultat.

Efter renovering ökade systemets styvhet och vindinducerade deformationer minskade, men den antagna täta luftspalten gav upphov till tryckrelaterade lastfall som blev avgörande vid låga utomhustemperaturer. Det lilla fönstret uppvisade högre lokala dragspänningar i glaset nära upplag och hörn, medan det stora fönstret visade större globala deformationer till följd av sin större spännvidd. Spänningarna i gjutjärnsramen låg under konservativa referensvärden, medan glasets spänningar i många lastfall överskred antagna gränsvärden för historiskt glas.

Sammanfattningsvis förbättrar renoveringen brukbarheten vid vindlast, men kan samtidigt öka risken för skador i det historiska glaset under kalla klimatförhållanden på grund av kavitetstryck. Åtgärder såsom kontrollerad tryckutjämning i luftspalten rekommenderas därför för att minska tryckinducerad belastning på det historiska glaset.

Acknowledgements

This master's thesis concludes my five years of studies at Lund University, Faculty of Engineering (LTH). The work was carried out at the Division of Structural Mechanics.

I would like to thank my supervisor at LTH, Professor Kent Persson, for his guidance and valuable input throughout the entire process. I would also like to thank my examiner, Associate Professor Susanne Heyden, for her feedback and support.

This master's thesis is dedicated to my beloved father, ***Mustafa***, who passed away. I carried him in my heart throughout this journey, and I hope this work honours everything he meant to me. I also dedicate this thesis to my beloved sister, ***Rasha***, who passed away as well. Her faith in me and her words of encouragement stayed with me, and I will always remember how strongly she believed in my future.

I am deeply grateful to my mother ***Ghinwa***, for her constant prayers, endless love, and unwavering support. Her faith and strength have been a source of comfort and guidance throughout my studies and this thesis.

From the bottom of my heart, I thank my husband, ***Mohamad*** for standing by my side with constant love, patience, encouragement, and support, especially during the most demanding moments of this work.

I am also truly grateful to my sister, ***Dalia***, who supported me from the very beginning and stayed close to me through every step until the end.

I would also like to thank my brothers, ***Ahmad***, ***Abdulrahim***, and ***Tamer***, for their support and encouragement.

My sincere thanks go to my dear friends ***Lina***, ***Jumana***, and ***Samah*** for their kindness, support, and uplifting words.

I also extend my appreciation to my mother-in-law, ***Nashwa***, and my sisters-in-law, ***Rouaa*** and ***Bayan***, for their care and support.

Finally, I want to thank my daughter, ***Nashwa***, for her patience, love, and understanding while I worked on this thesis. Her presence has been my greatest motivation.

I dedicate this thesis to grandchildren: ***Ghinwa, Zinea, Mustafa, Maha, Mustafa, Ahmad, Logain, Shahid, Omar, Qusay, Lana, Fatima, Sham, Ahmad and Lama.***

This achievement belongs to all of you as much as it belongs to me, and I will always carry your love and support with me.

Lund, 2026

Zuha Mustafa Alshaar

Table of contents

1 Introduction

1.1 Background

The preservation and adaptive reuse of historic industrial buildings require renovation strategies that improve indoor comfort and energy performance while maintaining protected architectural features. The Machine and Assembly Hall at the former Kockums shipyard in Malmö (constructed in 1912) is a representative case where the external appearance of the historic façade must remain unchanged under municipal preservation requirements, meaning that the original cast-iron windows must be retained.

To meet modern thermal and acoustic requirements without altering the façade, the renovation concept introduces an additional inner window installed approximately 500 mm inside the original, creating an air cavity between the historic outer window and the new inner glazing. While this solution can enhance performance, it may also fundamentally alter the mechanical loading environment of the historic window system. In particular, a sealed or partially sealed cavity can develop pressure differences due to temperature changes and atmospheric variations, potentially introducing load cases that were not critical before the retrofit.

The original window components are also associated with uncertainty and vulnerability typical of early 20th-century construction: cast iron behaves as a brittle material with limited tensile capacity and sensitivity to defects, and the exact glass type and condition may be uncertain due to age and possible replacements over the building's service life. Against this background, the structural integrity of the historic windows must be evaluated under the altered loading conditions introduced by the retrofit.

1.2 Purpose and aim

The aim of this master's thesis is to assess whether the historic cast-iron framed windows in the Machine and Assembly Hall can safely withstand the altered loading conditions introduced by the installation of an inner insulating window. The assessment focuses on the structural response of both glass panes and cast-iron frames in terms of stresses and deflections under relevant load combinations.

Based on defined climate-related actions and conservative assumptions regarding material properties, numerical finite-element simulations are performed to evaluate the mechanical effects of the retrofit and to identify potential critical response regions in the original window system.

The following research questions are addressed:

- Does the loading situation change for the old window after renovation and if so, how much?
- Can the old window withstand the loads that occur after renovation?
- What measures could be taken to reduce the impact of the loads on the old window?

1.3 Method

The structural behavior of the historic windows will be evaluated using finite element (FE) analysis in Abaqus. The window geometry will be established from on-site measurements of the existing structures and translated into a three-dimensional FE model representing the cast-iron frame members and the glass panes, including their interfaces. Material properties for cast iron and glass will be adopted from the available literature and project documentation, using conservative values to account for uncertainty associated with historic materials and potential ageing effects.

Relevant load cases representing pre- and post-renovation conditions will be applied to the FE model, and the structural response will be assessed primarily in terms of stresses and deflections in both glass and cast iron. Post-processing and figure generation will be carried out using MATLAB to ensure consistent extraction of results.

1.4 Limitations

The results are subject to modelling and input uncertainties. The FE geometry includes idealizations (simplified cross-sections, alignments, uniform thicknesses and simplified connections), which may affect local stiffness and peak stresses near joints and the glass–frame interface.

Material properties for historic cast iron and glazing are uncertain; cast iron is modelled as linear elastic and existing defects (corrosion, microcracks, casting flaws) are not represented. Boundary conditions and glass–frame interaction are idealized, meaning local peaks near corners/contacts may reflect numerical concentration rather than physical values; therefore, interpretation emphasizes recurring stress patterns and trends.

Finally, the cavity condition (sealed versus leaky/ventilated) is a key uncertainty controlling cavity pressure actions. The effect of the ventilated cavity is not taken into account. Overall, these limitations mean that the FE model is suited for comparative assessment of the structural behavior before and after renovation and for identifying critical load cases and critical locations.

2 Kockum area

This chapter provides a historical and architectural overview of the Kockum industrial area in Malmö. It begins with a description of the site's development and significance during the late 19th and 20th centuries, highlighting its role as one of the city's most important industrial hubs. The section then examines the architectural evolution of the area and its characteristic building structures, with particular attention to the Machine and Assembly Hall. Finally, the ongoing renovation projects are presented, emphasizing the challenges of preserving cultural heritage while adapting the buildings to modern functional and energy requirements.

2.1 The history of Kockum area

For half a century, Kockum was the largest workplace in Malmö, peaking with 6,000 employees in 1962. Internationally, Kockum was known as a prominent shipyard, while locally it played a crucial role in shaping Malmö's industrial and social identity. The area, with its docks, quays, ship basin, and industrial buildings, still bears visible traces of its industrial past. Today, it remains a vibrant industrial landscape where the historical significance is both tangible and ever-present. During the late 19th and much of the 20th century, Malmö emerged as a major industrial hub, with Kockum Industries playing a pivotal role in that transformation. It could be argued that Malmö would not have reached its current scale and prominence without the influence of Kockum. [12]

The iconic gantry crane became a landmark and symbol for both Kockum and the city of Malmö. Kockum not only shaped the skyline but also contributed to reshaping the coastline through extensive land reclamation in the Öresund. While much of the former shipyard has since been repurposed for new activities and the gantry crane has been removed, the southern section of Stora Varvsgatan remains largely unchanged since the shipbuilding era, preserving its cohesive industrial environment. [12]

The Kockum area features numerous historic industrial buildings, including:

- The carpentry shop (1876)
- The foundry (1910)
- The machine and assembly hall (1912)
- The administration building (1912)
- The carriage workshop (1913)
- The warehouse (1917)
- The staff house (1947)
- The sheet metal warehouse (1947)
- The welding and boiler workshop (1954)

Many of these buildings are currently undergoing renovation and being revitalized with new functions and modern uses. [12]

The carpentry shop, built in 1876, was constructed using yellow brick, a common material for industrial buildings of the time providing both durability and insulation. It had a concrete and stone foundation, ensuring stability for industrial operations. Steel elements were used in the roof and other load-bearing components to allow for large open interior spaces. The roof

structure featured large trusses and tension frames, while the exterior walls were built of brick and stone for structural strength and protection from the elements. The building also featured large cast iron-framed windows with smaller panes, offering both functionality and an aesthetically robust appearance. [12]

The foundry, built in 1910 was constructed on a reinforced concrete foundation to support significant loads from furnaces, molding equipment, and other heavy industrial machinery. Steel framing was used to ensure structural integrity. The exterior walls were made of brick, a material well-suited for the high temperatures and fire resistance required in foundry operations. Cast iron was used for window frames to withstand the thermal and mechanical stresses typical in such environments. [12]

The machine and assembly hall, constructed in stages in 1912 and 1923, was designed to accommodate large industrial machinery and ship components. The concrete floors were built to support substantial loads, while large windows were incorporated to ensure ample natural lighting crucial before electric lighting became widespread. These windows were divided into smaller panes to balance structural safety with flexibility. [12]

Adjacent to this was the administration building, built in 1912, which served as Kockum's headquarters. It housed offices for managers, central administrative functions, and the company’s board of directors. [12]

2.2 Renovations of Kockum area

To enhance the legibility and coherence of the site, it is essential to clearly differentiate between new and existing architectural elements. Modern additions, such as newly constructed buildings or extensions, should be designed in a contemporary style according to *Varvsstadens* historical report [22], while still reflecting the defining characteristics of the original structures. Inspiration for new designs can be drawn from existing or even demolished buildings for example, by replicating historical volumes using modern and distinct materials. Furthermore, specific architectural details, such as roof angles or window placements, can be echoed in to create continuity. In certain cases, reconstructions of lost structures may be justified, though such interventions remain rare exceptions.

The former Kockum shipyard area has evolved into a vibrant and functioning industrial landscape with significant cultural and historical value. According to *Varvsstadens* historical report, the long-term preservation of buildings and environments is closely linked to their usability. Ideally, buildings should continue to serve their original purpose, allowing them to age and evolve naturally. However, the Kockum area is currently undergoing transformation, with plans for the existing industries to vacate in the coming years. As the area transitions to accommodate non-industrial functions, it is crucial to recognize and preserve its historical and cultural significance. The unique architectural qualities of the industrial buildings when carefully integrated with modern additions and new uses can foster a dynamic and inspiring environment. [22]

The placement of windows and doors often reveals much about a building's original function and usage. These elements are fundamental components of architectural design and merit careful consideration during renovation. According to *Varvsstaden’s* historical report, alterations to historic brick facades should be regarded as irreversible, as restoring such façades to a satisfactory condition is often extremely difficult. Therefore, the use of existing

wall openings such as original windows and doorways should be prioritized. New openings should not be introduced into these historically significant structures. [22]

Windows and roof lanterns are critical to the architectural identity of historic buildings and should be preserved wherever possible. In cases where replacement is necessary, new elements should replicate the original type with precision. The profile and proportions of these components play an important role in maintaining architectural integrity. Historical details and visible traces of previous functions contribute to the cultural narrative of a building and can serve as compelling features within a renewed environment. As such, these traces should be preserved and integrated thoughtfully into renovation efforts. [22]

The reconstruction of the Carpenter's Building began in 2022 and is currently ongoing. To preserve the structure, a spectacular engineering effort was undertaken to lift the entire building, which was situated too low in relation to the surrounding urban context. Approximately 200 tons of steel beams were installed through and around the building to create a lifting frame. After severing the old foundation wall, 42 powerful hydraulic jacks were used to raise the 2,200-ton structure. Once the new foundation slab is fully cured, the building will be carefully lowered onto its new, elevated base. [22]

Historically, the Carpenter’s Building housed woodworking and interior design workshops, including production for external clients. As one of the smaller structures in the area, it offers an intimate character, with a timber interior that reveals signs of renovations carried out during the 1930s and 1970s. Located in the older part of the industrial site, facing the harbor basin and overlooking the city, the Carpenter's Building holds high cultural and historical value, See Figure 1. [23]

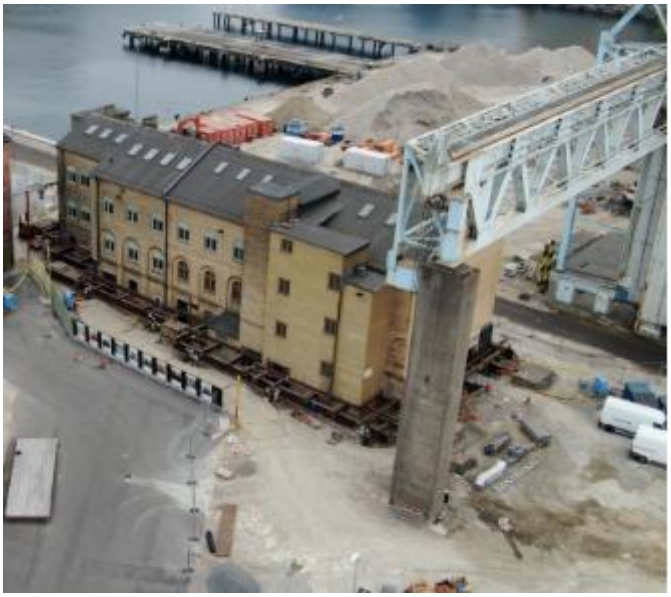

Figure 1 Carpenter's building now. Photo: Varvsstaden AB. Used with permission via email on 13 October 2025. [17]

After being empty and unused for many years the foundry has been carefully renovated in 2022. As much as possible, the old has been preserved, the existing bricks have been knocked down and reused, and inside the building the massive steel beams tower. The cast iron frame of the windows has been preserved, allowing the building to retain its original industrial

character. These frames are very robust and durable, which means they do not need to be replaced unless they are seriously damaged. The old glass has been replaced with energy efficient glass to improve energy performance and reduce heat loss. As old industrial windows are often single glazed, more modern glazing solutions may have been installed to increase the building's insulation and sound insulation, See Figure 2. [23]

Figure 2 Foundry building now. Photo: Varvsstaden AB. Used with permission via email on 13 October 2025. [16]

The administration building where Kockum's had its headquarters with premises for managers, central functions, and the board was built in 1912. In spring 2019, the administration building was renovated to a modern apartment hotel with 95 unique rooms for both business travelers and tourists. The renovation of the administration building took great care to preserve the unique qualities of both the area and the building, so that we can carry the story forward. Almost all the windows have been replaced with new windows. It was a complicated and time-consuming task because the windows were first to be cleaned of toxins, painted with three layers of linseed oil paint and glass replaced in cases where the panes have been broken. Where there were no old windows in the same style, it was chosen to order similar but newly produced ones with arched cultured glass, See Figure 3. [23]

The Carriage workshop was built in 1913. A historic hall will develop to be well suited for offices or other businesses. The warehouse, staff house, sheet metal warehouse, welding, and boiler workshop are still under renovation. [23]

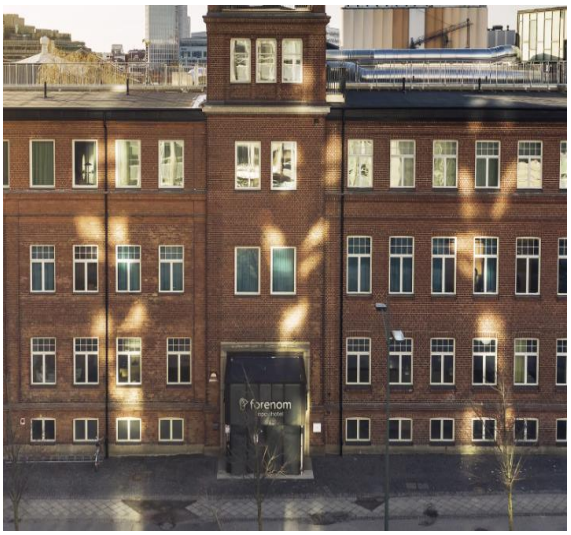

Figure 3 Administration building now. Photo: Varvsstaden AB. Used with permission via email on 13 October 2025. [14]

2.3 Windows in Kockum area

Cast iron windows were commonly used in the 19th and early 20th centuries, particularly in industrial and urban buildings. These windows were typically produced using a combination of casting techniques and skilled craftsmanship, resulting in elements that were both functional and decorative. The restoration of such windows today requires careful and specialized work to preserve their structural integrity and historical value, while also improving their functionality to meet modern standards.

The long-term durability of cast iron windows largely depends on the condition of key components such as putty, paint, and fittings. These elements protect the frames from corrosion and maintain their aesthetic appeal. However, prolonged exposure to the elements often leads to significant deterioration, particularly in the lower parts of the frame and arches. Despite their often-poor visual appearance, metal casement windows are frequently in better condition than they seem. Rust, which expands in volume compared to the original iron or steel, can give the impression of extensive damage, but much of it can be reversed through professional restoration. With appropriate repair and regular maintenance, cast iron windows can continue to function and often outlast modern replacements. [5]

Common repair methods include filling pits and small holes with metal filler or epoxy to restore the surface and prevent further degradation. In more serious cases involving structural damage, welding or patching may be necessary. Specialized cast iron welding techniques can be employed to repair cracks or larger sections of missing material. These interventions enable the windows to regain both their visual appeal and functionality while preserving their historical authenticity. [5]

One of the primary limitations of historic cast iron windows is their inadequate thermal and acoustic insulation. As single-glazed systems without effective sealing, their performance is significantly lower than modern standards. Contemporary retrofit strategies, including improved glazing systems and enhanced airtightness measures, can substantially increase thermal and acoustic performance without compromising the historic character of the façade [21].

3 Renovation of windows in the Machine Hall

The Machine and assembly hall were built in 1912 and 1923 respectively. The machine and assembly hall were built to handle large machinery and equipment, as well as to enable the assembly of ships and other large industrial products. The concrete floor was designed to withstand very heavy weights and loads. [22]

To create a good working environment, especially in a time before electric lighting was common, the building was designed with large windows to maximize light. This was crucial to ensure that workers had enough natural light while working. The large windows were divided into smaller sections to provide flexibility and safety, See Figure 4.

Figure 4 Machine and assembly hall, exterior and interior views. Photo: Varvsstaden AB. Used with permission via email on 13 October 2025. [15]

The windows are old, and the functions of the windows are limited, such as thermal insulation and sound insulation. To reach the requirements of today, the building will have an old window (The existing window) and a new inside window (The additional window). The renovation is to apply an additional window 500 mm inside the old window, which creates a cavity between the windows, see Figure 5. [23]

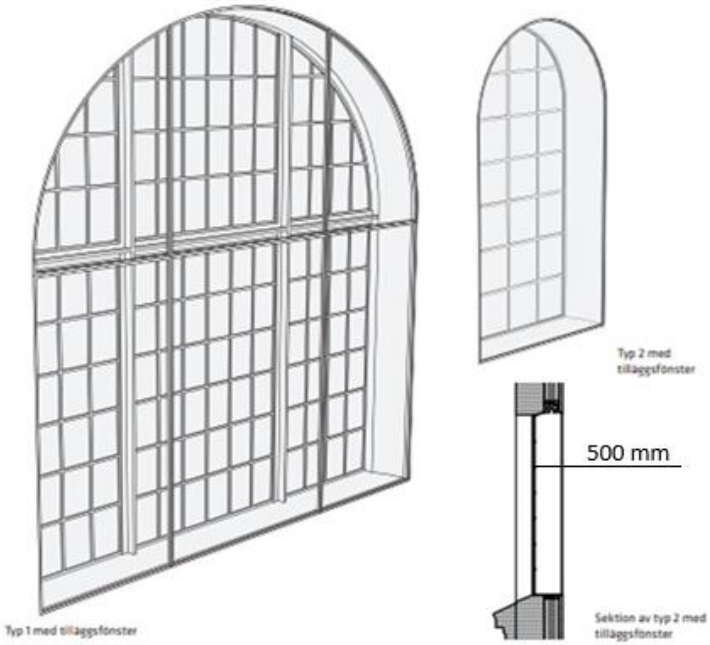

Figure 5 The additional window inside the old window. The photo is taken from rapport Fönsteranalys. [22]

The old windows will be exposed to more loads than weather loads after renovation such as pressure change in the cavity due to temperature changes from outside and inside the building. The aim of this master's thesis is to see if the existing windows will accept all the loads such as wind force, thermal induced pressure and changing in atmospheric pressure without any problem. The thermal induced pressure could be created in the cavity from temperature changing between outside and inside the building.

By using Finite Element analysis, we can see how much the existing window will be affected by this renovation. In this project, two windows will be analyzed, a small and large window. In the next steps all materials properties and the calculation of all types of loading will be presented clearly.

4 Material

In this chapter, the mechanical properties of the window materials are presented, including values such as Young's modulus and Poisson's ratio. These properties are essential inputs for finite element analysis and directly influence the calculation of stress distribution and deflection under various loading conditions. Special attention is given to the stiffness of each material, as it plays a critical role in the structural response of both the cast iron frame and the glass pane.

4.1 Cast iron

Cast iron contains 2-4% carbon, 1-3% silicon and a smaller number of minor elements. The cast iron can be optimized before being cast by adding a small quantity of manganese, cerium, nickel, copper, and vanadium. There are two types of cast iron, white cast iron and grey cast iron depending on silicon content. Cast iron may be treated under a high temperature which can produce a malleable or ductile cast iron. [5]

In 1800 the iron ore was mined from mines, mainly hematite or magnetite, and transported to smelters. In blast furnaces, the iron ore was melted together with coal (coke) to create molten iron, where the iron oxide was reduced to metallic iron. The molten metal, which contained a high carbon content, was poured into sand molds to create objects such as window frames, doors, and other components. After cooling, the cast iron was hardened and worked to remove casting joints. The objects were painted or treated to protect against rust. This manufacturing method, which was a central part of the industrial revolution, allowed the mass production of durable and robust materials for a growing industry and construction sector. Cast iron became a cornerstone of modern industry in the 19th century and continued to be widely used throughout the 20th century. Adding a minor element in cast iron, like silicon, molybdenum, copper or chromium can improve the corrosion resistance. [5]

4.1.1 Bending strength

Cast iron is a widely used engineering material known for its excellent compressive strength, wear resistance, and ease of casting. However, its brittle nature, particularly in gray cast iron, limits its tensile and flexural strength compared to ductile materials. The mechanical properties of cast iron vary significantly depending on the specific type. [20]

The tensile strength of cast iron varies depending on its grade and microstructure. For gray cast iron (EN-GJL-250), which is commonly used in structural components, the typical bending strength is approximately 200 MPa. Below are typical values for gray cast iron (EN-GJL-250), which is commonly used in structural and mechanical applications. See Table 1, these values are representative and can vary depending on the casting method, section thickness, and microstructure. [20]

Table 1 Mechanical properties of gray cast iron.

Property	**Value**
Compressive strength	800–1200 MPa
Tensile strength	150-250 MPa
Bending strength	200 MPa
Young's modulus	160-170 GPa

4.1.2 Deflection

Deflection in cast iron components is generally small compared to less stiff materials, owing to the relatively high stiffness of gray cast iron. Its modulus of elasticity typically ranges from 160-170 GPa, which provides good resistance to elastic deformation under load. However, unlike steel or aluminum, gray cast iron exhibits very limited ductility. Once the elastic limit is exceeded, it is prone to brittle fracture rather than significant plastic deformation, meaning failure can occur suddenly with minimal visible deflection. [20]

The amount of deflection in a cast iron structure under a given load depends on factors such as the geometry of the component**,** type and magnitude of loading**,** and support conditions**.** Since gray cast iron is brittle, deflection is not typically used as a safety indicator because it may fail without much prior deformation. Instead, stress analysis and fracture mechanics are more relevant for predicting failure [20].

4.2 Glass

The old glass production in Sweden was dependent on three methods, cylinder glass method, the moon glass method and crown glass method. The crown glass method is the oldest method which was used until the beginning of the 19th century. First, a large glass ball was blown and then flattened and attached to a dowel. [1]

Glass is highly susceptible to surface imperfections such as excrescences and micro-cracks. When subjected to tensile loading, these flaws act as stress concentrators, which largely explains its inherently low tensile strength. In addition, the instantaneous strength of glass is time-dependent, since under sustained loading its effective strength decreases over time due to crack growth and stress corrosion. [6]

At room temperature, glass behaves as a brittle material with no ductility [6]. It does not undergo plastic deformation and instead deforms elastically under stress until it fractures. Its tensile strength is significantly lower than its compressive strength, and its mechanical behavior is considered ideally elastic. [6]

4.2.1 Bending strength

Since glass behaves as a brittle material with limited tensile capacity, its resistance to bending stresses is a decisive factor in determining its load-bearing ability. Due to its susceptibility to high stress concentrations and surface defects, the mechanical strength of glass is inherently low. Common values for the mechanical properties of glass are summarized in Table 2.

Table 2 Mechanical properties of glass.

Property	**Value**
Compressive strength	880 – 930 MPa
Tensile strength	30 – 90 MPa
Flexural strength	30 – 100 MPa
Young's modulus	70 – 75 GPa

The bending strength of float glass can be calculated using a specific design formula, according to prEN 16612 that accounts for several factors. [7]

$$f_d = \frac{k_{mod} k_{sp} f_{k,float}}{\gamma_{M,float}}$$

$$k_{mod} = 0.74$$

$$k_{sp} = 1$$

$$f_{k,float} = 45 \text{ MPa}$$

$$\gamma_{M,float} = 1.8$$

$$f_d = \frac{0.74 \cdot 1 \cdot 45}{1.8} = 18.5 \text{ MPa}$$

f_d= design strength.

$f_{k,float}$= characteristic strength.

k_{mod}= factor that considers the load duration.

$\gamma_{M,float}$= material factor for glass strength.

k_{sp} = factor that depends on how the surface is treated, example, sun protection coating, wire glass. Without treatment, this is set to 1.0.

The calculated bending strength of 18.5 MPa corresponds to newly manufactured float glass under standardized laboratory conditions. However, applying this value directly to historical windows introduces a significant degree of uncertainty. The original glass has been exposed to environmental and mechanical degradation for approximately a century, which has likely reduced its strength.

Weathering effects such as temperature fluctuations, humidity variations, UV radiation, and frost can induce surface corrosion and microcrack formation. In addition, mechanical actions such as wind pressure, vibrations, and repeated opening and closing of the window may further contribute to fatigue and crack propagation. The manufacturing process of historical glass, often less controlled than modern float production, may also have introduced internal stresses, thickness variations, and surface imperfections that reduce bending capacity.

Considering these factors, it is reasonable to assume that the bending strength of the historical glass lies in the range of approximately 6–9 MPa. This reduction corresponds to roughly one-third of the strength of new float glass and provides a conservative yet realistic estimate. Although this assumption introduces uncertainty into the analysis, it allows for a more representative assessment of the actual behavior of the glass under loading.

4.2.2 Deflection

When float glass is subjected to external loads such as wind pressure, thermal loads, or point loads, it will deflect (bend). The amount of deflection depends on the geometry, support conditions, and material properties of the glass pane.

For a rectangular float glass pane simply supported on four edges and subjected to a uniform load, the maximum deflection can be approximated by:

$$w_{max} = \alpha \cdot \frac{q \cdot a^4}{E \cdot t^3}$$

Where:

w_{max}= maximum deflection (m)

q = uniform surface load (N/m²)

a = shorter side of the glass plate (m)

E = Young's modulus of glass (~70 GPa for soda-lime float glass)

t = glass thickness (m)

α = constant depending on the aspect ratio and support conditions

According to EN 16612 [7], the maximum allowable deflection is often limited to $l/60$ to $l/100$, where l is the span (shorter edge of the pane). For a glass window of 300*400 mm and the thickness 2 mm the acceptable deflection is typically 3-5 mm.

5 Computational model

5.1 Modelling limitations and assumptions

The finite element model represents the quasi-static structural response of the historic outer window under prescribed pressure actions before and after renovation. The analyses aim to capture global stiffness, load transfer and elastic stress patterns, and are therefore intended for comparative evaluation (before/after, load-case ranking and identification of critical zones) rather than direct prediction of cracking or ultimate failure.

Reference state and load definition.
The glazing system is assumed to be installed at a reference state of $T_0 = 20°\text{C}$ and $p_0 = 1\text{atm}$, and the window is considered stress-free under these reference conditions. All subsequent load cases are applied as deviations from this reference state (temperature and/or pressure changes). Long-term atmospheric pressure variations are assumed to act equally on the interior and exterior of the hall, i.e., no permanent indoor overpressure is modelled.

Cavity condition and pressure actions.
The air space between the original outer window and the new inner window is modelled as a sealed cavity, meaning that no intentional ventilation and no pressure equalization with ambient air are allowed. Under this assumption, changes in cavity temperature and ambient atmospheric pressure result in changes in cavity pressure, which introduces additional pressure loading on the glazing. Since the sealed versus leaky/ventilated condition is a key uncertainty for the post-renovation configuration, the resulting cavity pressure loads should be interpreted as scenario-dependent and are treated as assumptions whose influence on the predicted structural response is discussed.

Material modelling.
Both cast iron and glass are idealized as linear elastic, isotropic materials. This approach is suitable for service-level stiffness and elastic stress distributions, but it does not represent brittle fracture of cast iron or glass, existing defects, joint slip, local crushing, or cracking. Consequently, reported stresses are interpreted as elastic demand indicators used to compare cases and locate critical regions, not as direct predictions of damage initiation or ultimate capacity.

Geometric nonlinearity.
Geometric nonlinearity (NLGEOM) is enabled in all analyses. This ensures that stiffness and pressure loading are evaluated on the updated (deformed) configuration, which is relevant for follower-type surface pressures acting on glazing and for cavity pressure acting together with wind/pressure changes. Material behavior remains linear elastic throughout; hence, the only nonlinearity included is geometric. While deformations are generally small, keeping NLGEOM provides a consistent framework across load cases and reduces the risk of underestimating second-order effects in combined pressure scenarios.

Cavity temperature approximation.
The cavity air temperature is approximated by the outdoor temperature in the load definition. In reality, the cavity temperature depends on heat transfer, solar effects, and potential leakage/ventilation. This simplification can affect the magnitude of the thermally induced

cavity pressure and is therefore treated as an important modelling assumption when interpreting the post-renovation results.

Interpretation notes.
Due to idealized supports and simplified interaction modelling, stress concentrations may occur near restraints and along glass–frame contact regions. For this reason, post-processing focuses on consistently defined monitoring regions and recurring stress bands rather than isolated numerical peaks at sharp corners.

5.2 Geometry

This section describes the geometry of the two windows before and after the renovation.

5.2.1 Original windows

5.2.1.1 Small window

The Foundry building has probably the same windows material as the Machine and assembly hall, that's why the small window has been taken from the Foundry building to Lund university to conduct some experiments, the shape of the small window is shown in Figure 6. The small window has float glass with a thickness of 2 mm. The dimensions and cross-sectional details of the small window are shown in Figure 7 and Figure 8.

Figure 6 The shape of small window.

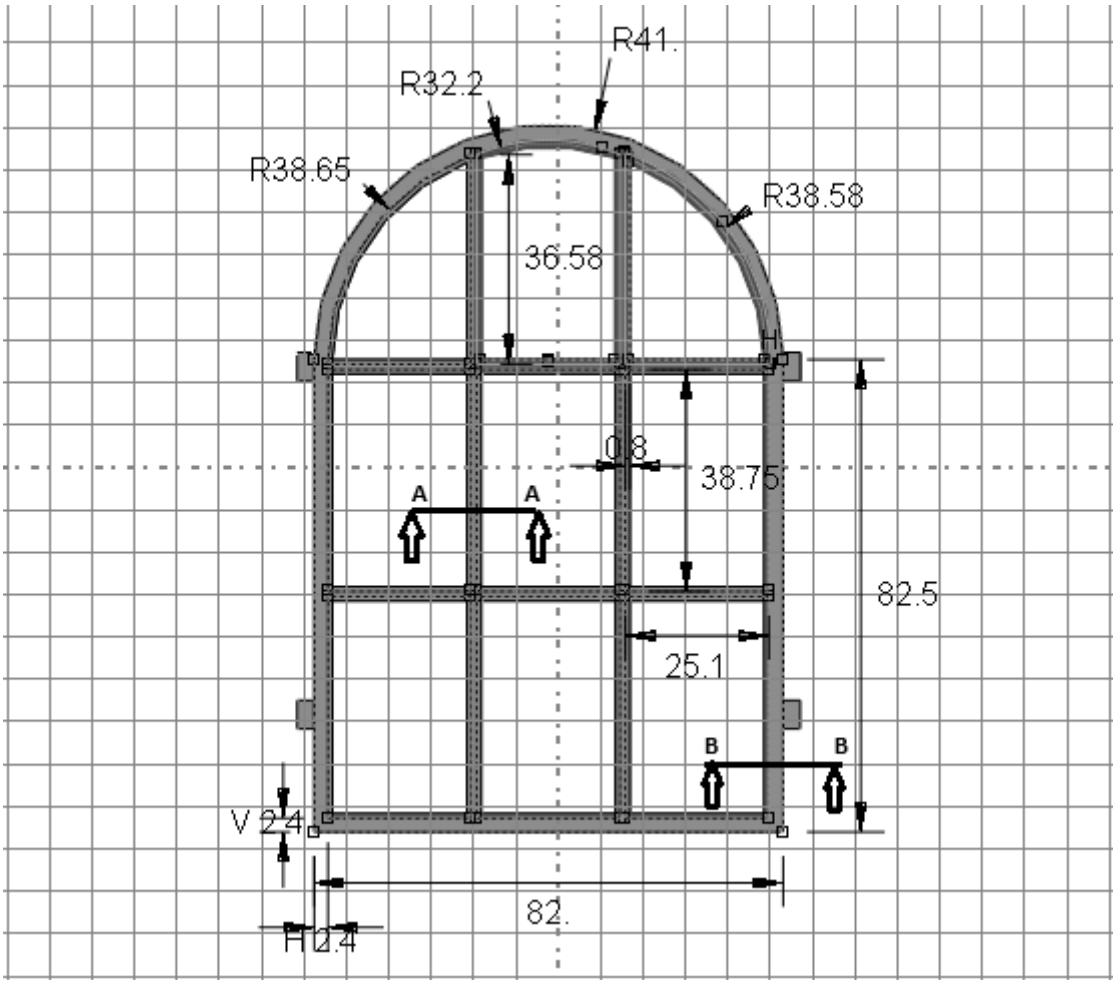

Figure 7 The geometry of the small window in cm.

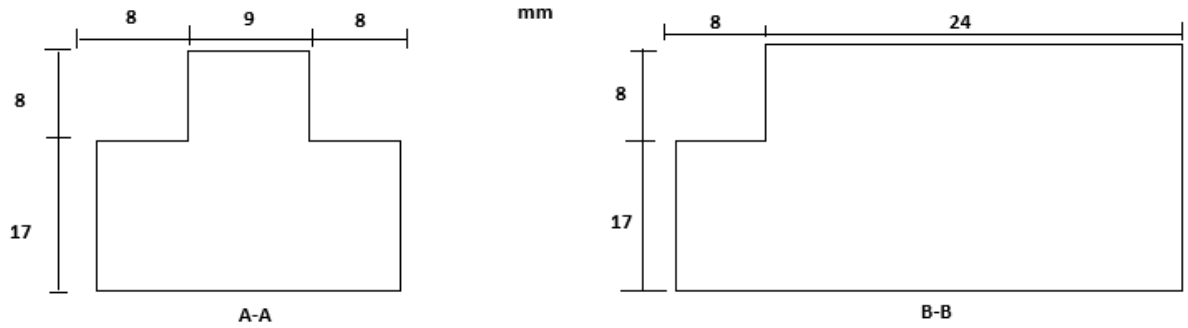

Figure 8 Cross-sectional dimension of the small and large window in mm.

5.2.1.2 Large window

To keep the computational model tractable, only the central portion of the large historic window was included in the Abaqus model, see Figure 9 and Figure 10. This sub-model approach reduces geometric complexity while retaining the critical structural behavior of the window system (load transfer through the main frame members and glazing segments). The dimensions of the large window are shown in Figure 10 and Figure 11. The large window has float glass with a thickness of 2 mm. The cross-sectional dimensions and thickness of the large window are the same as for the small window, see Figure 8.

Furthermore, the central large window could not be robustly created and meshed as a single Abaqus part due to the high level of geometric detail (many slender members, intersections, and sharp corners), which led to unstable analyses. Therefore, the model was divided into four assembled parts: (i) an upper semicircular (arched) segment, (ii) a left middle segment, (iii) a right middle segment, and (iv) a lower segment. As a result, each segment is assigned its own effective span, which influences deflection and stress distribution compared with an uninterrupted single pane.

Figure 9 The large historic window on the south façade of the Machine and Assembly Hall, showing the segmented glazing arrangement with an upper arched portion and multiple rectangular panes. Photo by Varvstaden AB. Used with permission via email on 13 October 2025.

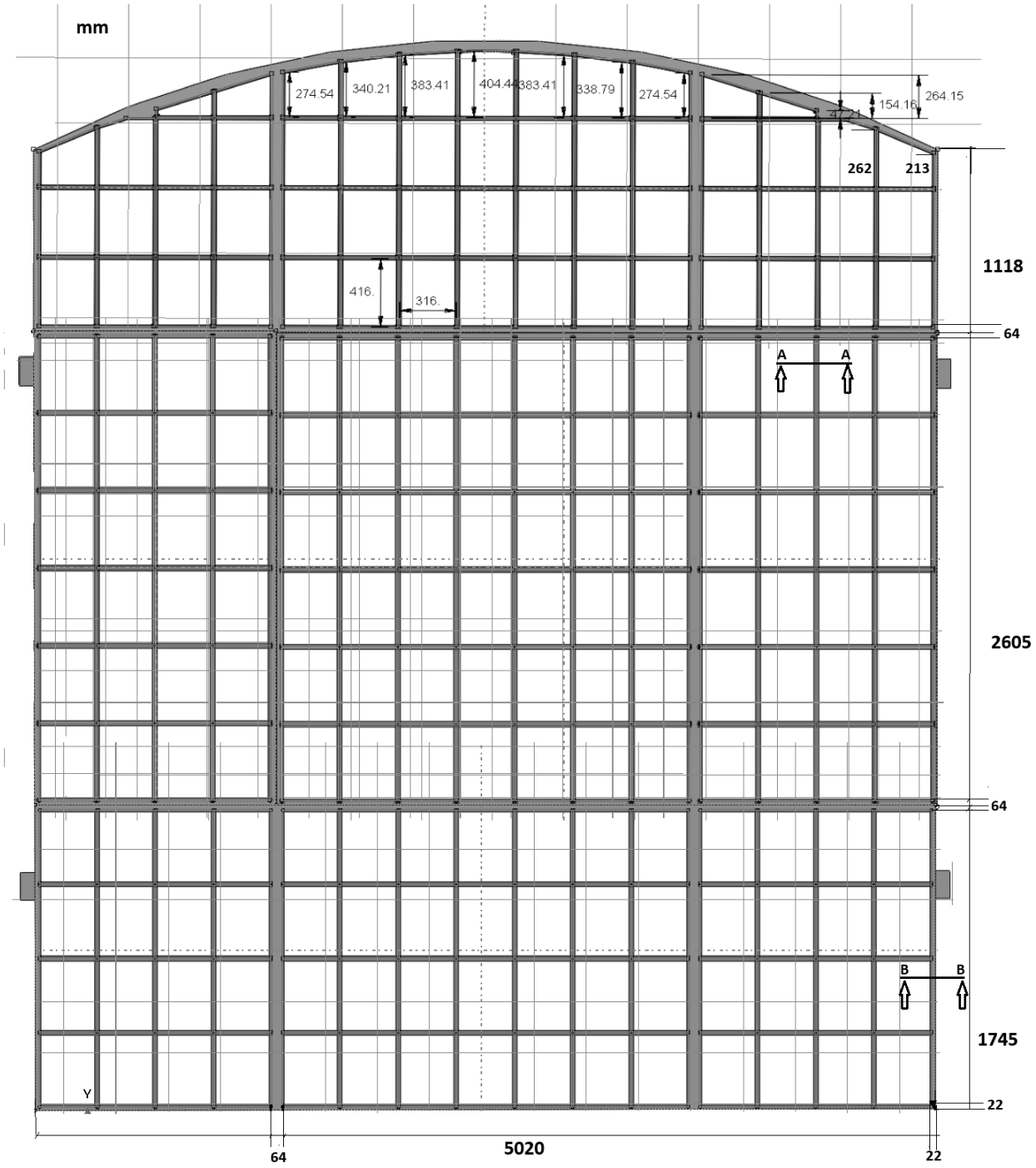

Figure 10 Geometry of the large window (dimensions in mm).

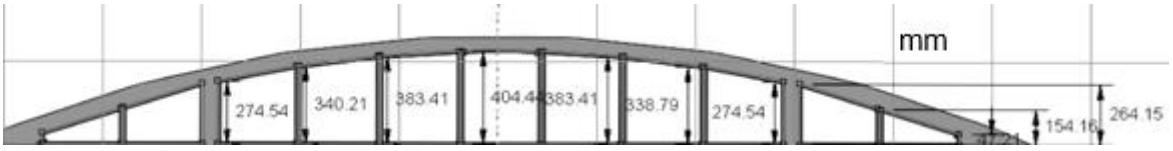

Figure 11 Detail view of the upper curved section of the large window (dimensions in mm).

5.2.2 New windows

The existing windows retain the same geometry, but an additional inner window is introduced. According to Varvstaden AB [22], the newly added window consists of double-glazed insulating panes. For modelling purposes in Abaqus, this configuration was simplified to a single-glazed pane. This simplification reduces computational complexity and focuses on the structural behavior of the old glass. The mechanical response of a double-glazed unit can be reasonably approximated by a single pane with equivalent stiffness under static loading conditions.

The new inner window was modelled using glass thicknesses chosen to provide realistic stiffness for the two window sizes and to avoid unrealistically flexible inner panes in the coupled system response. For the small inner window, a glass thickness of 5 mm was adopted, which is commonly used for small panes and provides sufficient stiffness without unduly increasing the structural rigidity of the retrofit element. The large inner window, on the other hand, was assigned a 10 mm glass thickness to reflect the increased span and expected higher bending stress under wind pressure, see Figure 12 to Figure 15 in the next pages.

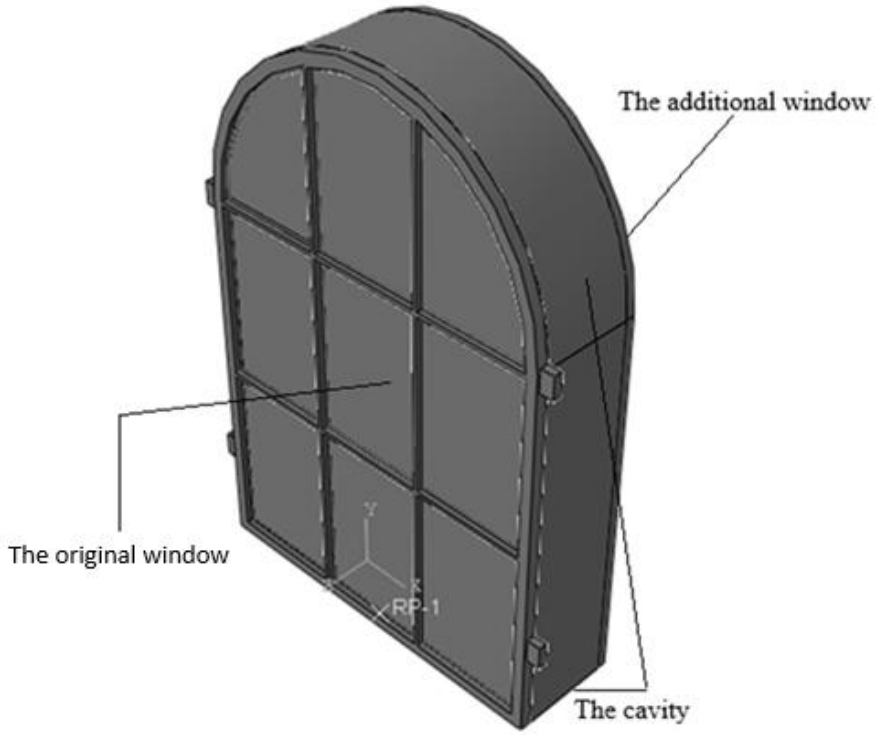

Figure 12 Finite element representation of the small historic window after renovation, showing the original window, the added inner window, and the sealed cavity (view from the exterior).

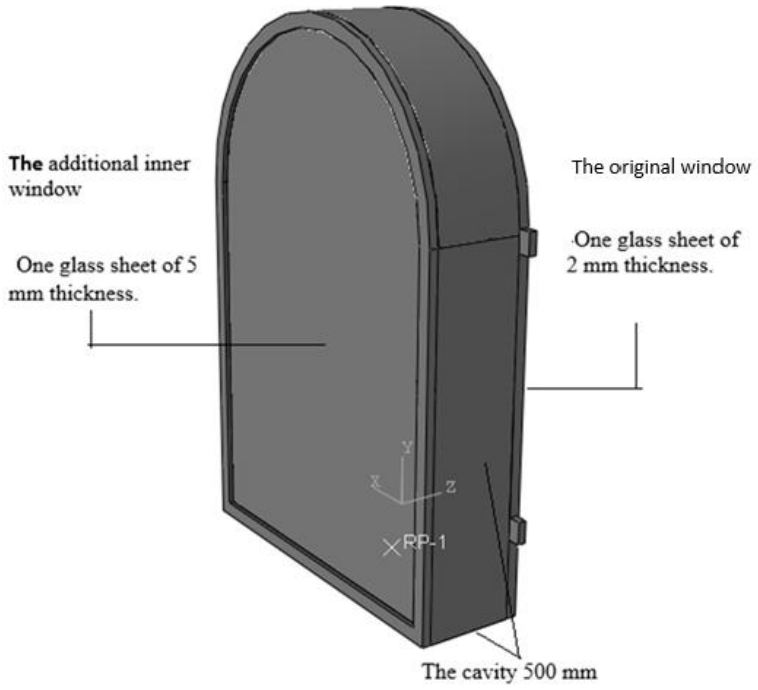

Figure 13 Finite element representation of the small historic window after renovation, showing the original window, the added inner window, and the sealed cavity (view from the interior).

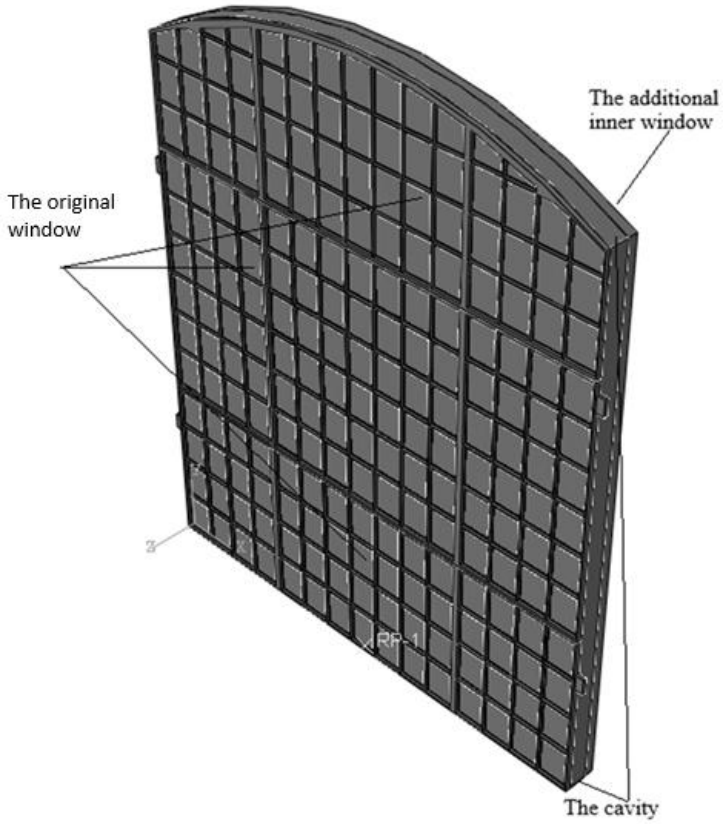

Figure 14 Finite element representation of the large historic window after renovation, showing the original window, the added inner window, and the sealed cavity (view from the exterior).

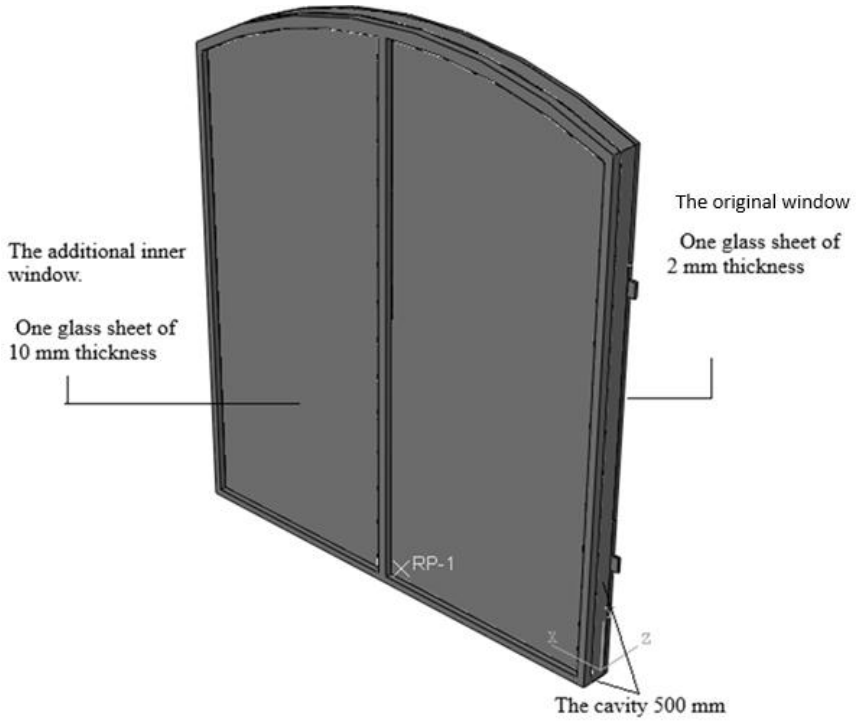

Figure 15 Finite element representation of the large historic window after renovation, showing the original window, the added inner window, and the sealed cavity (view from the interior).

5.3 Material

All windows are composed of a cast iron frame and glass. This section describes the material properties used in the simulations.

5.3.1 Cast iron

The cast-iron frame is modelled as linear elastic and isotropic. This is a simplification, since cast iron is a brittle material and its structural capacity is strongly influenced by defects and microstructure. Fracture and damage evolution are not modelled in the present study. The linear-elastic assumption is therefore used to obtain stress distributions and identify critical locations rather than to predict crack initiation explicitly. According to Davis, J.R. [5]. The Young's modulus is set to 165 GPa**.** Poisson's ratio is set to 0.25, meaning that for every unit of axial strain, there is 0.25 units of strain in the perpendicular direction [20]. Fracture is not considered in the cast iron, but a bending strength value 200 MPa is used for comparison with the calculated stress.

5.3.2 Glass

Glass is also modelled as a linear elastic and isotropic material. Its Young's modulus is set to 70 GPa. Poisson's ratio is set to 0.20 in glass. The value of 18.5 MPa represents the calculated bending strength of newly manufactured float glass (see Section 4.2.1). However, since the strength of glass decreases significantly over its service life (up to 100 years), this value is not used directly for design purposes. Instead, a reduced design strength is adopted, in the following sections, a pre-renovation analysis is performed, and the maximum stress value observed in the glass is used for comparison with the calculated stress, see section 6.3.

5.4 Load

In this section, all anticipated load types acting on the renovated window structure are presented. These include static loads resulting from environmental conditions such as wind, temperature fluctuations, and internal pressure

5.4.1 Self-load

The self-weight of the window components is neglected in this study, as wind loads and thermally induced pressure have a far greater influence on the structural response. Since the windows are mounted vertically, gravity acts mainly in the plane of the glass and frame, producing only minor in-plane compression and no significant bending. However, neglecting self-weight remains a simplification, and in a detailed long-term analysis, its cumulative effect on the lower parts of the frame could be considered for completeness.

5.4.2 Wind load

Wind load is determined according to Eurocode 1 (SS-EN 1991-1-4), which considers building height, terrain category, and geographic location. In this study, internal wind pressures are disregarded. Only the most unfavorable external pressure is considered to simplify the analysis. [8]

The wind load is calculated according to Eurocode 1 SS-EN 1991-1-4 General loads – Wind load. [8]

$$w_k = q_p(z_e) \cdot c_{pe}$$

Basic Data

The following basic data were used for Malmö, Kockum area:
- Basic wind speed (v_{b0}) = 26 m/s
- Terrain category = Category II
- Building height = 15 m (assumed)

The characteristic velocity expression ($q_p(z_e)$)

According to Eurocode the Figure 16 below shows the value of characteristic velocity pressure in kN/m².

Linear interpolation at 15 m and the interpolation will be between 12 m and 16 m:

$$q_p(z_e) = q_p(z_e \text{ in } 12 \text{ m}) + \frac{15-12}{16-12}(q_p(z_e \text{ in } 16 \text{ m}) - q_p(z_e \text{ in } 12 \text{ m}))$$

$$q_p(z_e) = 0.96 + \frac{3}{4}(1.04 - 0.96) = 1.02 \text{ kN/m}^2$$

höjd	$v_b = 25$m/s Terrängtyp					$v_b = 26$m/s Terrängtyp				
(m)	0	I	II	III	IV	0	I	II	III	IV
2	0,77	0,67	0,50	0,45	0,41	0,84	0,73	0,55	0,49	0,44
4	0,90	0,81	0,64	0,45	0,41	0,98	0,87	0,69	0,49	0,44
8	1,04	0,95	0,79	0,55	0,41	1,13	1,03	0,86	0,60	0,44
12	1,13	1,04	0,89	0,65	0,45	1,22	1,13	0,96	0,70	0,49
16	1,19	1,11	0,96	0,72	0,52	1,29	1,20	1,04	0,78	0,56
20	1,24	1,16	1,01	0,78	0,58	1,34	1,26	1,10	0,84	0,63
25	1,29	1,22	1,07	0,84	0,64	1,40	1,32	1,16	0,90	0,69
30	1,33	1,26	1,12	0,89	0,69	1,44	1,37	1,21	0,96	0,74
35	1,37	1,30	1,16	0,93	0,73	1,48	1,41	1,25	1,00	0,79
40	1,40	1,33	1,20	0,97	0,77	1,51	1,44	1,29	1,04	0,83
45	1,43	1,36	1,23	1,00	0,80	1,54	1,48	1,33	1,08	0,87
50	1,45	1,39	1,26	1,03	0,83	1,57	1,51	1,36	1,11	0,90

Figure 16 Characteristic velocity pressure $q_p(z)$ at height z for v_b = 26 m/s.

Pressure Coefficient (c_{pe})

In this project a c_{pe1} will be used because it is a local form factor for a loaded area of 1 m². It is used when dimensioning fasteners and small elements. Two types of pressure coefficient will be used: [10]

- c_{pe1}= -1.4 in zone A, as external suction.
- $c_{pe1} = 1.0$ in zone D as external pressure.

In the absence of external temperature effects, the maximum design load of zone A is generally applied.

Calculation of characteristic wind load (w_k)

The total wind load is calculated by:
$w_{k\,1\,(\text{suction})} = q_p(z_e) \cdot c_{pe}$

$$w_{k(\text{suction})} = 1.02 \cdot (-1.4) = -1.428\ \text{kN/m}^2$$

$w_{k2\,(\text{pressure})} = q_p(z_e) \cdot c_{pe}$

$$w_{k(\text{pressure})} = 1.02 \cdot (1.0) = 1.02\ \text{kN/m}^2$$

Design loads in ultimate limit states (ULS):

According to EN 1990: Eurocode – Basis of Structural Design, structures are classified into different consequence classes (also called safety classes) based on the potential consequences of failure. These classes influence the choice of partial safety factors and reliability requirements. [4]

In this case, $\gamma_d = 0.73$ is used, which corresponds to Safety Class 0.
Safety Class 0 is typically applied to non-critical components or structures where the consequences of failure are considered low such as temporary structures**,** non-load-bearing elements, or components not affecting structural stability or safety**.** [4]

The partial factor γ_d is applied to action effects or design values in ultimate limit state calculations. The value 0.73 reflects a reduced level of safety, which is acceptable when justified by the low risk associated with the element or system in question. [4]

$$q_{d,wind1(suction)} = \gamma_d \cdot 1.5 \cdot w_{k\,1\,(\text{suction})} = 0.73 \cdot 1.5 \cdot (-1.428) = -1.564\ \text{kN/m}^2$$

$$q_{d,wind2(pressure)} = \gamma_d \cdot 1.5 \cdot w_{k2\,(\text{pressure})} = 0.73 \cdot 1.5 \cdot (1.02) = 1.117\ \text{kN/m}^2$$

Wind load as a combined load

Since there are no established procedures for combining wind load, temperature effects, and air pressure in a single load case, the chosen approach is to treat the wind load as a secondary action. Temperature and air pressure are therefore considered as the main loading conditions.

In accordance with EN 1990: *Eurocode – Basis of Structural Design* [4], a combination factor of $\psi_0 = 0.3$ is applied to the secondary load (wind). This approach allows for a consistent representation of the combined effects while acknowledging the absence of a standardized method. The calculated values for both wind suction and pressure are presented below.

$$q_{d,combined\ wind\ load(suction)} = \gamma_d \cdot 1.5 \cdot \psi_0 \cdot w_{k(suction)}$$

$$q_{d,combined\ wind\ load(suction)} = 0.73 \cdot 1.5 \cdot 0.3 \cdot (-1.428) = -0.469\ \mathrm{kN/m^2}$$

$$q_{d,combined\ wind\ load\ (pressure)} = \gamma_d \cdot 1.5 \cdot \psi_0 \cdot w_{k(pressure)}$$

$$q_{d,combined\ wind\ load\ (pressure)} = 0.73 \cdot 1.5 \cdot 0.3 \cdot (1.02) = 0.335\ \mathrm{kN/m^2}$$

5.4.3 Pressure load

In the renovated window system, a sealed air cavity is formed between the original exterior window and the newly installed interior window. Since the cavity is assumed to be completely airtight, changes in temperature and atmospheric pressure will alter the density of the trapped air. This creates a pressure difference across the two glass panes, which acts as an additional load on the structure. The pressure load therefore consists of two main components: thermally induced pressure and variations in atmospheric pressure.

The indoor reference temperature used in this analysis is 20 °C. According to Boverket's building regulations, living and working spaces should maintain at least 18 °C, and hygiene or care rooms 20 °C or higher [13]. This provides a realistic design reference for the analysis. However, the assumption of a completely airtight cavity is an idealization; in practice, small leakages may occur through joints or material interfaces, which would reduce the actual pressure variation compared with the theoretical values.

5.4.3.1 Thermal induced pressure

Reflected solar radiation can increase the air temperature within the cavity, thereby affecting internal pressure [9]. Since the cavity is assumed to be completely sealed, temperature changes will produce either negative or positive pressure inside the cavity. This effect could be prevented by including a ventilation port, which would allow the air volume to adjust and equalize with the surrounding atmosphere. In this simulation, however, no ventilation port is assumed, and the cavity is considered perfectly sealed.

According to Buddenberg et al. [3], the pressure in insulating glass units is directly affected by temperature variations according to the ideal gas law:

$$pV = nRT$$

where
p= pressure (Pa)
V= volume (m^3)
n= amount of gas (mol)
R= universal gas constant (8.314 J/mol·K)
T= temperature (K)

Because the cavity is assumed to be sealed, the amount of gas n remains constant. However, the cavity volume V is not strictly constant, since the glass panes deform under pressure. The pressure–temperature relationship is therefore described by the ideal gas law between two equilibrium states:

$$\frac{p_1 V_1}{T_1} = \frac{p_2 V_2}{T_2}$$

This formulation accounts for the coupling between pressure change and volume change due to glass deflection. When the temperature decreases, the pressure inside the cavity reduces. The resulting pressure difference causes the glass to deflect inward, which slightly reduces the cavity volume until a new equilibrium state is reached. Conversely, an increase in temperature raises the cavity pressure, producing outward deformation of the panes.

In reality, the cavity is unlikely to remain perfectly airtight, allowing partial pressure equalization. As a result, the theoretical pressure calculated from the ideal gas law probably overestimates the actual load. Nevertheless, this assumption provides a conservative estimate, ensuring that the analysis covers the most critical loading conditions for the historic windows.

5.4.3.2 Atmospheric pressure changes

In this study, a pressure variation of ±30 hPa is applied to represent realistic atmospheric pressure changes. This value is based on observed weather patterns in Northern Europe, where atmospheric pressure commonly ranges between approximately 980 hPa and 1040 hPa during strong low-pressure and high-pressure systems. According to the Swedish Meteorological and Hydrological Institute [25], variations of 25–35 hPa are typical during pronounced weather transitions, especially in coastal regions influenced by maritime climates.

The normal atmospheric pressure at sea level is approximately 1013 hPa.

- During strong low-pressure systems: $p_{low} \approx 980$hPa (−30 hPa)
- During strong high-pressure systems: $p_{high} \approx 1040$hPa (+30 hPa)

Because atmospheric pressure acts uniformly across the glass surface, a difference of 30 hPa corresponds to approximately 3000 Pa, or 3 kN/m². This is significant, as it is of the same order of magnitude as the design wind pressure used in structural analysis. Consequently, atmospheric pressure variations can generate loads comparable to wind loads and must therefore be included in the structural evaluation of the historic windows.
Although ±30 hPa represents a realistic upper limit for Scandinavian coastal regions, such extreme differences rarely coincide with peak wind or temperature loads. The assumption thus provides a conservative but reasonable estimate for the most critical design scenario.

5.4.4 Combined load

5.4.4.1 Wind load and temperature

In this study, 20 °C is defined as the reference temperature at which the cavity air pressure equals the surrounding atmospheric pressure. This represents the neutral or stress-free condition of the window system.

When the temperature falls below 20 °C, the air inside the sealed cavity contracts, creating a lower internal pressure and resulting in inward bending of the glazing. Conversely, when the temperature rises above 20 °C, the air expands, increasing the internal pressure and causing outward bending of the glass.

To represent the most critical load combinations, wind pressure is applied in the same direction as cavity-induced pressure. Therefore, wind load is applied as pressure (inward) for cases where $T < 20°C$, and as suction (outward) for cases where $T > 20°C$. This ensures that both effects act simultaneously in the same direction, capturing the maximum possible load on the historic window system, see Figure 17.

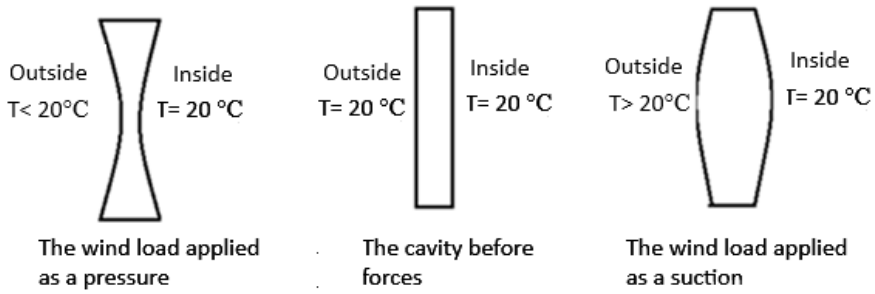

Figure 17 The cavity shape under forces at different temperatures.

5.4.4.2 Wind load and atmospheric pressure

At 20 °C outside the cavity is defined as neutral (no net cavity pressure), so the critical external actions are the synoptic atmospheric pressure state and the wind action. To envelope the most unfavorable response, both are taken as suction at 20 °C. The atmospheric term is represented by a low-pressure weather scenario (outside pressure lower than inside), which acts outward on the plane.

For the wind action, façade suction is typically more severe than positive pressure because the negative external pressure coefficients on cladding are larger in magnitude; consequently, the design wind effect is also taken as suction. In the load combination, wind is treated as a secondary action (with the prescribed combination factor), and both actions wind load and atmospheric pressure are applied in the same outward direction, (see Section 5.4.2). The combined wind load is:

$$q_{d,combined\ wind\ load(suction)} = -0.469\ \mathrm{kN/m^2}$$

This choice maximizes the resultant load on the glazing at the cavity-neutral condition and is therefore used as the critical combination for design checks.

5.4.4.3 Atmospheric pressure and temperature

In this analysis, the effect of atmospheric pressure depends on outdoor temperature because temperature changes cause the air inside the cavity to either expand or contract.

When the temperature falls below 20 °C, the air in the sealed cavity contracts, leading to a lower internal pressure than outside. In this case, the atmospheric pressure acts inward (pressure load), coinciding with the same direction as the cavity-induced pressure. Conversely, when the temperature exceeds 20 °C, the air inside the cavity expands, producing a higher internal pressure and pushing outward. To represent the most critical combination, the atmospheric pressure is also taken as suction (outward) for these conditions. In both situations, the loads act in the same direction, resulting in the maximum total effect on the glazing.

5.4.4.4 Temperature, wind and air pressure.

When the outside temperature falls below 20 °C, the air inside the sealed cavity cools and contracts, producing an internal under pressure relative to the outside air. This pressure difference causes the exterior glass to bend inward. At the same time, an external wind load and an increased atmospheric pressure of +30 hPa also act inward on the outer glass surface. These combined effects result in the most critical inward loading condition on the glazing, as shown in Figure 18.

When the external temperature rises above 20 °C, the air inside the cavity expands, leading to an internal overpressure relative to the surrounding air. This pressure acts outward on the glazing. In this case, the load combination includes a wind suction (outward) and a low atmospheric pressure of −30 hPa, both acting in the same direction as the cavity pressure. Together, these loads create the most critical outward loading condition, see Figure 17.

Although these cases represent extreme combinations of temperature and pressure, they are included to assess the maximum possible stress conditions in the historic window system. In practice, such simultaneous extremes are rare but analyzing them provides a conservative basis for evaluating the structural safety of the glazing.

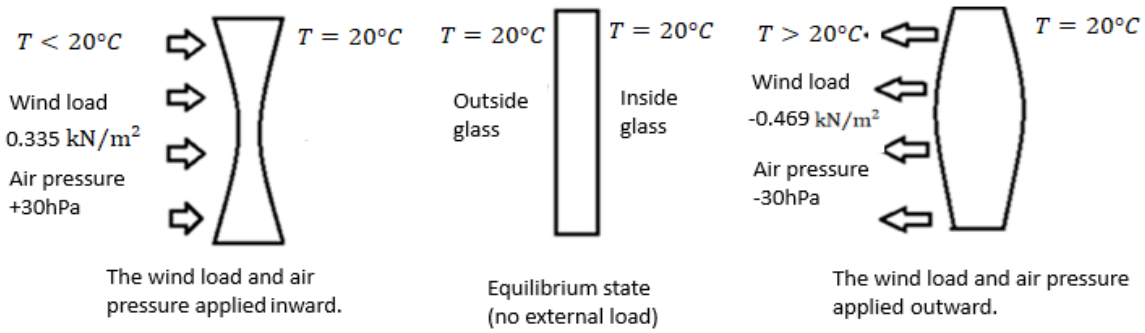

Figure 18 Cavity deformation in different loading cases.

5.4.5 Design load

5.4.5.1 Before Renovation

Before the installation of the inner window, only external wind load was applied, see Table 3. This was modelled as a uniform surface pressure on the exterior glass pane in Abaqus. This method enables analysis of deformation and stress distribution under realistic wind conditions.

Table 3 Design load for windows before renovation.

Loading case	Wind load (kN/m^2)	Temperature (°C)	Atmospheric pressure change (kN/m^2)
Only wind load	$0.73 \cdot 1.5 \cdot (-1.428) = -1.564$	20	-

5.4.5.2 After Renovation

After renovation, the window must withstand a combination of:

- Wind pressure
- Thermal pressure
- Atmospheric pressure changes

A combined load analysis was conducted for the following cases:

1. Wind + Temperature (W+T)
2. Wind + Atmospheric Pressure (W+A)
3. Temperature + Atmospheric Pressure (T+A)
4. Wind + Temperature + Atmospheric Pressure (W+T+A)

The Table 4 in the nest page shows all load cases.

Table 4 Design load for windows after renovation.

Loading case	Wind (kN/m^2)	Temperature (°C)	Atmospheric pressure change (kN/m^2)	Explanation
Wind load	-1.564	20	-	Only Wind load. Max wind load value.
Temperature	0 0 0 0 0 0 0	-20 -16 -5 0 10 20 34	0 0 0 0 0 0 0	Only Temperature.
Atmospheric pressure	0	20	3	Only air pressure.
Temperature and wind load	$0.3 \cdot 1.117 = 0.335$ $0.3 \cdot 1.117 = 0.335$ $0.3 \cdot (-1.564) = -0.469$ $0.3 \cdot (-1.564) = -0.469$	-20 -5 20 34	0 0 0 0	At low temperatures, the wind load acts as pressure, and at high temperatures, it acts as suction.

Wind load and atmospheric pressure	$0.3 \cdot (-1.564) = -0.469$	20	-3	Both contribute to a combined inward acting force.
Atmospheric pressure and temperature	0	-20 -5 10 20 34	3 3 3 -3 -3	Higher temperature increases internal pressure, which pushes outward on the glass.
Temperature, wind force and atmospheric pressure	$0.3 \cdot 1.117 = 0.335$ $0.3 \cdot 1.117 = 0.335$ $0.3 \cdot 1.117 = 0.335$ $0.3 \cdot (-1.564) = -0.469$ $0.3 \cdot (-1.564) = -0.469$	-20 -5 10 20 34	3 3 3 -3 -3	Cold outside air causes internal under pressure and inward wind load. Warm outside air causes internal over pressure and outward wind suction.

5.5 Finite element model

Finite element analysis was performed in Abaqus to evaluate the structural response of the historic cast-iron windows (small and large) before and after renovation under the defined environmental load cases. The purpose of the FE models is to obtain stress and deflection distributions, identify the most critical load cases, and locate critical regions (particularly along the glass–frame interface and at frame junctions) [18]. The models are intended for comparative assessment between pre- and post-renovation scenarios rather than certification-level prediction of exact failure loads.

To keep the large-window model computationally manageable, only the central portion of the large window was represented. Due to the high geometric complexity (many slender members, intersections, and local details), this portion could not be robustly created and meshed as a single Abaqus part; therefore, it was modelled as four assembled, this

partitioning improved mesh generation and numerical stability while preserving the actual segmentation and support conditions of the glazing fields.

5.5.1 Computational procedure

The simulations were carried out as quasi-static analyses for a set of load cases representing wind pressure, thermally induced cavity pressure, atmospheric pressure variations, and their combinations. Temperature cases were evaluated over the interval −20 °C to +34 °C, representing winter and summer extremes used in the project. The cavity between the historic outer window and the new inner window was assumed to be fully sealed (no intentional ventilation and no pressure equalization with the ambient air). Under this assumption, pressure actions in the cavity were computed using an ideal gas (see section 5.4.3.1) based approach accounting for temperature changes and atmospheric pressure variations and applied as differential pressure on the relevant cavity surfaces. The cavity air pressure at the reference state is taken as normal atmospheric pressure (1013 hPa).

5.5.2 Element types

Three-dimensional solid elements were used to represent the cast-iron frame and glass panes.

- Cast-iron frame: C3D8R (8-node brick, reduced integration). This element provides good efficiency for relatively stiff structural components and reduces the risk of shear locking.
- Glass panes: C3D8 (8-node brick, full integration) to obtain stable stress fields in the brittle glass material.

To apply cavity pressure efficiently without modelling the air as a physical 3D solid, S4R shell elements were used to represent cavity pressure application surfaces (“cavity walls”), since the cavity itself is not a load-bearing solid.

Stress peaks may occur near sharp corners, tied constraints, or idealized contacts. Therefore, interpretation focuses on recurring stress bands and critical regions rather than isolated single-element peak values.

5.5.3 Boundary conditions

The boundary conditions were applied to simulate realistic constraints. All boundary constraints were assigned on the backside (interior-facing side) of the window model, representing the support provided by the surrounding wall and anchorage conditions, see Figure 19 and Figure 20.

- The entire outer edge was fixed in the *z*-direction to prevent out-of-plane displacement
- One point on the left base corner was fixed in the *y*-direction
- One point on the right base corner was constrained in both *x* and *y* directions to eliminate rigid body motion

The restraint stiffness of historic anchorage and masonry interaction is uncertain. The chosen boundary conditions represent an idealized support condition; sensitivity to support assumptions is therefore discussed when interpreting peak stresses near support.

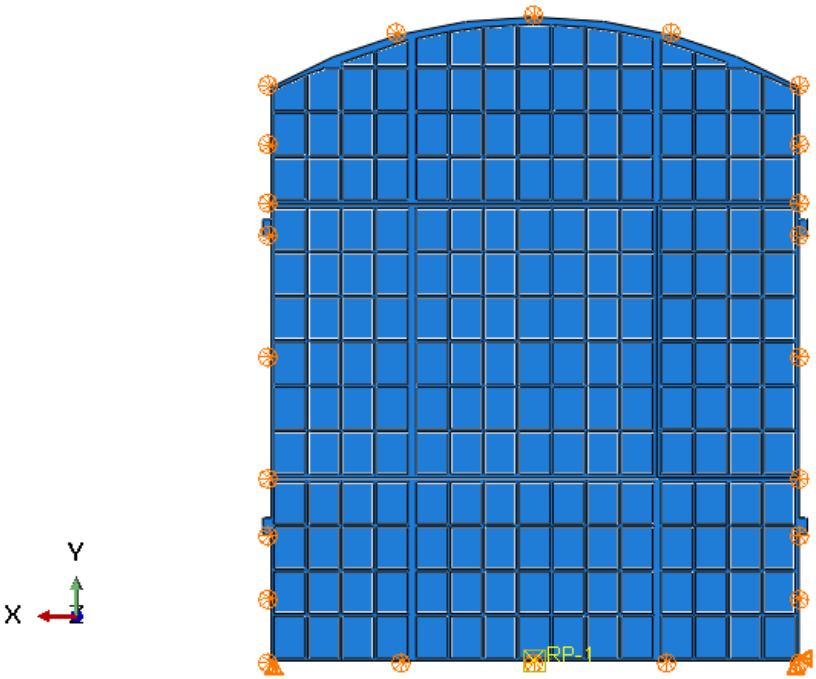

Figure 19 Boundary conditions large window.

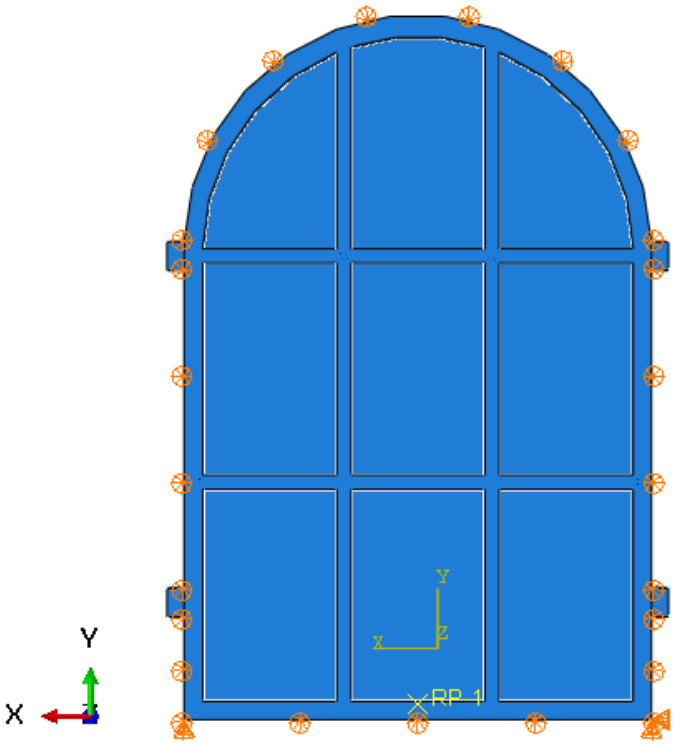

Figure 20 Boundary conditions small window.

5.5.4 Mesh

Meshing was performed in Abaqus using an automatic free meshing approach, selected to handle the complex geometry of the historic window, including the curved arch, numerous frame intersections, and multiple glass panes. No manual local mesh controls were applied; instead, mesh density was governed by globally defined element sizes for each component.

For the large window model, a global element size of 150 mm was used for the cast-iron frame and 50 mm for the glass panes. For the small window model, a global element size of 10 mm was applied to both cast iron and glass. The automatic meshing algorithm naturally generated a denser element distribution in geometrically complex regions, such as near pane corners and frame junctions, while maintaining coarser elements in regions with smoother geometry.

Mesh quality was verified using the Abaqus/CAE verify mesh tool by checking element shape metrics, including distortion, corner angles, and aspect ratio. No mesh errors were reported, although a limited number of elements were flagged with warnings in highly detailed regions. These warnings were considered acceptable and are typical of complex three-dimensional geometries.

Since local stress concentrations may occur near sharp corners and idealized constraints, mesh adequacy was assessed primarily through a mesh convergence study rather than through further manual refinement. Stress and deflection results were therefore interpreted based on stable response patterns and predefined monitoring regions rather than isolated peak values at individual elements, see Figure 21 and Figure 22.

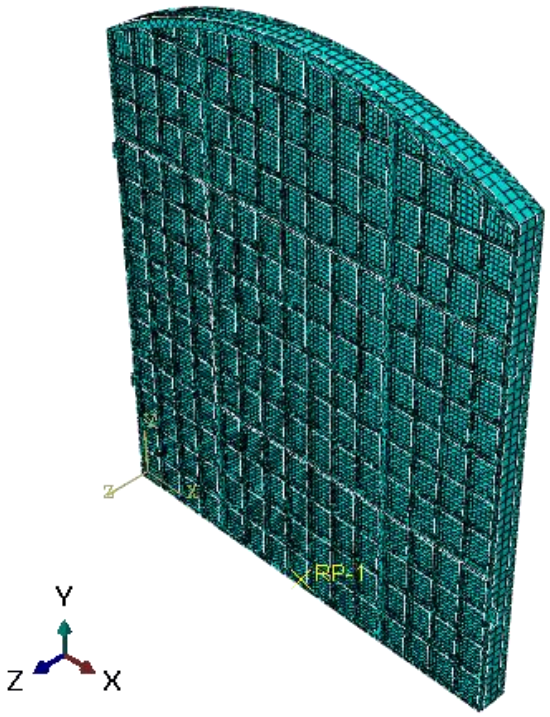

Figure 21 Mesh, large window.

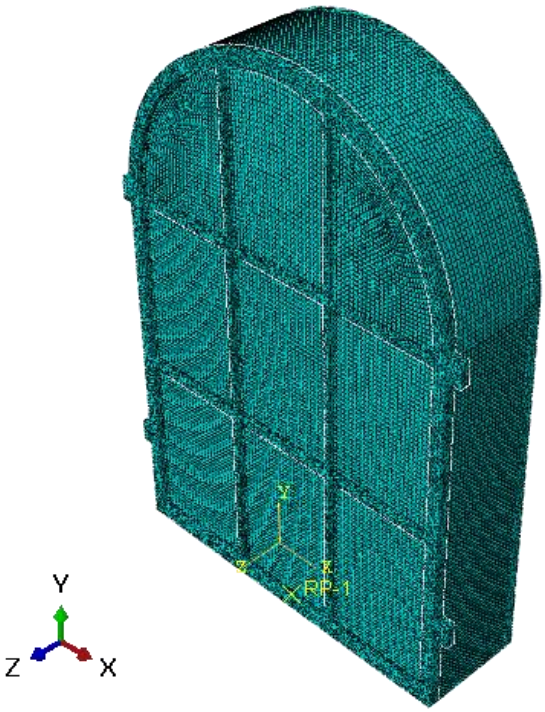

Figure 22 Mesh, small window.

5.5.5 Convergence

To ensure the reliability of the numerical results, a mesh convergence study was performed. The most critical load case was analyzed using progressively refined meshes, and the resulting stresses and deflections were compared between mesh levels. Convergence was considered achieved when the variation in the selected response quantities between successive refinements was below 3%, indicating that the results were not significantly influenced by mesh density.

The procedure started with an initial coarse mesh, followed by two refinement steps obtained by reducing the global element size. For each mesh level, maximum deflection and stress values were extracted from predefined monitoring regions in the glass panes and cast-iron frame (e.g., along pane edges and at the glass–frame interface). These monitoring regions were used to avoid relying on isolated peak values that can be mesh-sensitive near sharp corners and idealized constraints.

The convergence study showed that further refinement led to only minor changes in the global deformation pattern and the stress distribution in the monitoring regions. Based on these results, the final mesh was considered sufficiently refined to provide stable and reliable outputs for the comparative assessment of the historic windows before and after renovation.

6 Results

This chapter presents the finite element results for the historic cast iron–framed windows in the Machine and Assembly Hall, with the objective of assessing whether the original window system can withstand the load effects introduced by the renovation strategy, where an insulating inner window is installed 500 mm behind the historic glazing.

The results are organized in a clear verification sequence. First, stress and deflection concentration zones are identified and used to define monitoring regions for consistent post-processing. The structural response is then reported for wind loading, cavity-pressure effects due to temperature changes, atmospheric pressure variations, and combined scenarios. Results are presented for both small and large window configurations and for both before renovation and after renovation conditions, where relevant.

Finite element solutions may exhibit highly localized peak stresses or displacements near constrained boundaries, sharp geometric transitions, and interaction interfaces. Such peaks can be sensitive to mesh density and modelling idealizations and therefore do not necessarily represent the overall structural response. For this reason, assessment and subsequent reporting are based on representative stresses and deflections extracted from predefined monitoring regions located along the principal load-transfer paths, i.e., where forces are transferred from the glass to the frame and redistributed through the structure.

In the evaluation of stresses, different stress measures are used for the cast-iron frame and the glass panes, reflecting their fundamentally different material behaviour. For the cast-iron frame, the von Mises equivalent stress is adopted as the primary indicator, as it provides a suitable scalar measure of the combined stress state and is commonly used to assess demand in metallic structural components. For the glass panes, the maximum principal tensile stress is used as the critical stress measure. This choice is motivated by the brittle, flaw-sensitive nature of glass, where failure initiation is controlled by tensile cracking rather than yielding. Therefore, a principal stress criterion is more physically relevant for glass than an equivalent stress measure. Deflection is evaluated using the displacement magnitude, U representing the maximum response under the applied loading condition.

6.1 Basis for results evaluation

This section presents and interprets the numerical results for both window configurations in the post-renovation state under wind loading only. It defines the post-processing and interpretation framework used to identify critical stress and deflection locations and to establish monitoring regions for consistent extraction and comparison of results between the small and large window models. Local peak values occurring near restraints, contacts, and glass–frame interfaces are treated with caution, as they may be influenced by mesh density, idealized boundary conditions, and constraint/contact formulations. The interpretation therefore distinguishes between physically meaningful stress concentrations associated with load transfer and recurring edge bands, and isolated numerical artefacts at sharp corners or constraint-dominated zones. Model characteristics that may affect the numerical response are also noted, including potential symmetry/asymmetry effects in the large-window model arising from partitioning, connectivity, and idealized joints.

6.1.1 Interpretation location

Finite element contours may exhibit localised critical peak stresses near constrained boundaries, sharp geometric transitions, and contact/interface regions. In these zones, reported maxima can be strongly influenced by mesh discretisation, stress extrapolation, and simplified boundary/contact idealisations, and may therefore not be representative of the global response.

Based on these stress measures, local maxima are observed in specific regions of the window system. In the small-window cast iron frame, the highest stresses occur adjacent to restrained frame corners (Figure 23Figure 24), where boundary conditions force bending and shear to develop over a short distance. In the large window, local maxima of principal tensile stress in the glass appear near supported edges and along glass–frame connection regions (Figure 25Figure 26), where restrained plate bending produces high curvature and where deformation compatibility with the stiffer frame amplifies local tensile stresses.

These locations are physically meaningful because they coincide with load introduction and restraint; however, the absolute peak magnitudes in these zones may be sensitive to mesh discretisation and to the idealisation of supports and contact. Consequently, such peaks are used to identify potential critical regions, while critcal values reported in the following sections are extracted from predefined monitoring regions along the main load-transfer paths, representing the distributed structural response rather than isolated numerical peaks.

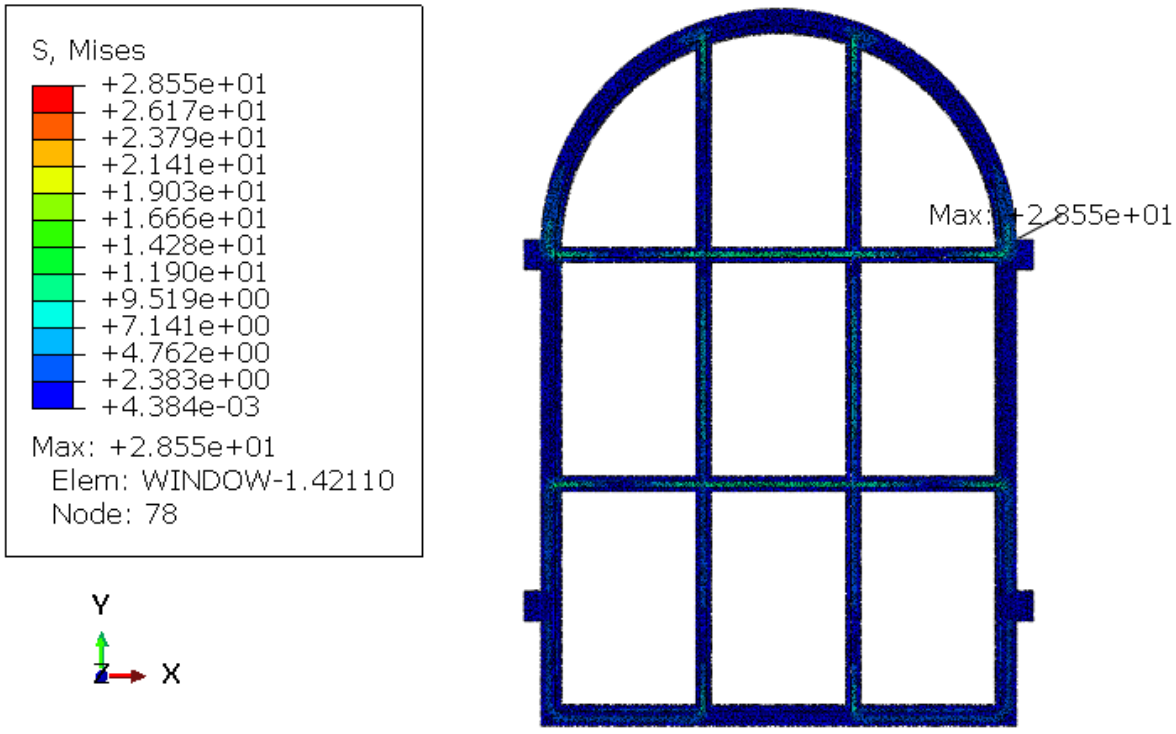

Figure 23 Location of peak von Mises stress in the cast-iron frame for the small window under wind loading after renovation.

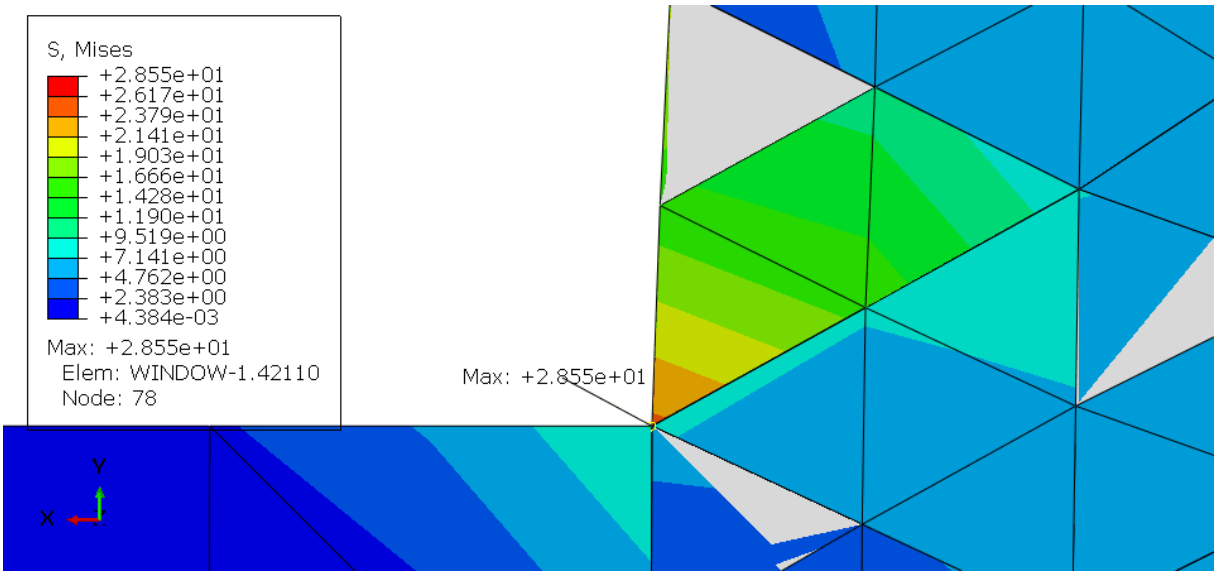

Figure 24 Close-up of the critical corner region where the peak stress occurs (cast-iron frame, small window after renovation).

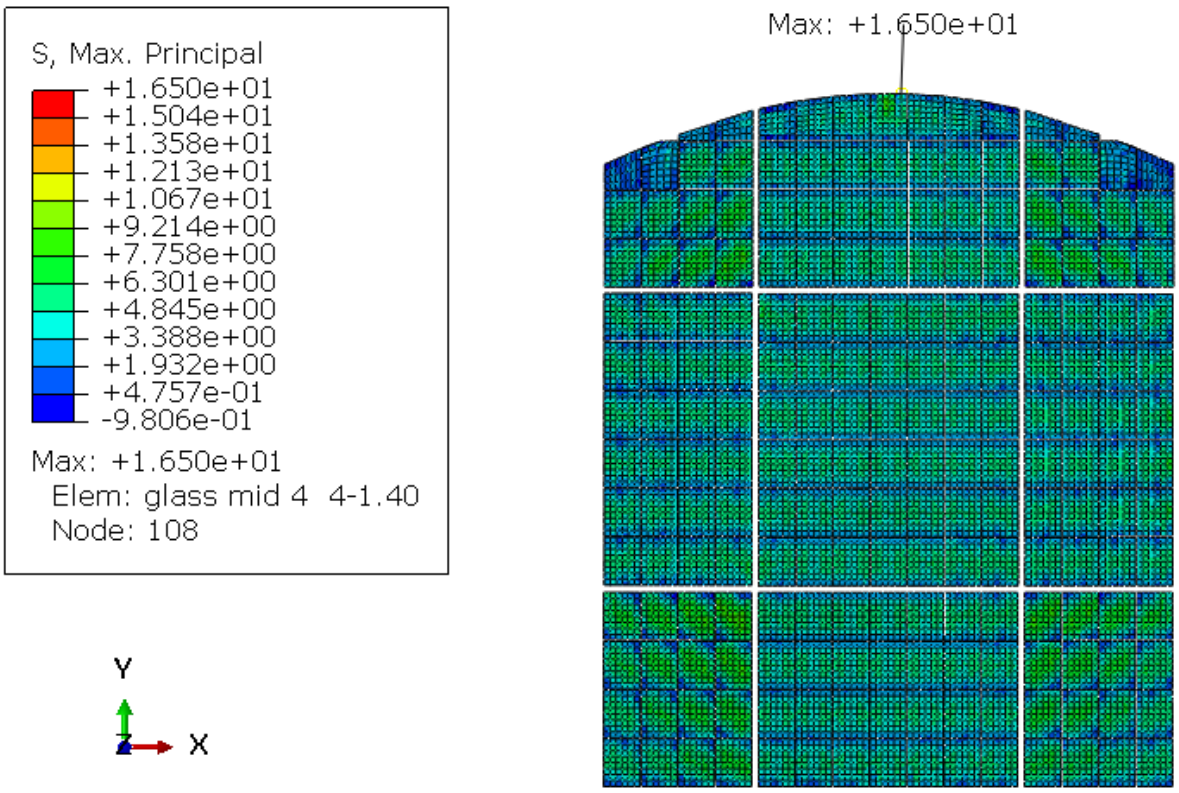

Figure 25 Location of peak max, principal stress in the glass for the large window under wind loading after renovation.

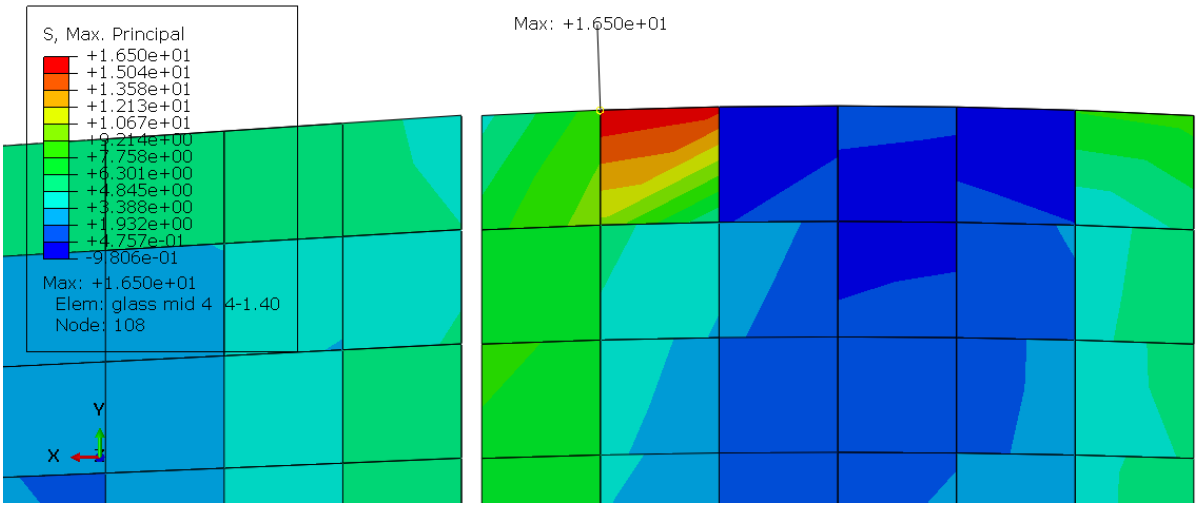

Figure 26 Close-up of the critical corner region where the peak stress occurs (glass, large window, after renovation).

6.1.2 Monitoring location

Localized point peaks can be dominated by numerical concentration effects. These isolated maxima are therefore not used as critical values in the assessment. Instead, critical stresses and deflections are reported as the maximum values extracted within predefined monitoring regions that follow the load-transfer paths (recurring edge bands and interface zones), ensuring consistent and physically meaningful comparisons between cases. For visual clarity, the contour range is occasionally limited so that the global distribution and the monitored response can be seen clearly.

The glass geometry and wind loading are symmetric for both window configurations. In the small-window model, the glazing is represented as one continuous part. The numerical response is therefore fully symmetric, with matching stress and deflection fields on the left and right sides. This indicates that the results are governed by the intended global load-transfer mechanism and are not influenced by modelling-induced asymmetry.

For the large-window configuration, the physical window system is also symmetric and modelled with uniform material properties. However, in the FE model the large windows frame (and associated components) is subdivided into four parts that are subsequently connected. Even though the parts are geometrically identical and connected consistently, the internal interfaces and interaction definitions can introduce small numerical differences in stiffness and load transfer across the model. Consequently, minor left–right differences in stresses and deflections may appear in the results.

This asymmetry is therefore interpreted as a numerical effect related to discretization and interface modelling rather than physical asymmetry of the window system. At a global level, the deformation shape and the overall load-transfer mechanism remain essentially symmetric. To ensure consistent evaluation, stresses and deflections are extracted from predefined monitoring regions representing the recurring response, and the small asymmetric observed in the large-window model is considered to have negligible influence on the interpretation and on comparisons between load cases.

6.1.2.1 Stress on Cast iron

For the cast iron frame, the monitoring regions were defined along the primary load-transfer paths, the main horizontal and vertical members and their intersections, where forces transferred from the glass are collected and redistributed through the frame. These regions are used consistently in the subsequent sections to extract representative stresses rather than isolated local peaks at corners, restraints, or interface artefacts.

For the small window before and after renovation, the critical stress locations remain stable and are observed in the same structural zones of the frame, mainly along the primary members and at their intersections, see Figure 27. Therefore, the same monitoring locations are retained for the small-window analysis before and after renovation, see Figure 27

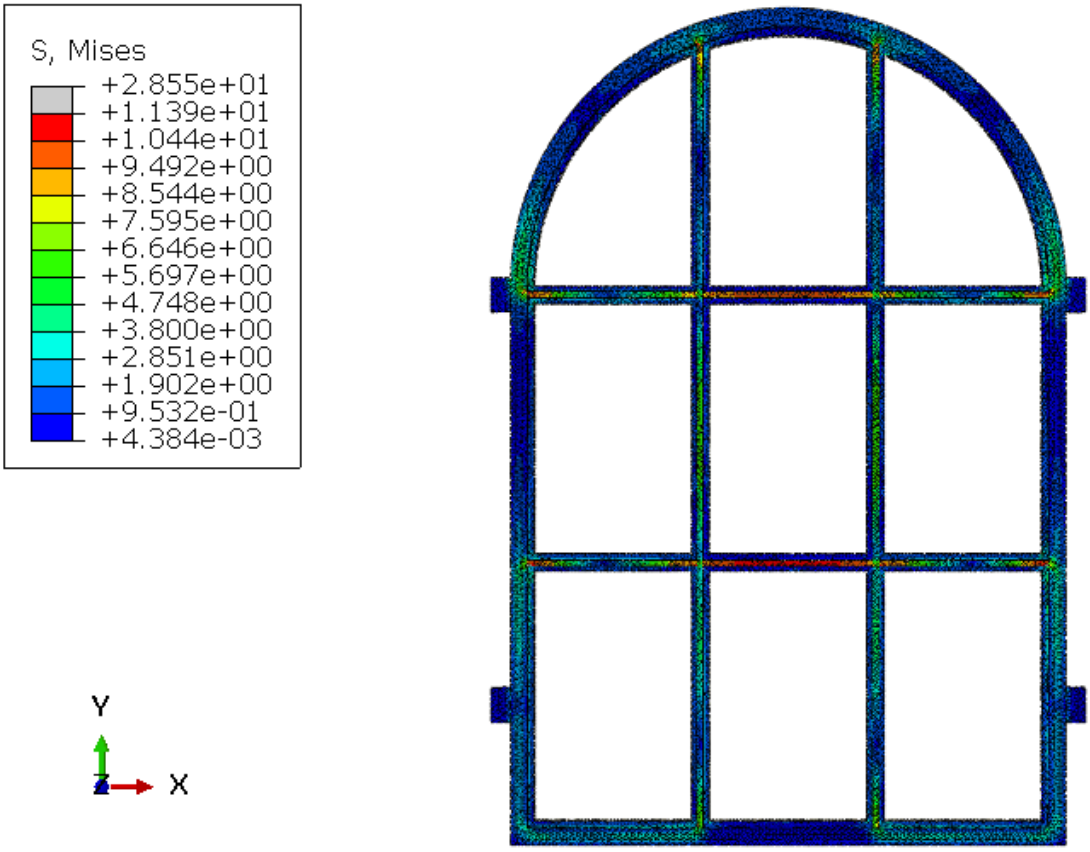

Figure 27 Definition of monitoring regions of von Mises stress; monitored areas are highlighted in red (cast-iron frame, small window after renovation, front side).

For the large window before renovation, the maximum frame stresses were consistently located near the upper frame region, particularly around the arched head. After renovation, the critical stress locations shifted toward the lower frame (sill) and the adjacent intersections with the vertical members, see Figure 28-Figure 29. In the results, maximum stress values were extracted for both configurations; however, in the post-renovation model the critical locations remained essentially the same across all investigated load cases, indicating a stable and recurring load-transfer path after the retrofit.

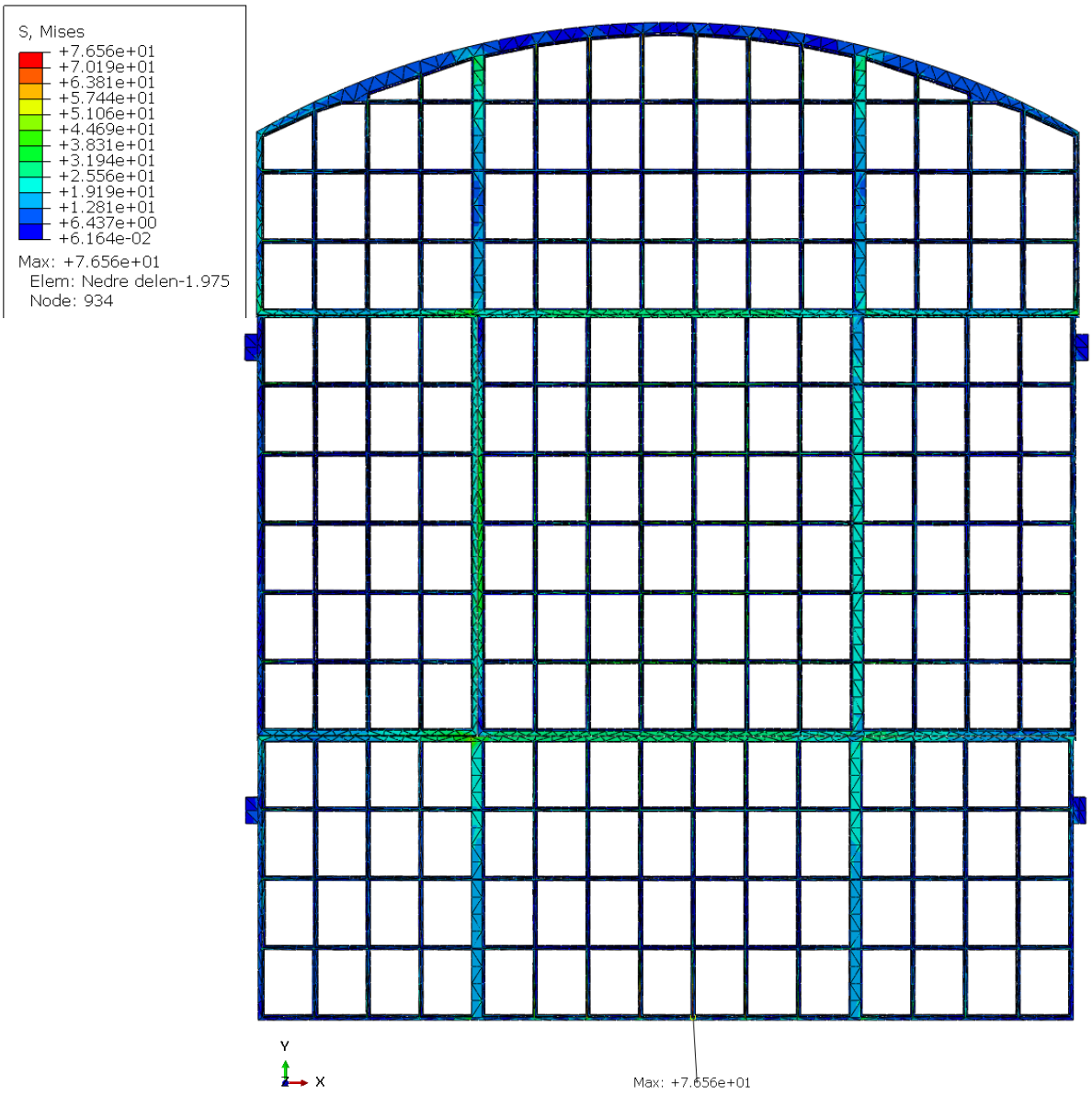

Figure 28 Definition of von Mises stress and the location of max stress value (cast-iron frame, large window after renovation, front side).

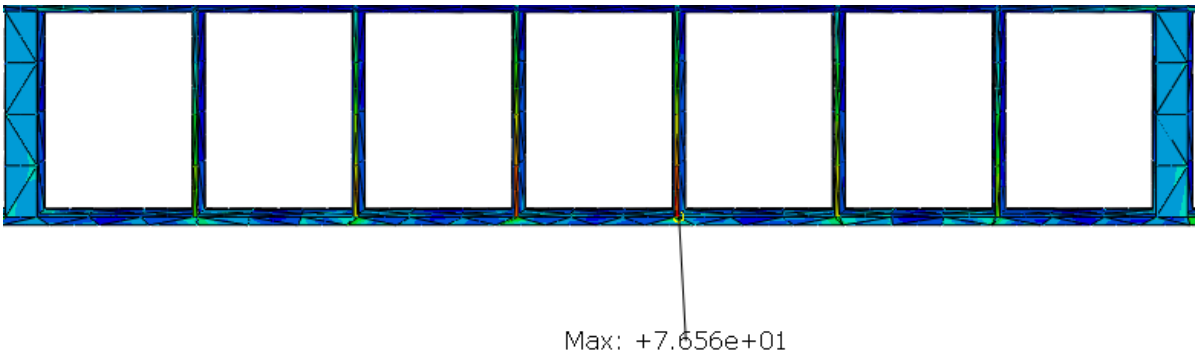

Figure 29 Definition of monitoring regions of von Mises stress; monitored areas are highlighted in red (cast-iron frame, large window after renovation, front side).

6.1.2.2 Stress on Glass

The critical tensile stresses in the glass are expected to develop mainly along the supported pane edges and at the glass–frame interface, where bending restraint and load transfer into the cast-iron frame are strongest. Local increases are also expected near pane corners and along internal frame lines between adjacent glass segments, where stiffness changes create short stress gradients. [2]

For the small window before and after renovation, Figure 30 and Figure 31, show that the critical glass stresses form continuous edge bands around the supported perimeter of the panes. These edge bands appear repeatedly along the frame-contact lines rather than as isolated mid-pane peaks, which is consistent with the physical load-transfer mechanism from glass to frame. Therefore, these perimeter edge bands are defined as the monitoring regions used for subsequent post-processing and comparison across load cases.

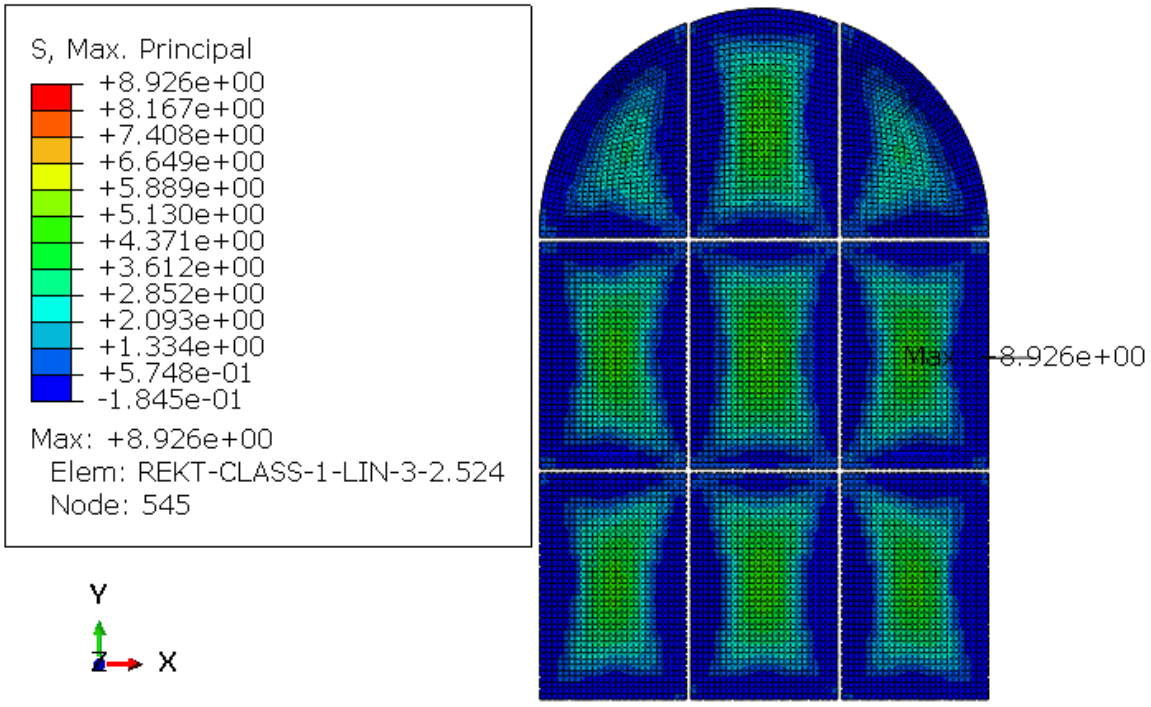

Figure 30 Maximum principal stress in the glass panes (glass, small window after renovation, front side).

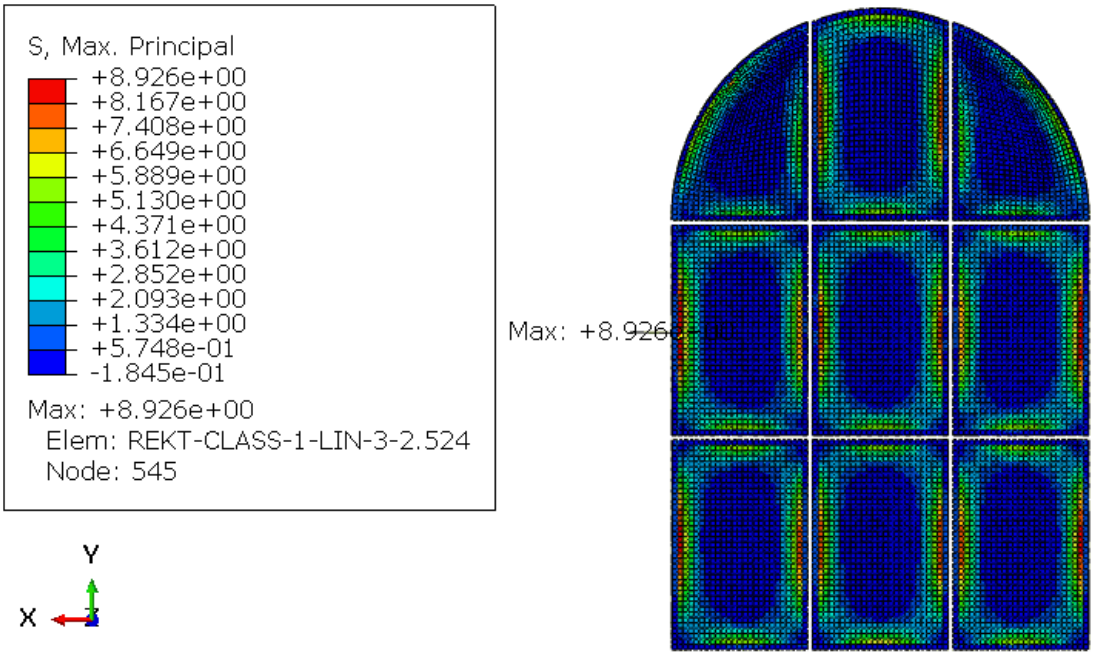

Figure 31 Definition of monitoring regions of maximum principal stress; monitored areas are highlighted in red (glass, small window after renovation, back side).

For the large window, the contour plot shows four clearly defined zones of elevated maximum principal tensile stress along the glass frame interface on both sides of the window. Two of these zones are in the upper arched region, near the junction between the curved arch and the vertical side frame members. The other two zones appear in the lower part of the window, again adjacent to the vertical frame members and close to the intermediate horizontal frame member separating the upper arched glazing from the lower panes, see Figure 32 and Figure 33. The stress distribution forms continuous edge bands rather than isolated mid-pane peaks, confirming that the highest tensile stresses develop near supported edges and frame junctions, where bending restraint and load transfer into the cast-iron frame are greatest.

The exact peak value in these red zones should be treated with caution. Stresses near connected corners/parts, and glass frame connections can be sensitive to mesh density and modelling choices, especially for the large window because it is modelled as several parts that are assembled and coupled. Such coupling and interface definitions can create local stiffness changes and may increase stress concentrations in these areas (for example, depending on how contact/tie constraints are defined and how sharp corners are represented). Therefore, the most reliable result is the repeated stress pattern (the same four interface zones), not a single maximum element value. For reporting, it is better to use these four zones as monitoring regions and extract a representative stress from a small edge/area band, instead of relying on one local peak.

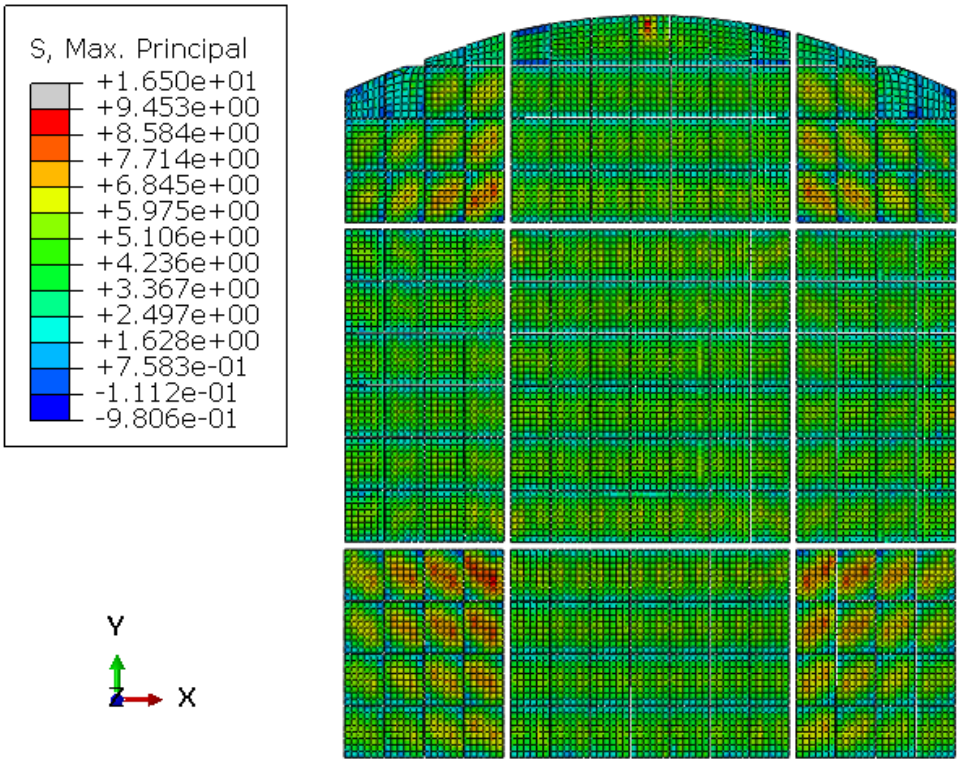

Figure 32 Definition of monitoring regions of maximum principal stress; monitored areas are highlighted in red (glass, large window after renovation, front side).

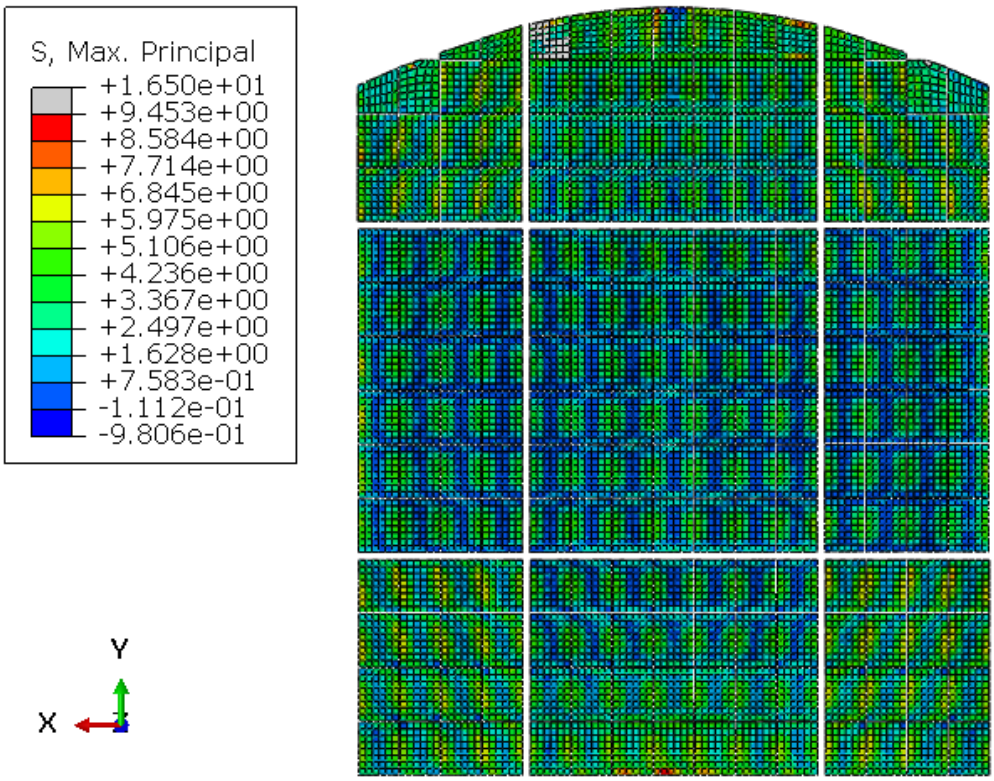

Figure 33 Definition of monitoring regions of maximum principal stress; monitored areas are highlighted in red (glass, large window after renovation, back side).

6.1.2.3 Deflection

Deflection is evaluated using the displacement magnitude U. Under wind loading, the response of the window system (glass + frame) is governed mainly by out-of-plane bending. Displacements are constrained close to supports and along frame boundaries, while the least restrained areas develop the largest out-of-plane deformation. Therefore, the critical deflection (before and after renovation) location is expected in the central, free-spanning regions of the system, where the bending curvature is highest.

Figure 34Figure 37, show the deflection monitoring location, which is defined in the central region of the system at the mid-panel area for the glass and the mid-span of the corresponding frame members so that the extracted deflection represents global.

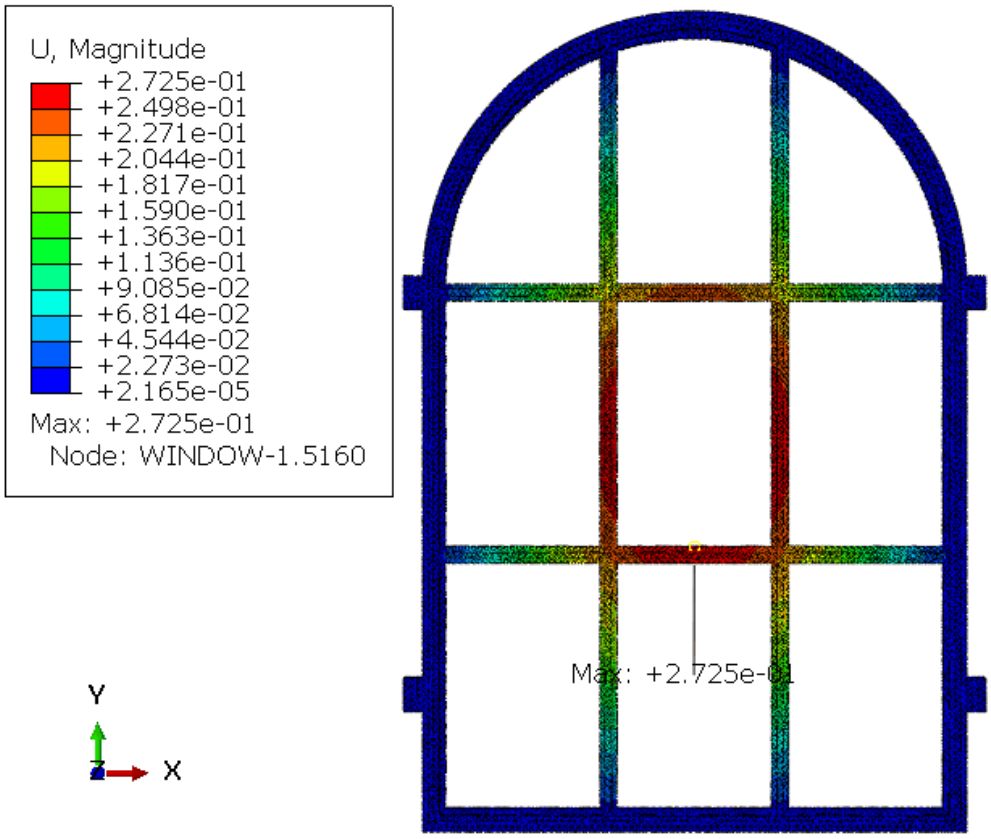

Figure 34 Deflection of the cast-iron frame in the small window. (only wind loading, cast iron frame, small window after renovation, front side).

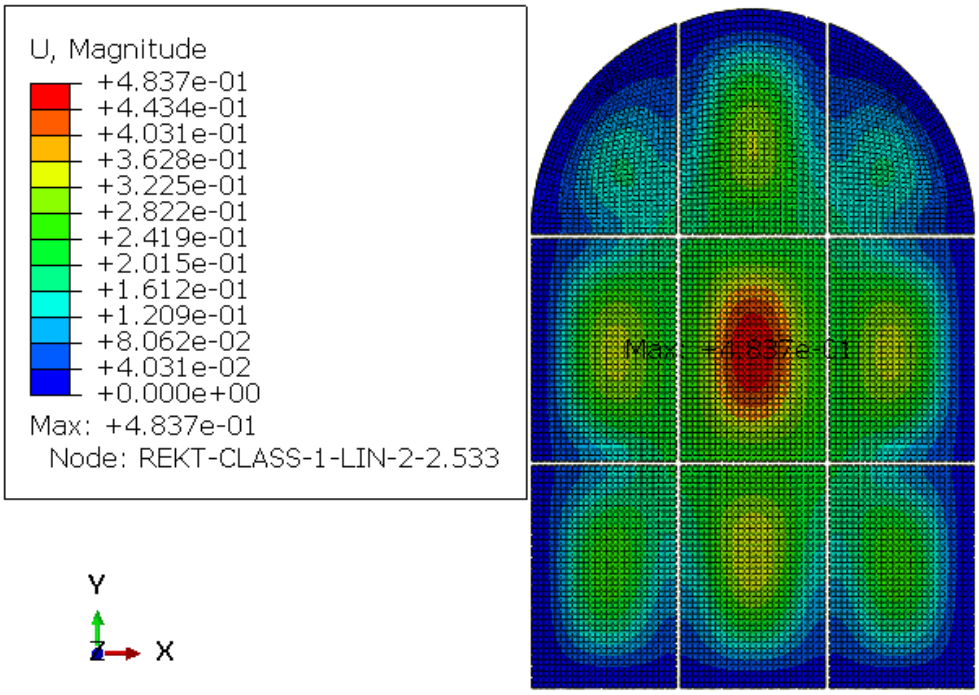

Figure 35 Deflection of the glass in the small window. (only wind loading, glass, small window after renovation, front side).

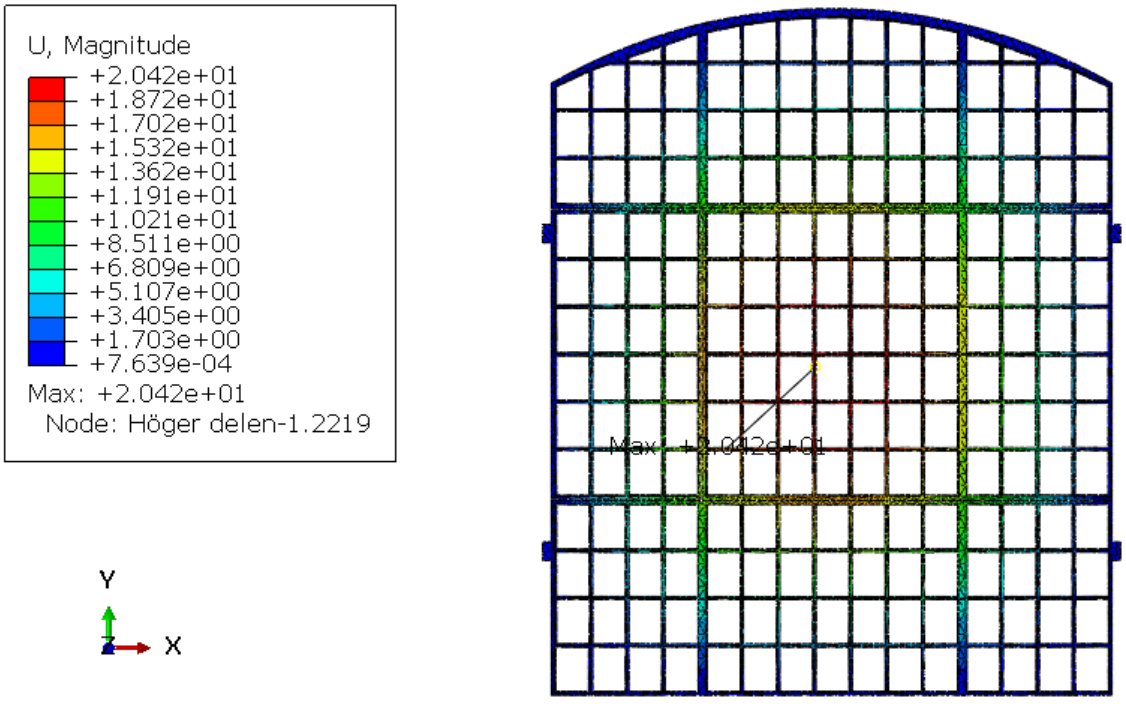

Figure 36 Deflection of the cast-iron frame in the large window. (only wind loading, cast iron frame, large window after renovation, front side).

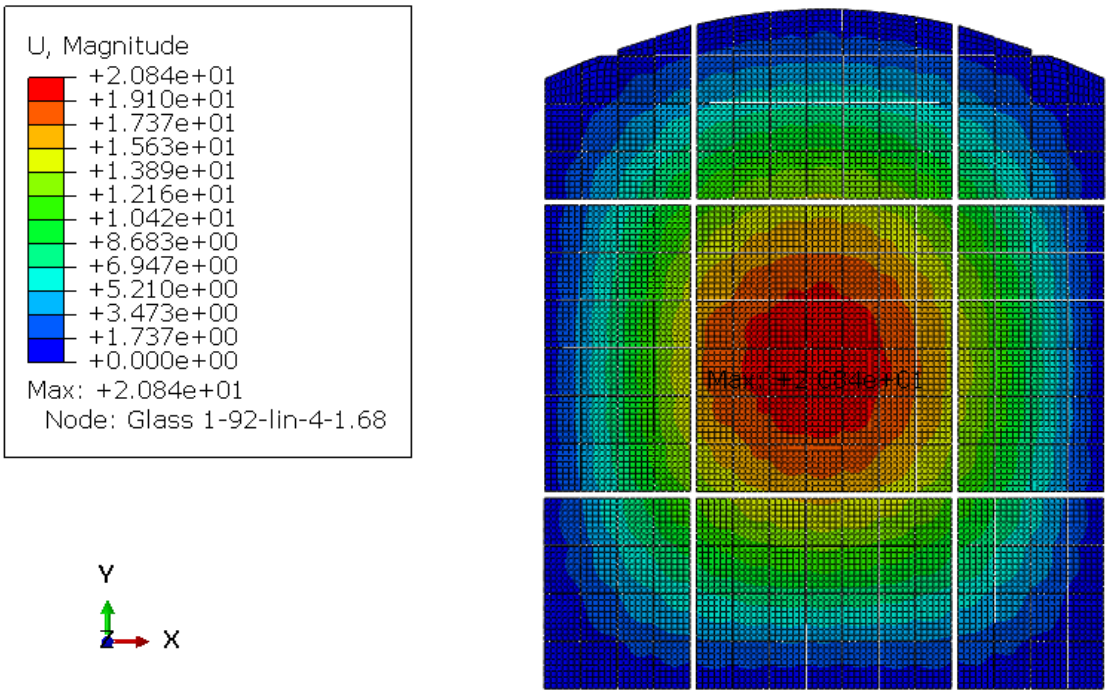

Figure 37 Deflection of the glass in the small window. (only wind loading, glass, large window after renovation, front side).

6.2 Nonlinear Response Analysis

Evaluating the response under wind pressure after renovation is important because the renovated window system may develop nonlinear system behavior at higher load levels due to geometric effects (large deflection), interaction/contact conditions, and load redistribution in the coupled glass frame assembly. A purely linear analysis assumes proportionality between load and response, which may become inaccurate once deflections are no longer small and the effective stiffness changes with deformation.

To characterize the wind-load response, a series of wind pressure levels was applied based on the values calculated in Section 5.4.2, covering the range 0.335–1.564 kN/m². Additional intermediate load levels were applied within this range to obtain a sufficiently dense set of response points. The outside temperature was kept at 20°C. Stresses were extracted from the predefined monitoring regions along the main load-transfer paths (Section 6.1.2). The corresponding stress load and deflection load relationships are presented in the figures below.

Linearity was assessed by checking proportionality between response and applied wind pressure. For a linear response, the ratio below would remain constant. In the present results, these ratios remain approximately constant at low pressures but vary at higher pressures, and the response curves show increasing curvature, indicating nonlinear system behavior at elevated wind loads.

$$\text{For stress } \frac{\sigma\ (stress)}{p\ (load)}\text{, for deflection } \frac{U\ (deflection)}{p\ (load)}$$

6.2.1.1.1 Stress distribution

For the small window, the stress–load curves remain close to linear over most of the investigated range. A mild deviation from linearity is observed at higher pressures: the representative stresses at the highest load level are approximately 8.926 MPa in the glass and 11.390 MPa in the cast iron. This is supported by a proportionality check, where the ratio σ/p remains nearly constant at lower to moderate pressures but shows a small variation near the maximum load, indicating a limited departure from strict proportionality while the overall response remains predominantly linear. Compared with the large window, the small window therefore behaves more stiffly and exhibits only minor nonlinear effects (Figures 37-40)

For the large window, both the glass and the cast iron frame show an approximately linear stress increase at lower wind pressures, followed by a more pronounced nonlinear increase beyond about 1.2 kN/m². At the highest-pressure level (~1.56 kN/m²), the representative glass principal stress reaches approximately 9.453 MPa, while the corresponding cast iron von Mises stress reaches approximately 76.560 MPa. The upward curvature indicates an increasing influence of nonlinear behavior at higher loads, consistent with a more flexible, larger-span configuration where membrane effects become more significant.

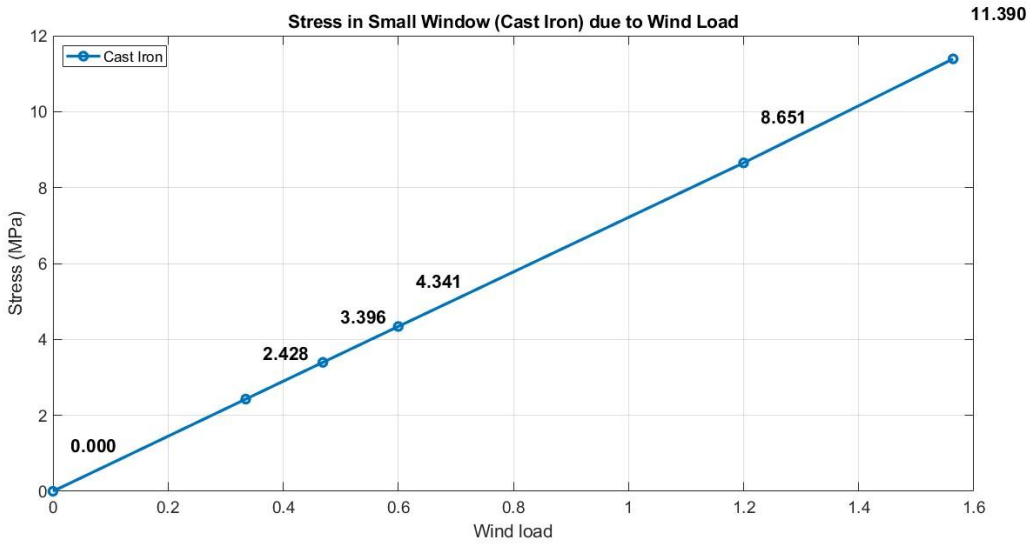

Figure 38 Stress-load curve for cast iron in small window.

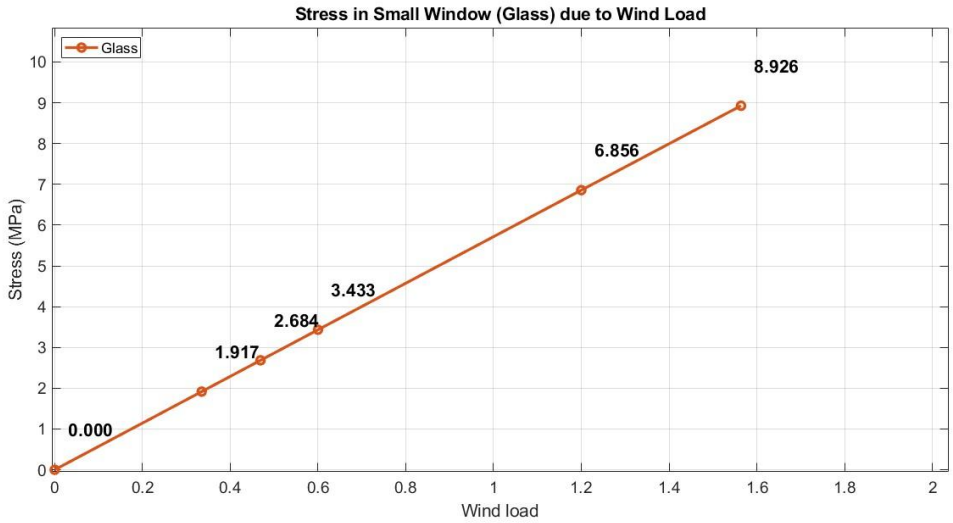

Figure 39 Stress-load curve for glass in small window.

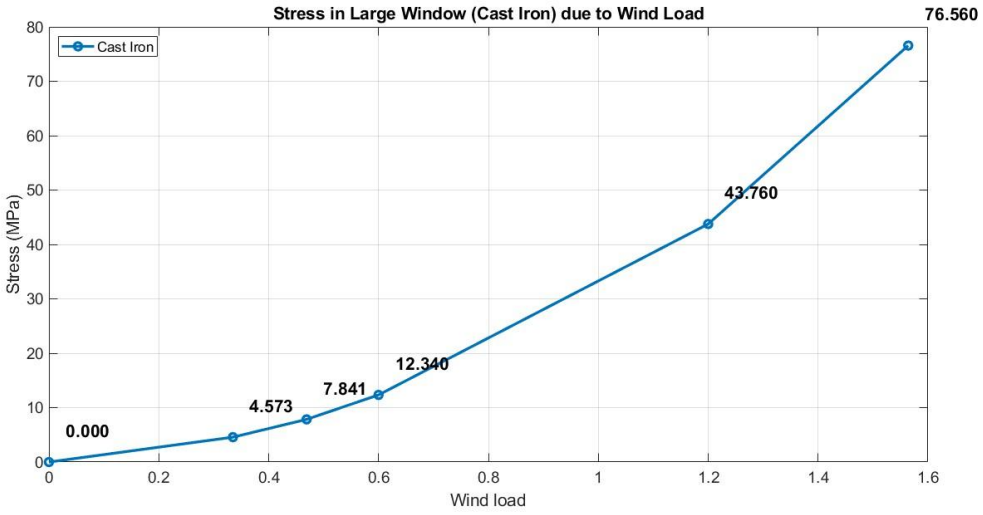

Figure 40 Stress- load curve for cast iron in large window.

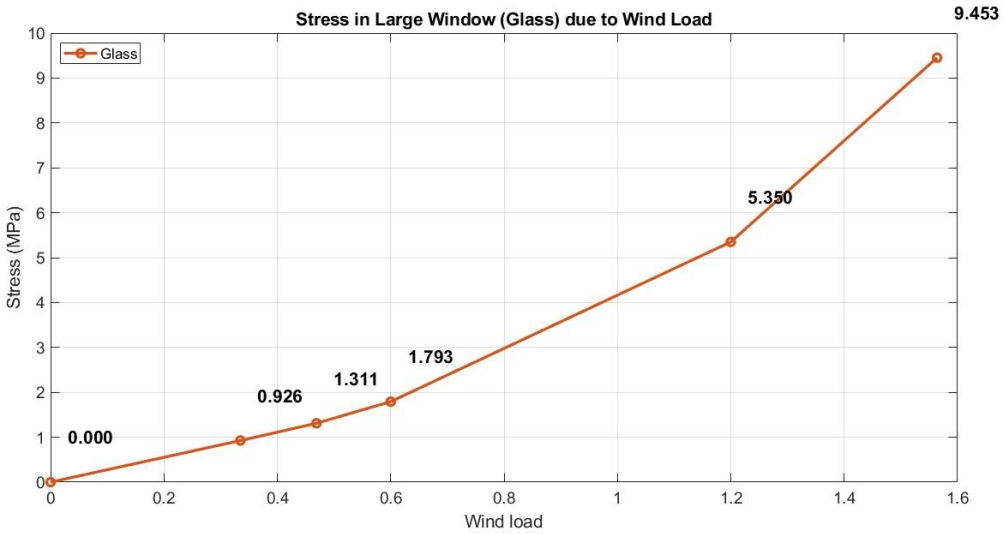

Figure 41 Stress-load curve for glass in large window.

6.2.1.1.2 Deflection

The deflection curves show a clear difference in stiffness and nonlinear response between the small and large window configurations. For the small window, deflections remain very small and the response is close to linear over most of the investigated range. At the maximum pressure level (1.56 kN/m²), the deflection reaches approximately 0.26 mm in the cast iron frame and 0.48 mm in the glass, which is consistent with an almost proportional response with only mild curvature at higher loads, see Figure 42-42.

In contrast, the large window exhibits a pronounced nonlinear deflection response. Deflection increases slowly at low wind pressures but accelerates markedly at higher pressures, reflecting increasing large-deflection effects and deformation-dependent stiffness as the system deforms and internal load sharing changes. At the maximum pressure level (1.56 kN/m²), the deflection reaches approximately 20.420 mm for the cast iron frame and 20.840 mm for the glass. The strong upward curvature beyond roughly 0.8–1.2 kN/m² indicates that large-deflection effects dominate the global response of the large window under high wind loading, see Figures 43-44.

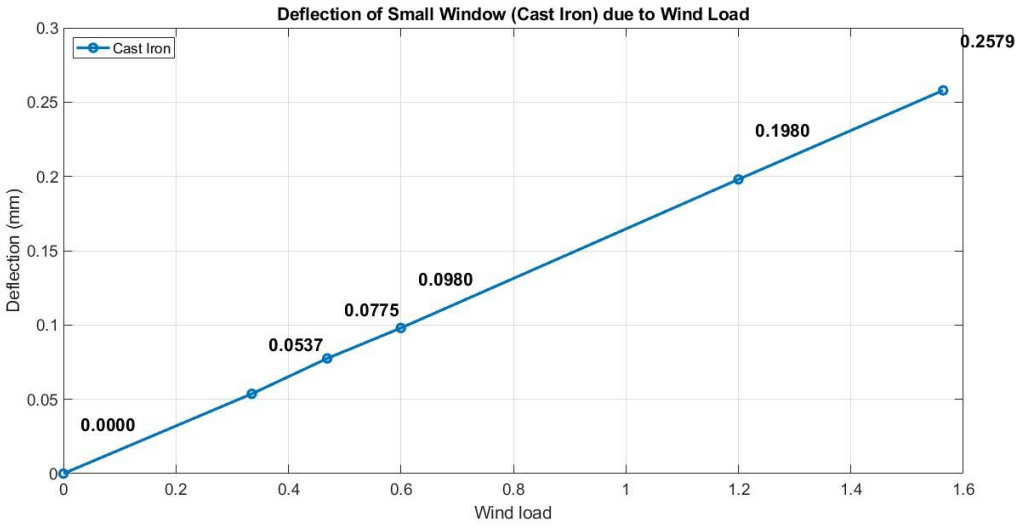

Figure 42 Deflection-load curve for cast iron in small window.

Figure 43 Deflection-load curve for glass in small window

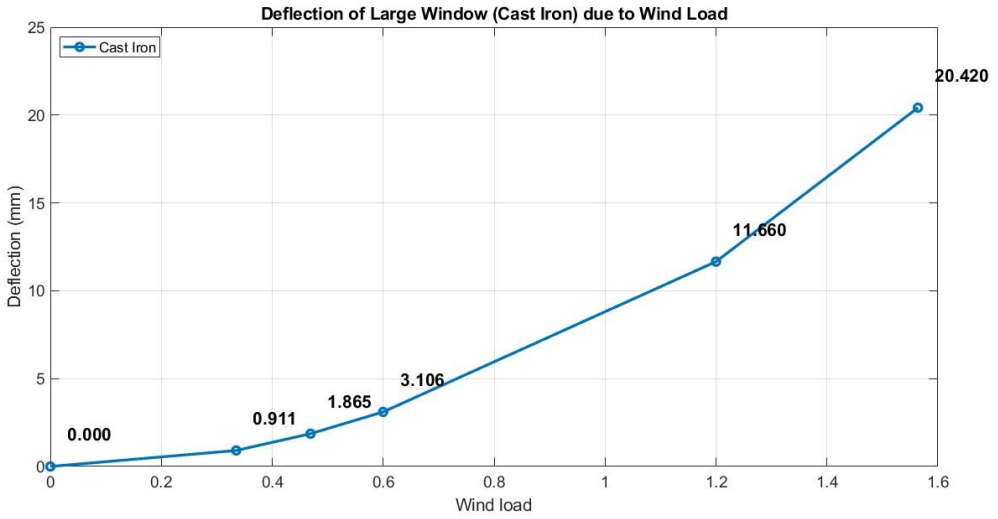

Figure 44 Deflection-load curve for cast iron in large window.

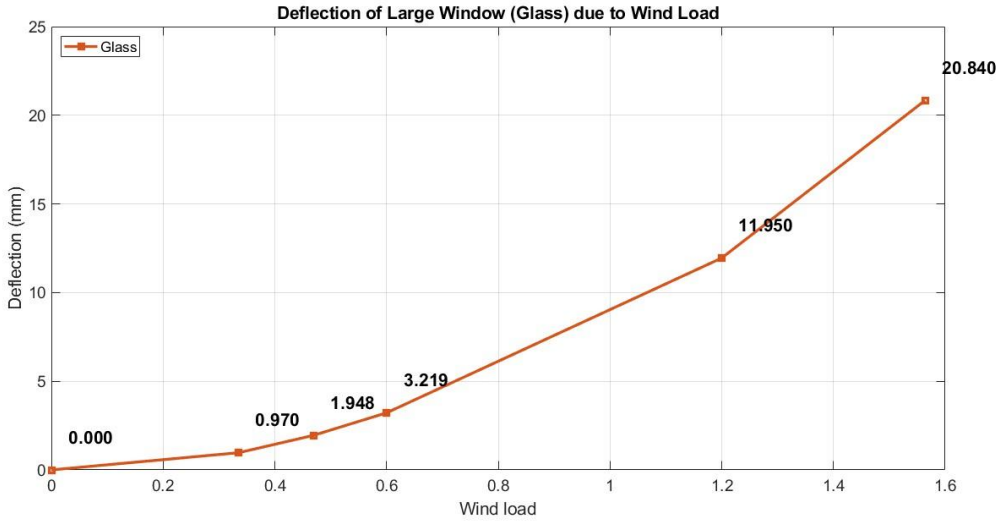

Figure 45 Deflection-load curve for glass in large window.

Overall, the results confirm that the large window is significantly more sensitive to nonlinear deformation effects than the small window, which remains comparatively stiff within the investigated wind-load range. While the absolute deflection magnitude is sensitive to support and interaction idealization, the observed trend that small window is nearly linear but large window strongly nonlinear at high pressures is robust.

6.3 Structural Response Before Renovation

The structural response of the historic windows before renovation is used as the baseline for evaluating the effect of installing the inner insulating window. In this configuration, the only external action is the design wind load (Section 5.4.5.1 and Table 3), applied in accordance with EN 1991-1-4. The purpose of the baseline is not to reproduce an observed event, but to establish a consistent reference case for later comparison of load effects.

Figure 46, summarizes the representative stress in the glass and cast iron under wind loading. The large window governs the baseline response. The representative maximum principal tensile stress in the glass reaches approximately 22.59 MPa for the large window, compared with 9.341 MPa for the small window. The corresponding representative von Mises stress in the cast-iron frame is approximately 146.72 MPa for the large window and 18.360 MPa for the small window. The baseline behavior is therefore governed by glass tensile stress, while the cast iron remains below the reference strength level 200 MPa, see section 5.3.1.

For verification, the glass stress should be compared with an adopted allowable/design resistance. A value around 18.5 MPa is associated with the assumptions used for newly manufactured float glass in Section 4.2.1.1, whereas historic glazing is expected to exhibit lower resistance due to ageing, surface flaws, and uncertainty in edge/support conditions. In this study, an allowable tensile stress of 9 MPa is adopted as a conservative screening value for subsequent assessment, corresponding to approximately 50% of the calculated strength of newly manufactured float glass and introduced to account for the uncertainty and expected strength degradation of the historic glazing.

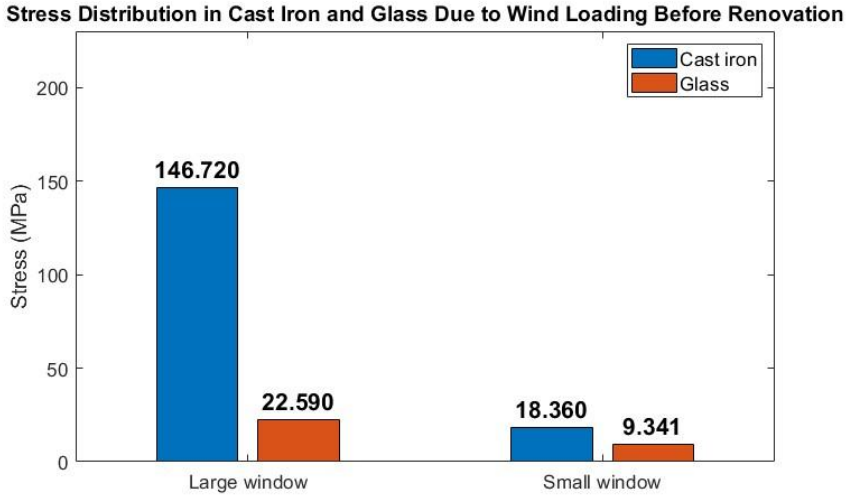

Figure 46 Stress Distribution Due to Wind Loading Before Renovation.

The deflection results show a pronounced scale effect between the two configurations (Figure 47). The small window exhibits very limited deflection, with maximum values of approximately 0.46 mm in the cast iron frame and 0.724 mm in the glass. In contrast, the large window shows substantially larger deflections, approximately 54.710 mm in the cast iron frame and 55.190 mm in the glass, see Figure 47. Global displacement is highly sensitive to the assumed boundary conditions and the restraint provided by the surrounding wall/anchorage. Since the FE model adopts simplified support, the predicted deflection should be interpreted as the response for the adopted idealized support conditions rather than as an exact in-situ deformation.

In both configurations, the glass exhibits slightly larger deflection than the cast-iron frame. This difference is not due to independent material flexibility, but rather to deformation compatibility within the coupled glass–frame system. Since the glass is connected to the surrounding frame, it follows the frame deformation while simultaneously undergoing plate bending, resulting in marginally higher displacement magnitudes in the glass.

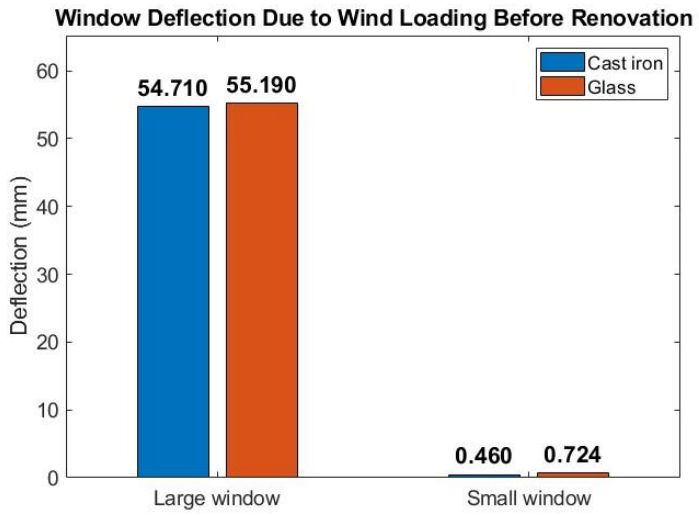

Figure 47 Window Deflection Due to Wind Loading Before Renovation.

6.4 Structural Response After Renovation

The installation of an additional inner insulating window approximately 500 mm behind the historic glazing introduces an enclosed cavity, which changes the load situation of the original window system (see Section 5.4.5.2 and Table 4). In addition to the external wind pressure acting on the outer window, the renovated assembly is subjected to cavity-pressure variations driven by temperature changes and atmospheric pressure variations, as well as relevant load combinations.

Because cavity-pressure effects depend on the modelling assumption of a sealed cavity and on the adopted reference pressure state, the results are interpreted as the response of the system for the defined cavity and boundary-condition assumptions, and comparisons are made consistently using the monitoring regions established in Section 6.1.

6.4.1 Wind load

Under wind loading after renovation, both window configurations show reduced stresses and reduced deflections compared with the pre-renovation baseline (Section 6.3). This indicates a stiffer global response of the retrofitted system. The reason for this is that due to the sealed cavity some of the wind load is transferred to the inner window.

In the case of external wind pressure, the large window shows higher stresses and deflections than the small window, both before and after renovation. This trend is consistent across materials and reflects the influence of window size on the structural response under lateral wind pressure.

6.4.1.1 Stress distribution

Figure 48 summarizes the representative stress. In the cast-iron frame, the representative von Mises stress remains non-critical under wind loading, reaching approximately 76.56 MPa in

the large window and 11.39 MPa in the small window. These levels are well below the reference strength adopted 200 MPa in section 5.3.1.

In the glass, the representative maximum principal stress reaches approximately 9.45 MPa in the large window and 8.93 MPa in the small window. Relative to the conservative screening value used for historic glass in this study (≈ 9 MPa), the small window remains close to the screening level, while the large window marginally exceeds it. This means that even though wind effects decrease after renovation, the glass still governs the wind-load case, and the glass in the large window remains the more critical configuration.

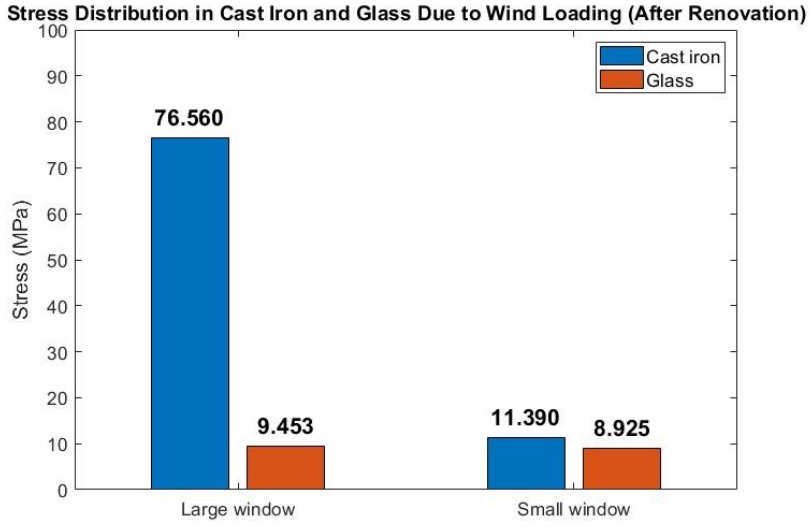

Figure 48 Stress Distribution Due to Wind loading after renovation.

6.4.1.2 Deflection

The large window remains the most flexible configuration, with peak deflections of approximately 20.42 mm in the cast-iron frame and 20.84 mm in the glass. The small window shows very limited deformation, approximately 0.258 mm in the cast iron and 0.483 mm in the glass (see Figure 49). In both window sizes, the glass shows slightly larger deflection than the cast iron frame due to deformation compatibility in the coupled system, with the glass following the frame deformation while undergoing plate bending.

Nevertheless, the qualitative findings are robust: deflection decreases after renovation, but the large window remains substantially more deformable than the small window under wind loading, which is accepted due to this larger span and simply supported boundary condition.

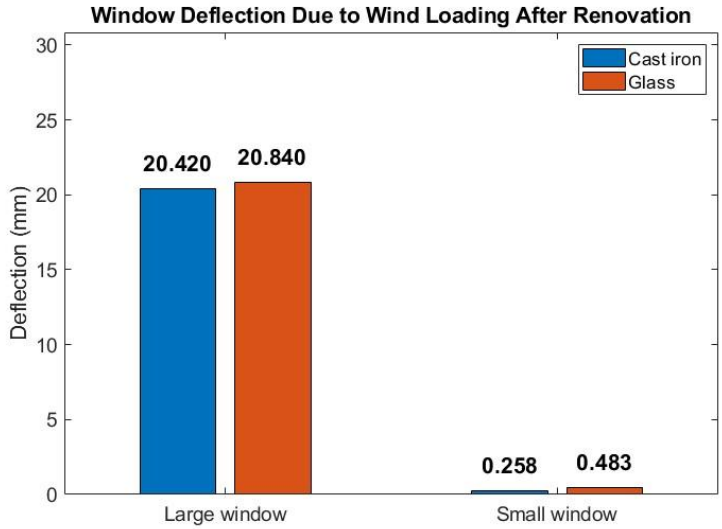

Figure 49 Window Deflection Due to Wind Loading After Renovation.

6.4.2 Thermal induced pressure

The results show a clear V-shaped response over temperature, with the structural demand approaching zero at 20 °C. This is expected because 20 °C is defined as the reference equilibrium condition in the model, where the cavity pressure equals the external atmospheric pressure and no net cavity-pressure load acts on the panes.

When the outdoor temperature deviates from 20 °C, the sealed cavity pressure departs from atmospheric. At low outdoor temperatures, cavity pressure decreases relative to ambient air, producing a pressure difference that drives the panes inward; at high outdoor temperatures, the cavity pressure increases and the pressure difference acts in the opposite direction, see section 5.4.3.1. Because the pressure magnitude scales with the temperature deviation, the highest stress and deflection occur at the temperature extremes, which explains the symmetric "V-shape". This load case is structurally important because it represents a new post-renovation mechanism: the retrofit does not merely change stiffness under wind load, it introduces an additional action (cavity-pressure loading) that can dominate the response under cold conditions.

6.4.2.1 Stress distribution

At -20 °C, the small-window glass shows higher maximum principal tensile stress within the monitoring regions than the large-window glass, approximately 58.0 MPa versus 15.5 MPa. In the cast-iron frame, von Mises stresses extracted in the monitoring regions reach approximately 108.9 MPa for the small window and 133.1 MPa for the large window, see Figure 50 and Figure 51.

For both window configurations, the extracted glass stresses exceed the conservative screening value adopted for historic glass (≈ 9 MPa). In contrast, the extracted cast-iron stresses remain below the adopted allowable (screening) stress level for cast iron (200 MPa Section 5.3.1),

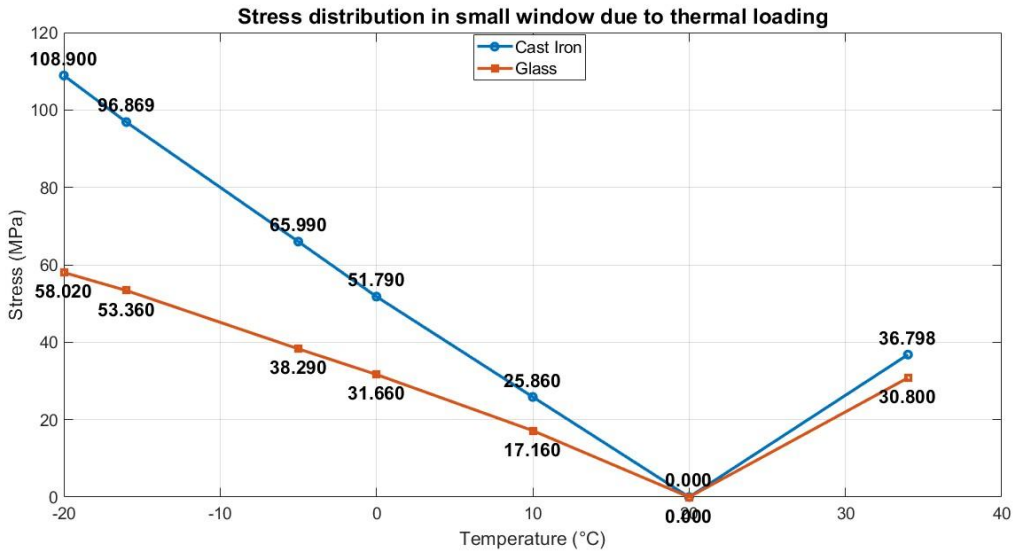

Figure 50 Stress Distribution in Small Window

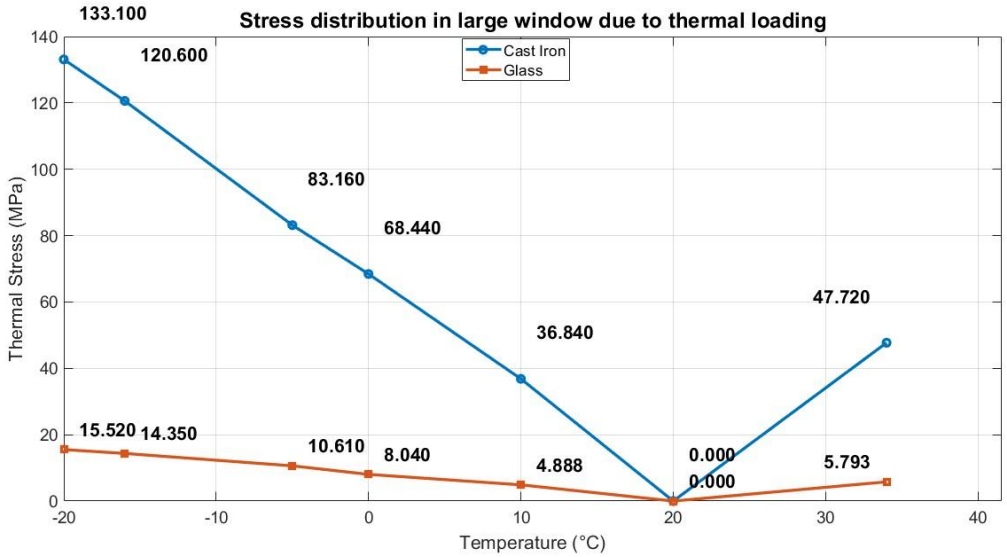

Figure 51 Stress Distribution in Large Window

6.4.2.2 Deflection

Across the full temperature range, the large window exhibits substantially larger deflections than the small window. At −20 °C, the large-window deflection reaches approximately 34.79 mm in the cast-iron frame and 36.50 mm in the glass, while at +34 °C the corresponding values are about 9.91 mm and 12.80 mm. In contrast, the small window remains comparatively stiff, with deflections of approximately 2.44 mm (cast iron) and 4.10 mm (glass) at −20 °C, decreasing further toward the reference condition, see Figure 52.

For the large window, the deflection curves of glass and cast iron remain close over the investigated temperature range, whereas a larger separation is observed for the small window. This similarity in the large-window response is consistent with a strongly coupled deformation of glazing and frame under cavity-pressure loading.

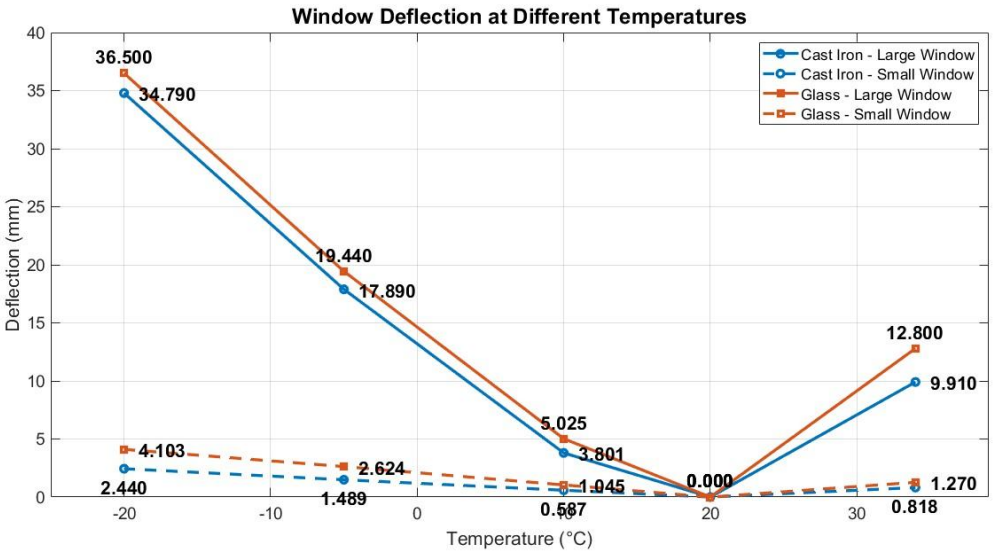

Figure 52 Window Deflection at Different Temperatures.

6.4.3 Atmospheric pressure

Figure 53 summarizes the representative stress under atmospheric pressure variation. The representative maximum principal tensile stress in the glass reaches approximately 14.62 MPa in the small window and 11.73 MPa in the large window. In both configurations, the extracted glass stresses exceed the conservative allowable stress adopted for historic glass (9 MPa). In the cast-iron frame, representative von Mises stresses within the monitoring regions are approximately 19.6 MPa for the small window and 89.7 MPa for the large window, which remain below the adopted allowable (screening) level for cast iron (200 MPa).

In terms of deformation, the large window shows substantially larger displacement magnitudes than the small window, see Figure 54. The maximum displacement magnitude reaches approximately 23.480 mm in the large-window glass and 22.940 mm in the large-window cast-iron frame, compared with approximately 0.851 mm (glass) and 0.458 mm (cast iron) in the small window.

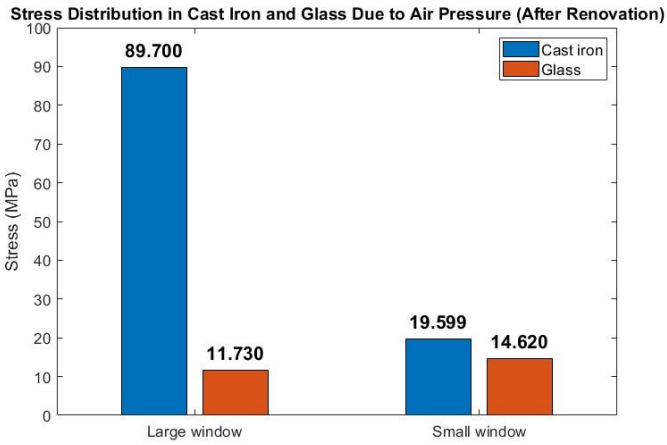

Figure 53 Stress Distribution Due to Air Pressure.

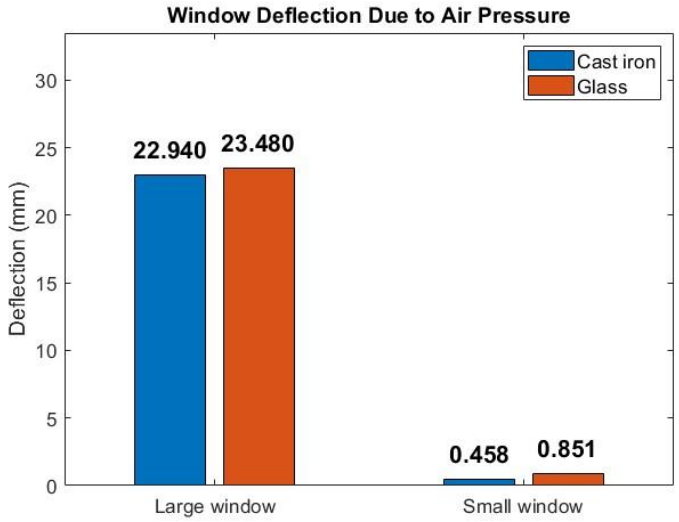

Figure 54 Window Deflection Due to Air pressure.

6.4.4 Combined load

When wind loading, atmospheric pressure variation, and thermally induced cavity pressure are applied simultaneously, the analysis is performed as a combined-load case in which all pressure components act together on the window system. The resulting net pressure on each pane depends on the combination of wind pressure, atmospheric pressure deviation, and the cavity pressure level. Accordingly, stresses and deflections are evaluated from the combined solution for each scenario, using the monitoring regions defined in Section 6.1 to ensure consistent extraction along the principal load-transfer paths.

Geometric nonlinearity is enabled (Section 5.1). Therefore, the combined-load response is evaluated directly from the nonlinear analysis results rather than by adding the single-load responses. The following subsections present the combined scenarios individually and report stresses and deflections for the glass and the cast-iron frame using the same post-processing procedure as for the single-load cases.

6.4.4.1 Wind load and thermal induce pressure

In this subsection, stresses and deflections are extracted from the predefined monitoring regions along the principal load-transfer paths (Section 6.1). The combined case includes wind pressure together with thermally induced cavity pressure arising from the sealed-cavity assumption after renovation. The cavity-pressure component is evaluated relative to the reference state at 20 °C, at this temperature the cavity-pressure contribution is zero, and the response corresponds to the wind-only case for the same wind level. For temperatures deviating from 20 °C, the cavity-pressure component increases in magnitude, and the combined response is reported as a function of temperature.

All results are presented within the modelling assumptions stated in Chapter 5 (linear elastic material behavior and idealized boundary restraint and glass–frame interaction).

6.4.4.1.1 Stress distribution

Figure 55 and Figure 56, present the representative stresses for the combined action of wind loading and thermally induced cavity pressure. For the small window, the representative maximum principal tensile stress in the glass increases from approximately 2.684 MPa at 20 °C to about 60.6 MPa at -20 °C. At the cold extreme, the extracted glass stress exceeds the conservative screening level adopted for historic glass in this study (9 MPa). In the cast-iron frame, the representative von Mises stress reaches approximately 111.9 MPa at -20 °C, remaining below the adopted allowable (reference) level for cast iron.

For the large window, the representative glass stress increases from approximately 1.311 MPa at 20 °C to about 18.12 MPa at - 20 °C. The corresponding representative von Mises stress in the cast-iron frame reaches approximately 139.6 MPa at minus 20 °C, which remains below the adopted allowable (reference) level for cast iron (200 MPa, 5.3.1.). At -20°C, the extracted glass stress also exceeds the adopted glass screening level.

Overall, the combined-load results show higher tensile glass stress in the small-window configuration than in the large-window configuration across the investigated temperature range.

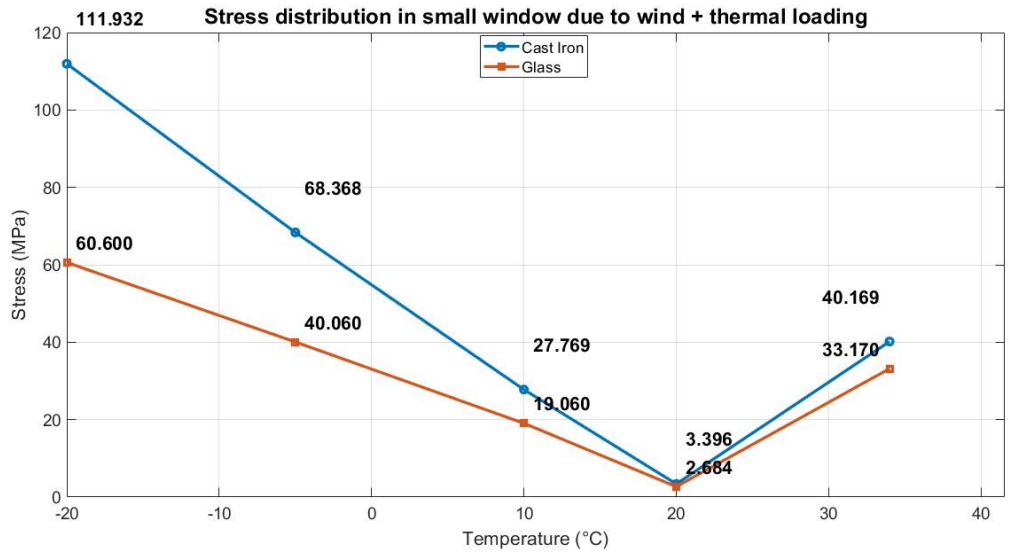

Figure 55 Stress Distribution in Small Window.

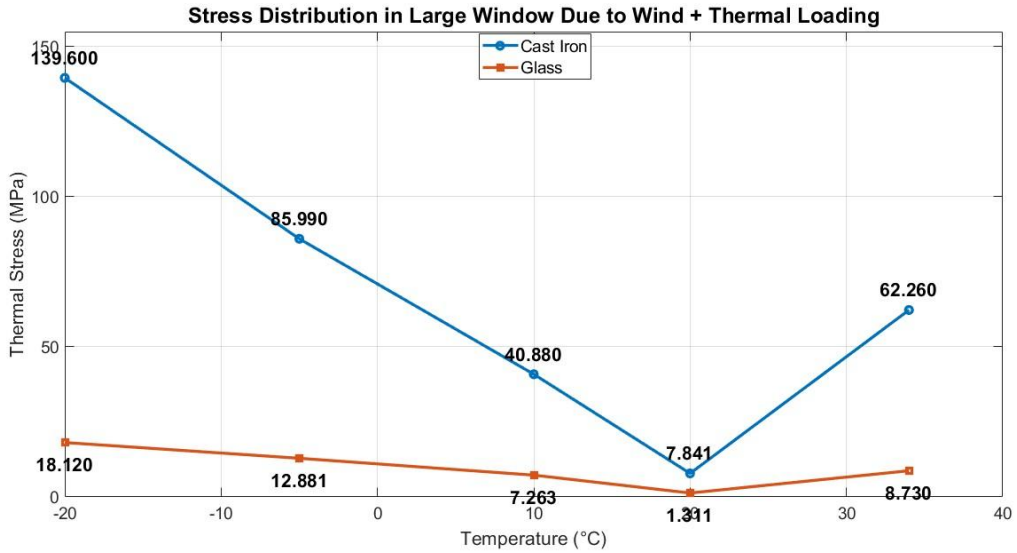

Figure 56 Stress Distribution in Large Window.

6.4.4.1.2 Deflection

Figure 57, presents the representative deflection response for the combined action of wind loading and thermally induced cavity pressure. A clear size effect is observed: the large window develops substantially larger out-of-plane displacements than the small window.

For the large window, the representative deflection reaches approximately 40.85 mm in the cast-iron frame and 41.81 mm in the glass at -20 °C. Near the reference condition (20 °C), the representative deflection is approximately 1.865-1.948 mm, increasing to about 18.63–19.80 mm at +34 °C. For the small window, the corresponding deflections remain much lower, reaching approximately 2.50 mm in the frame and 4.19 mm in the glass at -20 °C. In both configurations, the glass deflects slightly more than the cast iron. Across the investigated temperature range, the largest deflections occur at the temperature extremes, while the deflection levels are reduced to near 20 °C.

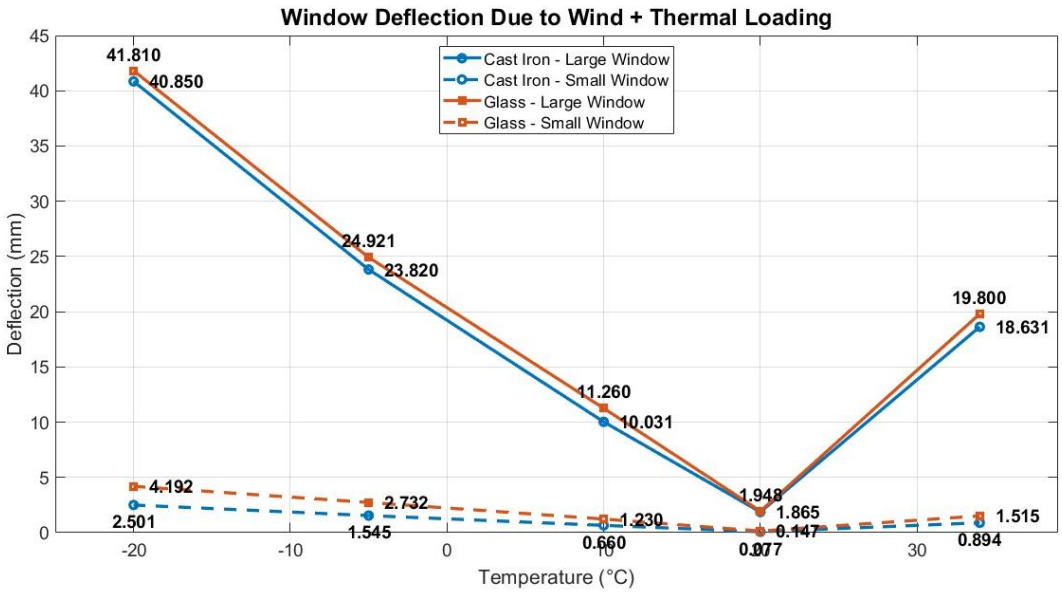

Figure 57 Window Deflection due to Wind + Thermal loading.

6.4.4.2 Wind load and air pressure

Figure 58 and Figure 59, present the response for the combined wind load and atmospheric suction case. The representative maximum principal tensile stress in the glass reaches approximately 17.11 MPa in the small window and 14.99 MPa in the large window. In both configurations, the extracted glass stresses exceed the conservative screening tensile strength adopted for historic glass in this study (9 MPa). In the cast-iron frame, the representative von Mises stress is approximately 22.39 MPa for the small window and 93.4 MPa for the large window, remaining below the adopted allowable (reference) level for cast iron (200 MPa).

The displacement response at 20 °C, reported as the displacement magnitude U, shows a clear size effect. The small window exhibits maximum displacement magnitudes of approximately 0.538 mm in the cast-iron frame and 0.965 mm in the glass. The large window exhibits substantially larger displacement magnitudes, approximately 24.550 mm in the cast-iron frame and 25.310 mm in the glass. In both window configurations, the glass displacement is slightly larger than that of the cast iron.

Overall, the results show that the small window develops higher tensile glass stress than the large window, whereas the large window develops substantially larger deflections than the small window.

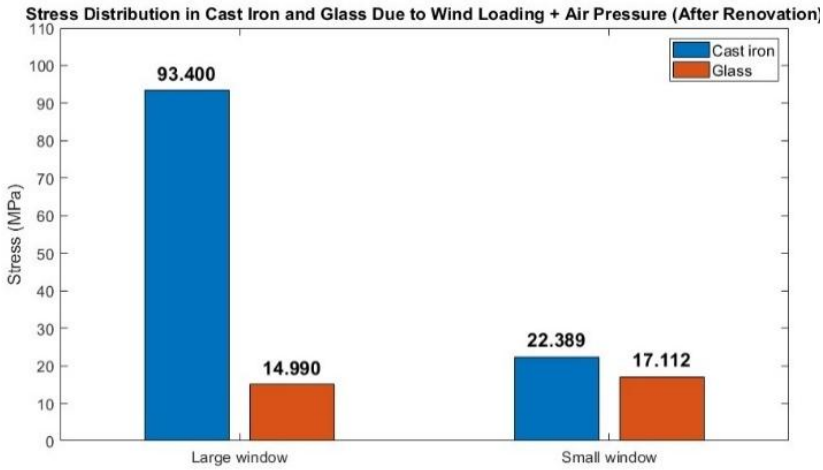

Figure 58 Stress Distribution Due to Wind + Air Pressure.

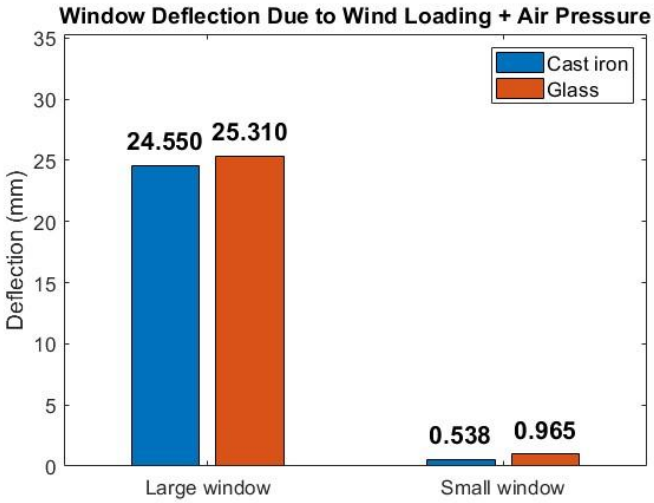

Figure 59 Window Deflection Due to Wind load + Air pressure.

6.4.4.3 Atmospheric pressure and thermal induced pressure.

This load combination superposes atmospheric pressure variation with thermally induced cavity pressure in the sealed cavity introduced by the retrofit. The response is therefore temperature-dependent: decreasing outdoor temperature amplifies the cavity-pressure component and increases demand, while at the reference condition (20 °C) the thermal contribution is minimal, see section 5.4.4.3. However, the total response does not vanish at 20 °C because the atmospheric pressure component still acts on the system. All results are interpreted within the modelling assumptions described in Chapter 5, and reported values are extracted from the predefined monitoring regions (Section 6.1).

6.4.4.3.1 Stress distribution

Figure 60 and Figure 61, show that the glass governs the response in both window sizes under this load combination. For the small window, the representative glass stress increases to approximately 69.53 MPa at −20 °C, with a minimum of about 14.620 MPa at 20 °C. For the

large window, the glass stress is lower but still exceeds the conservative screening level adopted for historic glass (≈ 9 MPa) even at the reference temperature, reaching about 31.110 MPa at −20 °C and about 11.73 MPa at 20 °C.

For the cast-iron frame, stresses remain below the reference strength adopted in Chapter 4, but the large window approaches the limit at low temperature: the representative von Mises stress reaches approximately 196.5 MPa at −20 °C, close to the assumed 200 MPa reference. The small window frame remains clearly lower, reaching about 131.8 MPa at −20 °C.

Overall, the tensile glass stress is higher in the small-window configuration than in the large-window configuration, and the extracted glass stresses exceed the adopted screening limit in both cases.

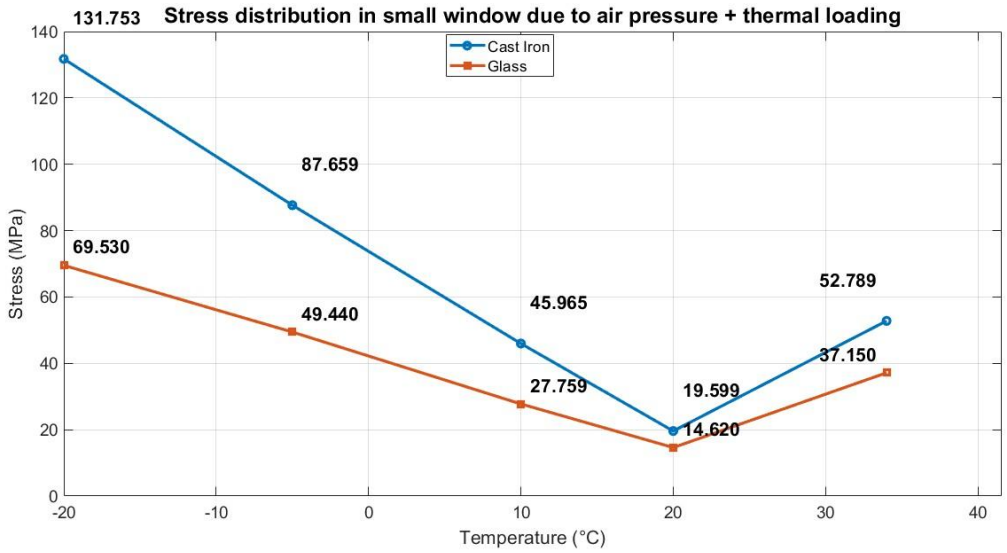

Figure 60 Stress distribution in small window.

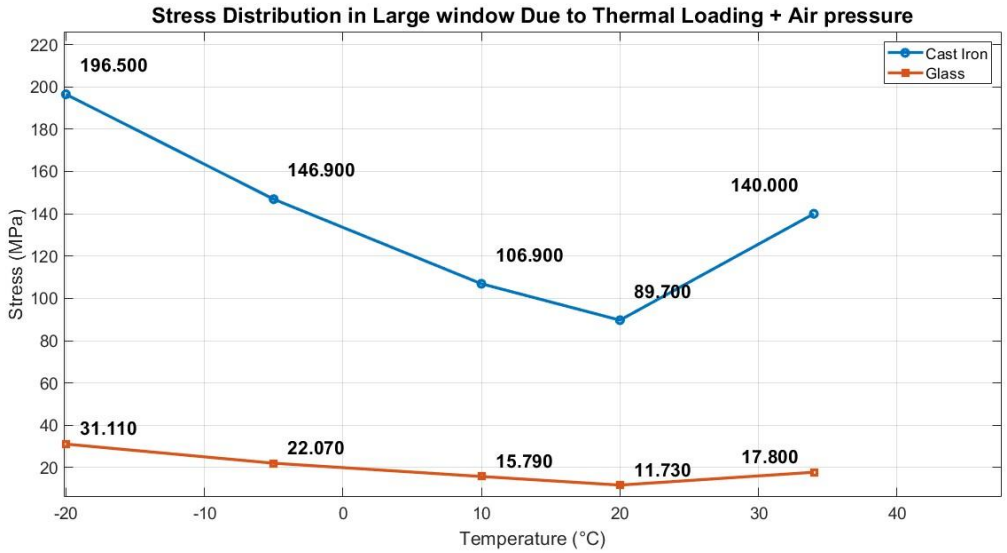

Figure 61 Stress distribution in large window.

6.4.4.3.2 Deflection

Figure 62, shows that the deflection response is strongly dependent on window size. The large window exhibits large out-of-plane displacements across the investigated temperature range, with representative maximum deflections of approximately 22.940 mm in the cast-iron frame and 23.480 mm in the glass at 20 °C, increasing to about 53.60 mm and 54.60 mm, respectively, at −20 °C. The deflection curves for glass and cast iron remain close to each other for the large window.

In contrast, the small window remains comparatively stiff. At 20 °C, the representative deflection is approximately 0.458 mm in the frame and 0.851 mm in the glass, increasing toward the cold case to approximately 2.896 mm and 4.840 mm, respectively, at −20 °C.

Overall, the large-window configuration exhibits substantially larger deflections than the small-window configuration across the investigated temperature range.

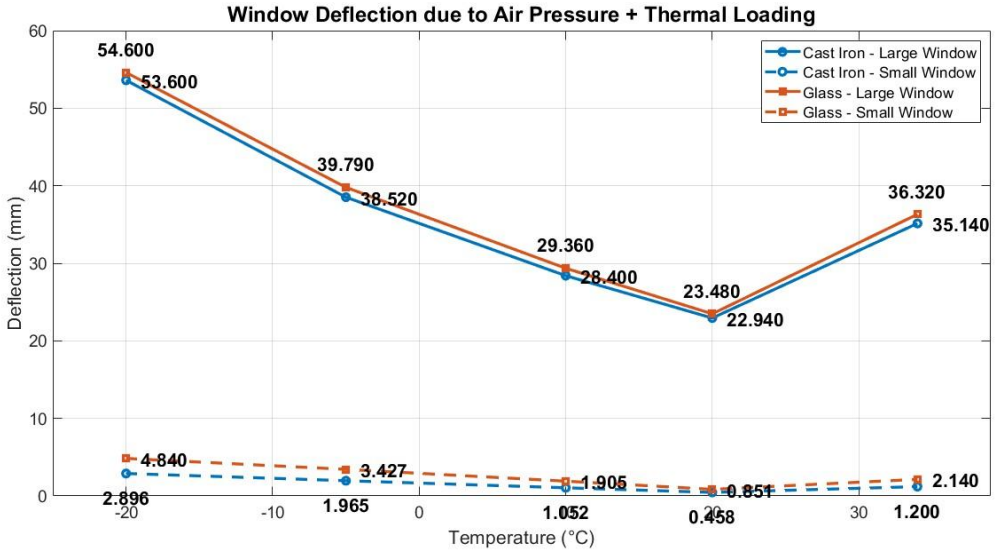

Figure 62 Window deflection due to Air pressure + Thermal Loading.

6.4.4.4 Thermal induced pressure, wind force and atmospheric pressure.

This section considers the combined action of wind pressure/suction, atmospheric pressure variation (±30 hPa), and temperature-driven cavity pressure in the sealed gap introduced by the retrofit. The response is strongly temperature-dependent because the thermal component changes magnitude (and direction) with outdoor temperature, while wind and atmospheric actions act as externally applied pressure effects.

6.4.4.4.1 Stress distribution

Figure 63 and Figure 64 present the representative stresses for this combined load case across the investigated temperatures. For both window configurations, the extracted maximum principal tensile stress in the glass exceeds the conservative screening level adopted for historic glass (≈ 9 MPa). In the small window, the representative glass stress reaches approximately 70.78 MPa at −20 °C and is approximately 17.11 MPa at 20 °C. In the large window, the corresponding glass stresses are lower but still above the screening level, reaching approximately 32.57 MPa at −20 °C and 14.99 MPa at 20 °C.

For the cast-iron frame, the representative von Mises stress in the large window reaches approximately 203.50 MPa at −20 °C, close to the adopted reference level of about 200 MPa. In the small window, the cast-iron stress remains lower, with a maximum representative value of approximately 133.98 MPa at −20 °C.

Overall, the extracted tensile glass stresses are higher in the small-window configuration than in the large-window configuration, while the highest cast-iron stresses occur in the large window at the cold extreme, and at cold temperature the cast iron exceeds adopted reference level.

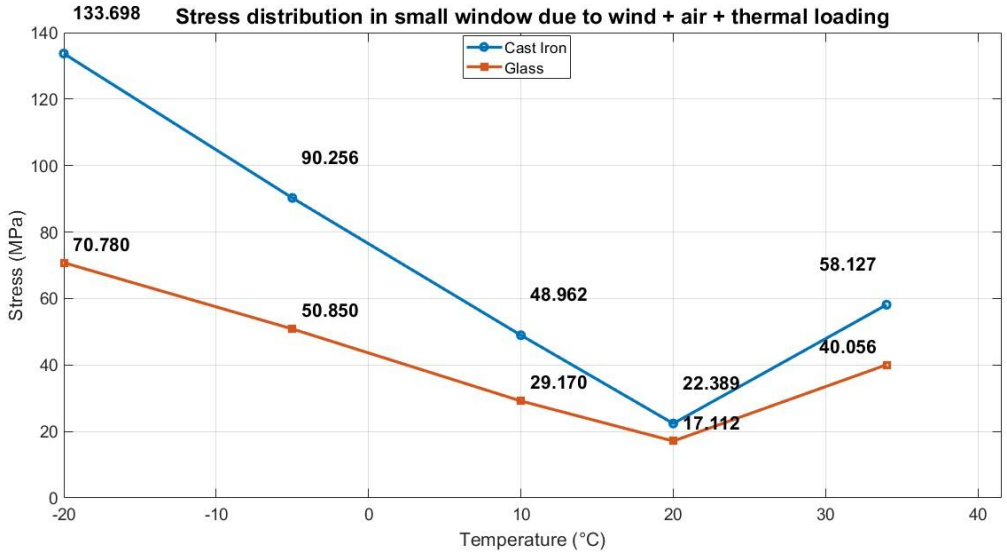

Figure 63 Stress Distribution in Small Window.

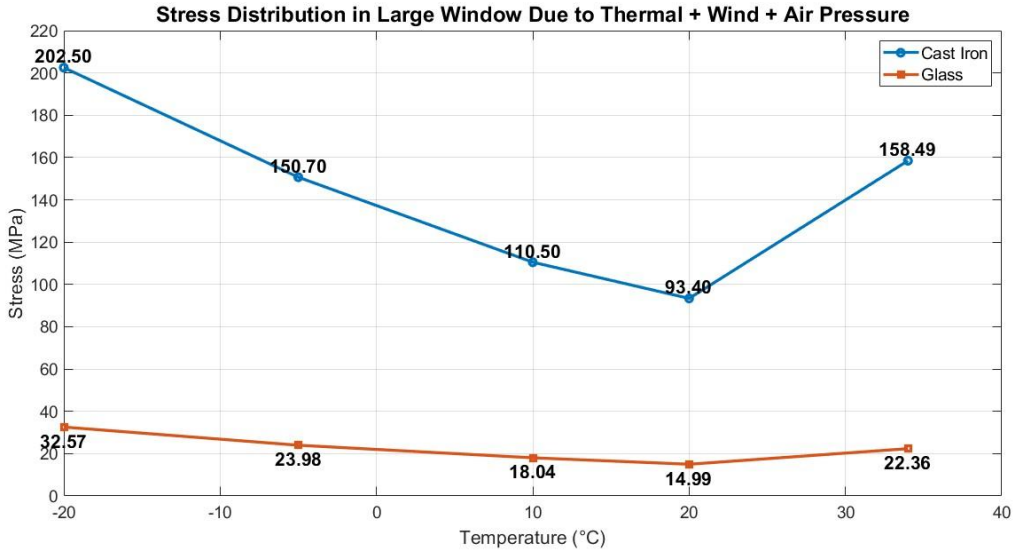

Figure 64 Stress distribution in large window.

6.4.4.4.2 Deflection

Figure 65, shows a pronounced size effect in the deflection response. The large window exhibits substantially larger out-of-plane displacements than the small window across the investigated temperatures. For the large window, the representative deflections in glass and cast iron remain close to each other, reaching approximately 57.48–58.96 mm at −20 °C, reducing to about 24.55-25.318 mm at 20 °C, and increasing again to approximately 41.74–42.45 mm at 35 °C.

In contrast, the small window remains comparatively stiff. The representative glass deflection ranges from approximately 4.92 mm at −20 °C to 0.965 mm at 20 °C and 2.210 mm at 34 °C. The corresponding cast-iron deflection ranges from approximately 2.953 mm at −20 °C to 0.538 mm at 20 °C and 0.9405 mm at +34 °C.

Overall, the large-window configuration exhibits substantially larger deflections than the small-window configuration across the investigated temperature range.

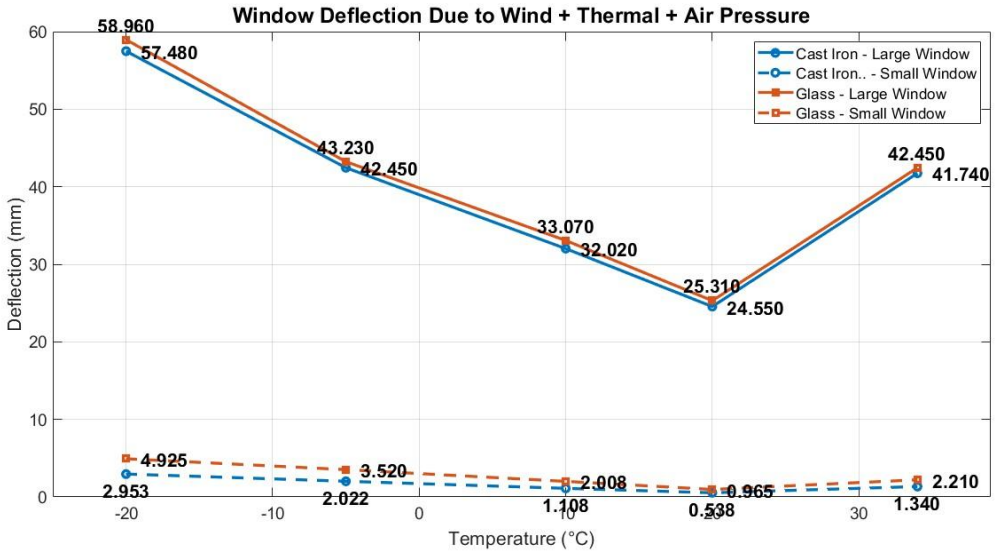

Figure 65 Window deflection due to wind +thermal+ air pressure.

6.5 Thermal Effects on Structural Deformation

This section synthesizes the results presented in Sections 6.2–6.4 and highlights the main temperature-dependent trends; no new numerical results are introduced. The section describes how representative stresses and deflections in the historic window system vary with temperature for the investigated load scenarios and compares the response of the small and large window configurations. The absolute magnitudes are influenced by the modelling assumptions in section 5.1 (the sealed-cavity condition, the idealized boundary restraint and connections). The trends are therefore used primarily for comparative evaluation across window sizes and load combinations.

Across the scenarios investigated, the response curves show a consistent V-shaped temperature dependence, with minimum response at the reference condition of 20 °C. The most severe stress and deflection levels occur at −20 °C, whereas the corresponding values at +34 °C are generally lower. Although the temperature-driven cavity-pressure contribution

vanishes at 20 °C, several pressure-related scenarios still produce representative glass tensile stresses above the adopted conservative screening value at this temperature. This demonstrates that temperature effects reduce demand relative to the extreme cold case, but they do not necessarily eliminate glass exceedance when atmospheric pressure variation and cavity-pressure mechanisms are included.

The results show four main response bands depending on whether atmospheric pressure variation is included. Load cases without atmospheric pressure (T and W+T) cluster at the lower response level, whereas load cases including atmospheric pressure (P+T and P+W+T) form a higher response band. This separation is observed for both window configurations and reflects the additional uniform pressure component introduced by atmospheric pressure variation.

At 20 °C, the temperature-dependent cavity-pressure contribution is zero, and the combined cases reduce to their corresponding mechanical-only cases. Accordingly, P+T at 20 °C coincides with the P-only case, and P+W+T at 20 °C coincides with the P+W case. The W+T case at 20 °C is not directly comparable to the wind-only case in this study, since the wind magnitude differs between the wind-only and combined load definitions (Section 5.4.5).

Stresses in the frame and glass follow the same overall temperature-dependent trend, but their relative levels depend on load case and window size. The large-window configuration shows greater separation between curves and larger overall deflections than the small window, particularly at temperature extremes. The small window exhibits a more consistent response over the range investigated.

In the large-window configuration, the temperature–response curves deviate more from an idealized linear trend than in the small-window configuration, as evidenced by the less uniform V-shape and the increased separation between load-case combinations at higher response levels. This behavior is consistent with the fact that the large window develops substantially larger out-of-plane displacements, for which geometric nonlinearity becomes more influential. Since NLGEOM is enabled in the analyses (Section 6.1.3), the reported response reflects the nonlinear equilibrium solution in the deformed configuration rather than a linear scaling with load. By contrast, the small-window response remains closer to linear over the investigated temperature range, with more regular curve shapes and smaller deviations between load combinations.

6.5.1 Cast iron

6.5.1.1 Stress

The large-window configuration exhibits higher representative von Mises stresses in the cast-iron frame than the small-window configuration across the investigated temperature range and load combinations (Figure 66 and Figure 67). The difference is most pronounced at low temperature: at −20 °C the large window reaches approximately 202 MPa in the most severe combined case, compared with approximately 134 MPa for the corresponding small-window case. At the reference temperature (20 °C), stress levels are substantially lower in both windows; however, the large window still shows a higher stress range than the small window. At +34 °C, the large window again reaches higher cast-iron stress levels than the small window. Overall, within the investigated range, the large window represents the critical configuration with respect to cast-iron stress demand.

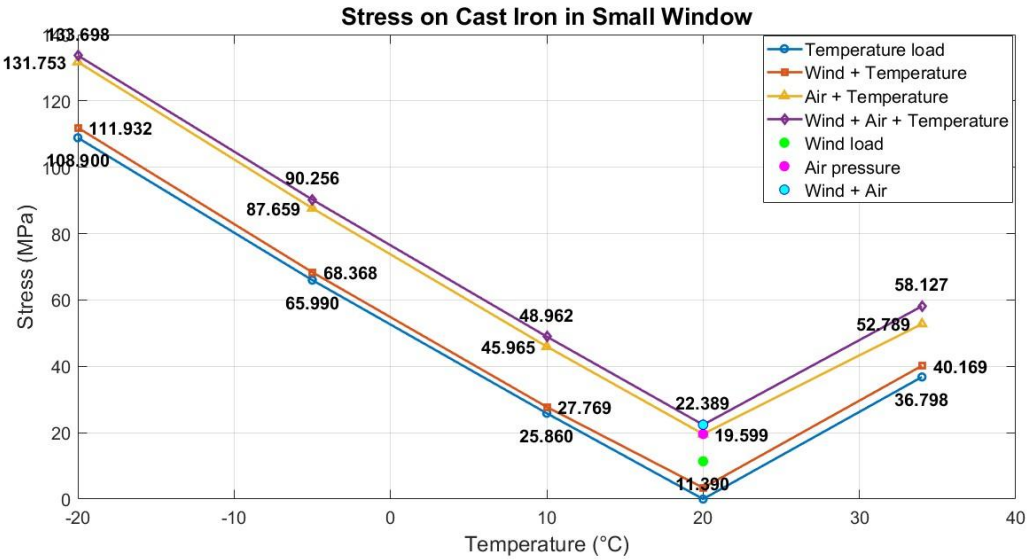

Figure 66 Stress on cast iron in the small window in different load cases.

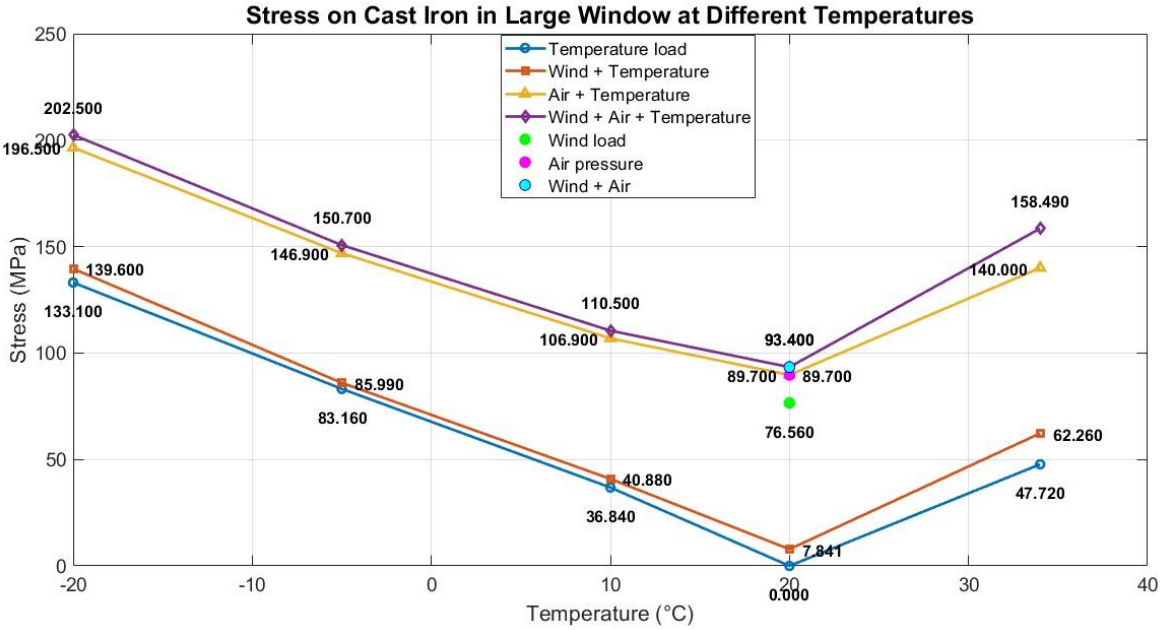

Figure 67 Stress on cast iron in the large window in different load cases.

6.5.1.2 Deflection

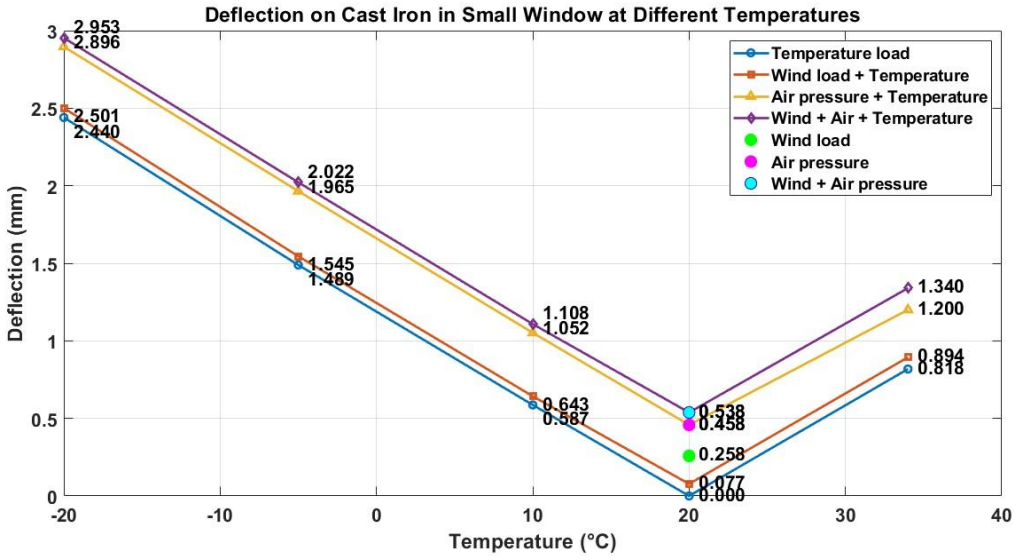

Figure 68 and Figure 69, show that the cast-iron frame in the large-window configuration exhibits substantially larger deflections than the small window configuration across the investigated load cases. The deflection varies with temperature and follows the same overall temperature-dependent pattern as observed for the other response measures, with minimum values near the reference temperature (20 °C) and increasing deflection as the temperature deviates from this condition. Across the investigated range, the large window therefore represents the critical configuration with respect to cast-iron deflection demand.

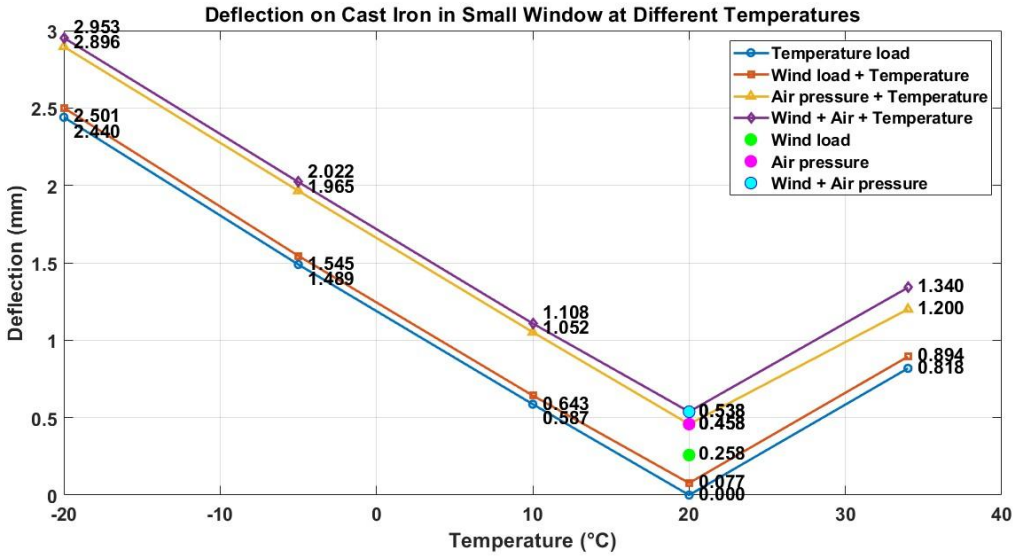

Figure 68 Deflection on cast iron in small window at different temperatures.

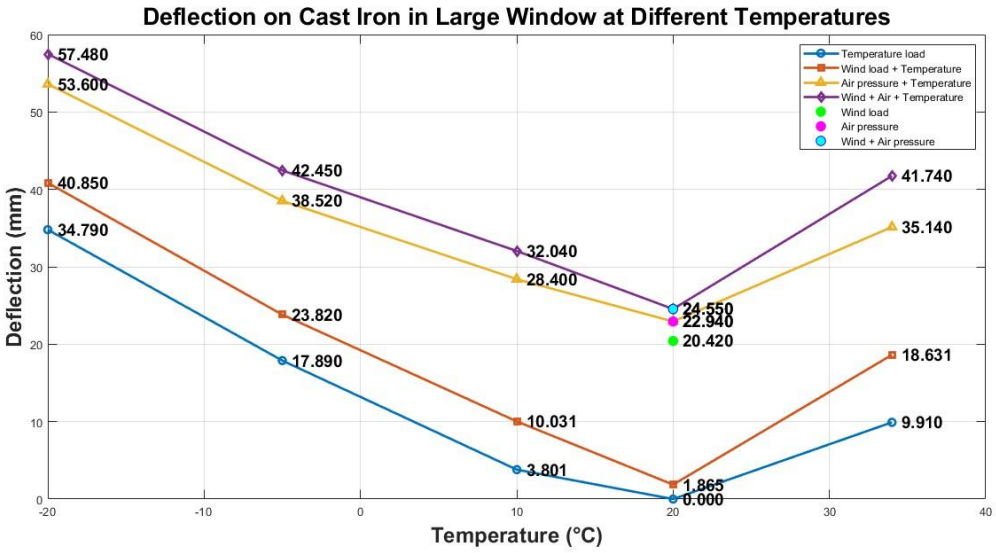

Figure 69 Deflection on cast iron in large window at different temperatures.

6.5.2 Glass

6.5.2.1 Stress distribution

In contrast to the stress response, the glass shows a different effect. The stress distribution plots indicate that the small window generally develops higher tensile stresses in the glass than the large window for the investigated load cases. This trend is consistent with a more restrained configuration, where pressure-related actions can produce higher local bending and stress concentrations, particularly near the supported edges and corners.

Figure 70 and Figure 71 further show that the critical glass stresses occur in similar regions for the different load cases, and that the highest stress levels are associated with the combined pressure-related scenarios at low outdoor temperatures. Overall, the stress distributions indicate that the small window governs the glass stress demand. When compared with the adopted reference value for glass strength 9 MPa, the calculated stresses exceed this level in both windows for several load cases.

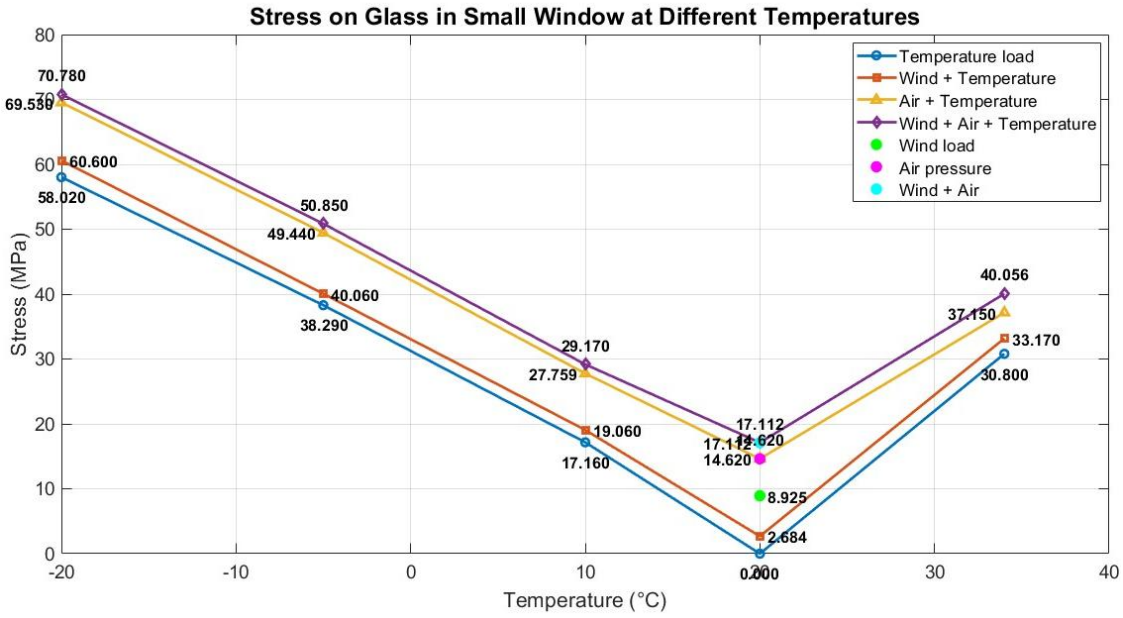

Figure 70 Stress on glass in the small window in different load case.

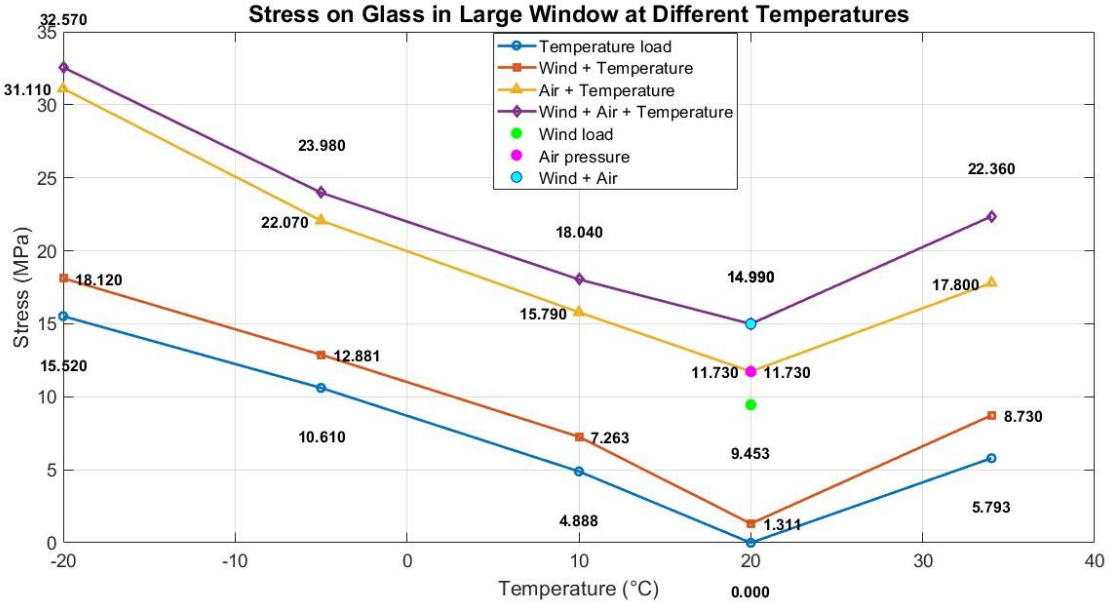

Figure 71 Stress on glass in the large window in different load case.

6.5.2.2 Deflection

The large-window configuration exhibits substantially larger out-of-plane deflections than the small-window configuration across the investigated load cases, see Figure 72 and Figure 73. For the large window, the representative maximum deflection reaches approximately 58.96 mm at −20 °C in the most severe combined cold case. In comparison, the small window shows markedly lower deflections, with a maximum representative value of approximately 4.93 mm in the worst case at −20 °C.

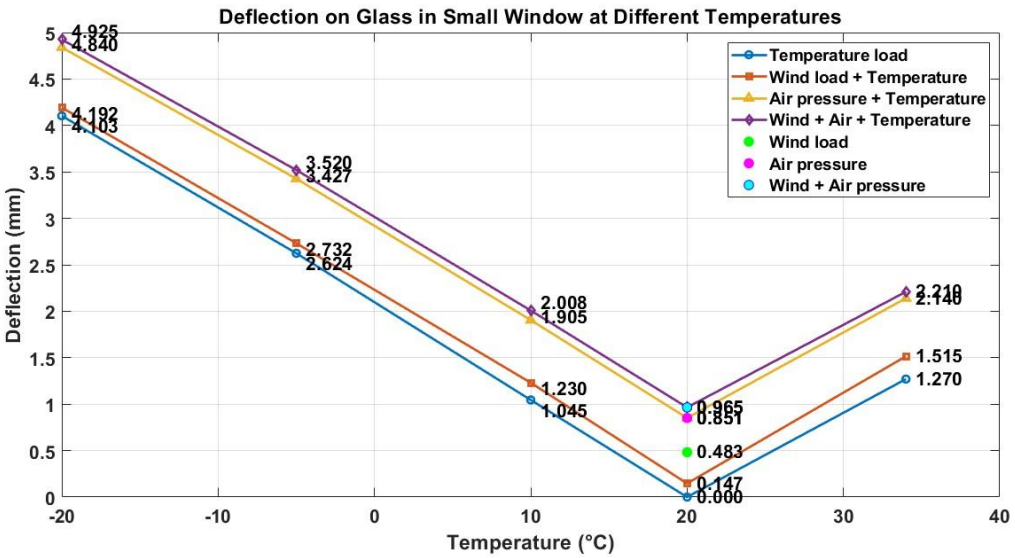

Figure 72 Deflection on glass in small window at different temperatures.

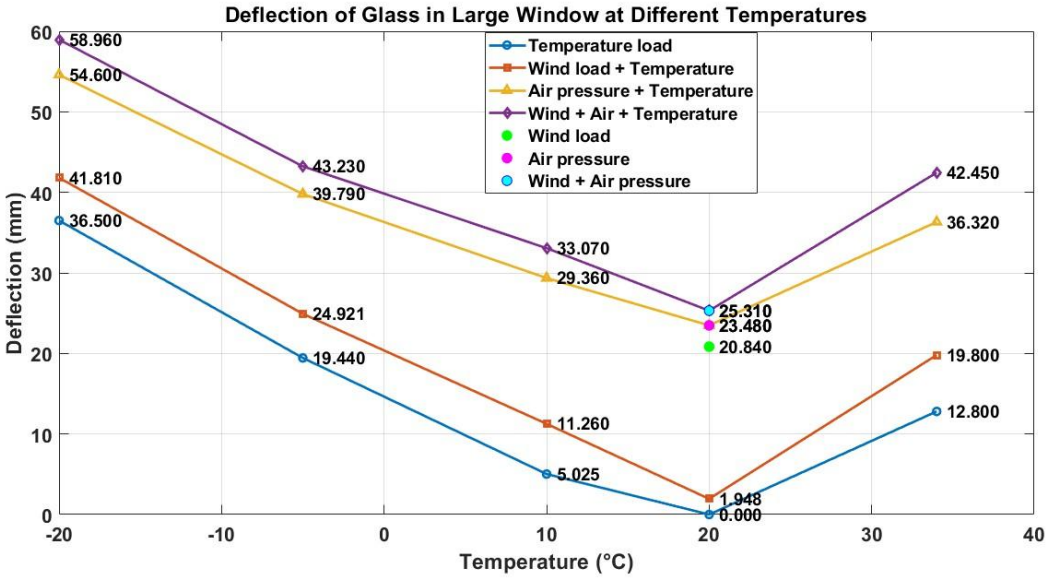

Figure 73 Deflection on glass in large window at different temperatures.

7 Discussion

The aim of this thesis was to investigate whether the historic cast-iron framed windows in the Machine and Assembly Hall can withstand the altered loading conditions introduced by the renovation, where a new insulating inner window was installed 500 mm inside the original. The results presented in Chapter 6 provide detailed insight into how stress and deflections develop under different load combinations. This discussion interprets those results in relation to the research questions, the broader context of heritage preservation and energy-efficiency retrofitting, and the methodological limitations of the numerical approach.

7.1 Change in Loading Conditions

Before renovation, the historic window behaves as a relatively open structural system. Wind acting on a single pane is the critical external action, and the response is primarily controlled by glass plate bending with load transfer into the cast-iron frame. Structural behavior is therefore dominated by one main load type and one main response mechanism.

After renovation, the behavior depends on which mechanism is activated. For loading due to wind pressure only, the numerical results show reduced wind-driven deflections and reduced stress levels compared with the pre-renovation configuration. This points to a stiffer global response in the wind-driven mechanism, which can be explained by an altered load-transfer path: the added inner window and the cavity configuration provide additional restraint and reduce global flexibility under lateral pressure. Under this wind-driven condition, the large window continues to exhibit higher stresses and deflections than the small window both before and after renovation, consistent with span effects in plate and frame bending under distributed pressure.

The renovation introduces a fundamentally different loading situation by creating a double-window system with a cavity between the panes. Under the modelling assumption of a sealed cavity, additional pressure-related actions become structurally relevant. Temperature variations generate thermally induced cavity pressure, while atmospheric pressure changes create further pressure differences across the panes. Since these actions act uniformly over the full pane area, they may reach magnitudes comparable to, and in certain scenarios exceeding, the wind pressure. Consequently, pressure driven effects can govern the structural response of the historic window system after renovation

Across the investigated scenarios, the response curves exhibit a V-shaped temperature dependence with a minimum near 20 °C, which corresponds to the defined reference state for the cavity. As the temperature moves away from 20 °C toward both −20 °C and +34 °C, the thermally induced cavity-pressure component increases in magnitude, and the stress and deflection response increases accordingly. The cold extreme (−20 °C) produces the highest response levels, while the warm extreme (+34 °C) generally results in lower demand than the cold case but higher demand than near the reference condition. It is also important to distinguish between temperature-driven and pressure-driven actions: at 20 °C the temperature-driven cavity-pressure component is zero, but load cases that include atmospheric pressure variation can still generate non-negligible glass stress. Glass stress exceedance relative to the adopted screening value is therefore primarily associated with pressure-related scenarios and

may occur even near the reference temperature depending on whether atmospheric pressure variation is included.

The cavity-pressure mechanism is particularly influential under cold outdoor conditions. When the outdoor temperature drops below the reference condition, the air in a sealed cavity contract, producing a pressure difference relative to the surrounding air and inducing inward pressure on the panes. This increases tensile stress in the historic glazing and, in some cases, can exceed the wind-driven stress. The retrofit therefore has a mixed structural effect: it can reduce wind-driven deformation under wind loading alone, while introducing pressure-driven mechanisms that did not exist in the original design and that may govern the response depending on airtightness and thermal conditions.

A key post-renovation observation is that the small-window configuration can develop higher tensile glass stresses than the large-window configuration, even though the large window exhibits substantially larger out-of-plane deflections. This behavior is mechanically plausible because tensile stress in brittle glazing is governed primarily by bending curvature and boundary restraint rather than by global displacement magnitude alone. The small window is more restrained after the installation of the inner window, which increases edge restraint and concentrates bending moments and tensile stresses along supported edges and near corners where load is transferred into the cast-iron frame. The large window, by contrast, remains globally more flexible and exhibits greater deformation compatibility between the glass and the frame, which can reduce local bending in the glass even when overall deflections are large.

The magnitude of the pressure-driven response is sensitive to assumptions that directly control the pressure level and load transfer. Any pressure equalization through leakage or intentional ventilation would reduce the pressure differential and thereby lower the pressure-driven stress and deflection. In addition, the cavity temperature is approximated by the outdoor temperature, whereas the real cavity temperature may deviate due to heat transfer, solar radiation and transient conditions, which would change the thermally induced pressure component. Nevertheless, the results demonstrate that pressure-driven scenarios are plausible and can become structurally critical after renovation. This means that cavity pressure cannot be ignored in design, and the pressure differential across the historic panes should be actively limited, for example through controlled pressure equalization or ventilation of the cavity.

At the same time, the very large deflection levels predicted for the large window in the most severe cases, on the order of about 59 mm, should be interpreted with caution. These magnitudes are influenced by geometric nonlinearity and are sensitive to modelling idealizations, in particular the assumed boundary restraint and the idealized connections between subdivided parts in the large-window model. Consequently, the comparative conclusion regarding the size effect is considered more reliable than the absolute deflection magnitude, and the large-window deflections should be viewed as conservative indicators of deformation under the adopted modelling assumptions rather than as exact predictions of in-situ behavior.

7.2 Structural Capacity of the Historic Window

The post-renovation capacity assessment is governed less by wind loading alone and more by cavity-related pressure actions introduced by the retrofit. This shift affects the components differently: the cast-iron frame reaches its highest utilization primarily in the large-window configuration, whereas the historic glazing becomes the most critical element in several combined scenarios. At a mechanism level, this conclusion is consistent across the investigated cases; however, the absolute demand levels remain scenario-dependent and are influenced by cavity airtightness and boundary restraint.

For the cast-iron frame, the small window generally remains below the adopted reference strength, while the large window reaches markedly higher utilization in the most severe combined cases and approaches the adopted reference level under cold conditions. This indicates that the large-window frame becomes relevant for verification after renovation. The near-limit stresses should be interpreted with engineering caution rather than as a direct prediction of cracking. Cast iron is brittle and has limited capacity for stress redistribution, and historic material condition may be affected by casting variability, corrosion and defects. Moreover, local maxima are sensitive to modelling idealizations in restraint, connections and contact definitions, particularly in the large-window model where subdivided parts may introduce local stiffness discontinuities. Even so, the consistent appearance of high utilization under combined pressure-related cases implies that the frame response cannot be dismissed as non-critical, and that mitigation focusing on pressure control is also beneficial for limiting frame demand in cold scenarios.

For the glazing, the results indicate limited margins in several post-renovation load combinations. In both window configurations, the extracted maximum principal tensile stresses exceed the conservative screening value adopted in this study in multiple pressure-related scenarios, most notably under cold conditions. This implies that the glazing becomes critical more frequently than the cast-iron frame in the post-renovation assessment.

This outcome must be interpreted critically, but it cannot be dismissed as a purely numerical artefact. The tensile capacity of historic glass is uncertain and depends strongly on edge quality, surface condition and flaw distribution, which are typically unknown in situ. Moreover, the adopted 9 MPa value represents a conservative screening stress rather than a verified failure threshold for the specific panes, and fracture initiation and crack development are not modelled. Exceedance should therefore not be read as a direct prediction of cracking in a specific case. Nevertheless, the repeated exceedance across several combined scenarios indicates limited margins and elevated sensitivity to pressure-driven actions. Given the brittle nature of glass and the lack of warning before failure, this represents a relevant structural risk that must be addressed in the retrofit design. From a practical perspective, this means that the tensile stress in the historic glazing must be reduced by limiting the cavity pressure differential acting on the panes.

Within the investigated scenarios, acceptable performance is most likely if cavity pressure is controlled through pressure equalization or ventilation. Under a fully sealed-cavity assumption, several combined cases produce glass stress exceedances relative to the conservative screening criterion, implying that the system cannot be considered reliably adequate without measures that reduce pressure differentials across the historic glazing.

7.3 Measures to Reduce Load Effects on the Historic Window

The findings in the results indicate that the post-renovation vulnerability is primarily associated with pressure-driven actions linked to the cavity, particularly under the sealed-cavity assumption. Consequently, the most effective measures are those that reduce the pressure differential across the historic glazing or mitigate how pressure-induced actions are transferred into the historic glass and the cast-iron frame. From a conservation perspective, priority should be given to solutions that are reversible, require minimal intervention and do not alter the historic appearance.

- Controlled pressure equalization through cavity ventilation (primary mitigation).

The most direct way to address the critical mechanism identified in the analyses is to allow the cavity to equalize pressure relative to the ambient environment. This can be achieved through controlled venting, intentional leakage paths or pressure-regulating detailing. Even partial pressure equalization is expected to reduce the pressure-driven tensile stress in the historic glass while maintaining the architectural concept of a secondary glazing system. [24]

- Reduction of tensile stress concentrations through edge and support detailing (secondary mitigation).

Since the highest tensile stresses consistently localize near supported edges and corners, measures that reduce local restraint and stress concentrations at the glass–frame interface can further improve performance. Examples include more compliant bedding materials, improved load distribution along supports, and avoidance of hard-point contacts that introduce local stress peaks. This is particularly relevant for the small-window configuration, where tensile glass stress is more demanding than global deflection in several combined pressure scenarios. [1,2]

In practice, cavity pressure and temperature vary over time and installation conditions are not perfectly uniform. Mitigation measures should therefore be designed to remain effective under partial ventilation and reasonable construction tolerances, so that performance is not overly dependent on ideal airtightness or perfectly uniform detailing.

7.4 Overall interpretation

The results show that the retrofit is not structurally neutral: it introduces cavity-pressure-driven actions that can become critical in cold conditions. This means that the key design question after renovation is cavity pressure which must be controlled and how loads are introduced at the glass edges. Consequently, the retrofit is best regarded as feasible if pressure equalization (or controlled ventilation) is ensured and edge detailing avoids hard contact and local restraint. With these measures, intervention can reduce risk while remaining consistent with conservation principles of minimal and reversible change.

8 Future Work

Future studies should extend this work in ways that reduce uncertainty and better represent real in-service behavior of historic windows after retrofit. A priority is model validation through laboratory tests and/or in-situ monitoring. Measurements should include cavity pressure, temperatures (indoor/outdoor/cavity), and structural response such as displacements (and strains where feasible) [11]. In the hall environment, documenting ambient vibrations may also be relevant for serviceability and long-term structural effects [19]. Such measurements would also allow calibration of boundary conditions, connection stiffness, and the degree of cavity sealing and pressure equalization.

A second key development is to move beyond deterministic strength checks by introducing probabilistic or fracture-mechanics-based glass assessment for aged/historic glass. Such approaches can account for strength scatter, surface flaws, edge damage, and ageing effects, and allow the results to be expressed in terms of failure probability rather than a single reference stress.

Further work should also address time-dependent and cyclic effects, including repeated temperature cycles, seasonal variations, and potential fatigue-like deterioration mechanisms in brittle materials and joints. This is particularly relevant for long-term durability, since critical conditions may occur repeatedly over many winters rather than as a single extreme event.

Finally, future modelling should implement coupled thermal–mechanical analysis. In this thesis, temperature effects were mainly represented through cavity-pressure changes, while internal thermal stresses in glass and cast iron caused by temperature gradients and restrained thermal expansion were not explicitly modelled. Applying temperature fields directly to the material domains would allow assessment of bending stresses from thermal gradients, combined thermal restraint effects at supports, and thermal shock scenarios under rapid cooling or asymmetric solar heating. This would provide a more complete fracture-risk evaluation and support more robust recommendations regarding cavity ventilation, glazing support detailing, and retrofit design strategies.

9 Bibliography

[1] Ashurst, J. and Ashurst, N. (1988). *Practical building conservation: Glass and glazing*. London: English Heritage.

[2] Block, D. and Schulz, M. (2014). Structural design of glazing systems. In: *Glass Performance Days Proceedings*.

[3] Buddenberg, L., Feldmeier, W., Kuntsche, J. and Nelles, O. (2016). Accurate determination of the static equilibrium in insulating glass units subjected to climate loads. *Journal of Façade Design and Engineering*, 4(2), pp. 69–85. https://doi.org/10.3233/FDE-160034

[4] EN 1990:2002+A1:2005. (2005). *Eurocode – Basis of structural design*. Brussels: European Committee for Standardization (CEN).

[5] Davis, J.R. (1998). *Metals handbook desk edition*. Materials Park, OH: ASM International.

[6] Duggal, S.K. (2012). *Introduction to structural analysis and design*. New Delhi: Tata McGraw-Hill.

[7] EN 16612:2019. (2019). *Glass in building – Determination of the lateral load resistance of glass panes by calculation*.

[8] EN 1991-1-4:2005. (2005). *Eurocode 1: Actions on structures – Part 1-4: General actions – Wind actions*. Brussels: European Committee for Standardization (CEN).

[9] ISO 52022-3:2017. (2017). *Thermal performance of windows, doors and shutters – Calculation of solar and daylight characteristics*.

[10] Isaksson, T., Mårtensson, A. and Thelandersson, S. (2020). *Byggkonstruktion*. 4th edn. Lund: Studentlitteratur.

[11] Lourenço, P.B. and Ramos, L.F. (2012). Structural monitoring of heritage buildings: Case studies and best practices. *Journal of Cultural Heritage*.

[12] Lund, C., Lundberg, M. and Schlyte, O. (2007). *Varvsstaden: Kockumsområdet söder om Stora Varvsgatan*. Available at: [insert full URL] (Accessed: 9 February 2025).

[13] Boverket (2011, with amendments). *Boverkets byggregler (BBR), BFS 2011:6*. Karlskrona: Boverket.

[14] Varvsstaden AB (n.d.). Administrationsbyggnaden [Image]. Available at: https://www.varvsstaden.se/administrationsbyggnaden (Accessed: 13 October 2025).

[15] Varvsstaden AB (n.d.). Byggnader som bevaras [Image]. Available at: https://www.varvsstaden.se/byggnader-som-bevaras (Accessed: 13 October 2025).

[16] Varvsstaden AB (n.d.). Gjuteriet [Image]. Available at: https://www.varvsstaden.se/gjuteriet (Accessed: 13 October 2025).

[17] Varvsstaden AB (n.d.). Snickeriet lyfter [Image]. Available at: https://www.varvsstaden.se/snickerietlyfter (Accessed: 13 October 2025).

[18] Ottosen, N.S. and Petersson, H. (1992). *Introduction to the finite element method*. London: Prentice Hall.

[19] Persson, P. (2016). *Vibrations in a built environment: Prediction and reduction*. PhD thesis. Lund University.

[20] SS-EN 1561:2011. (2011). *Foundry – Grey cast irons*. Brussels: European Committee for Standardization (CEN).

[21] Tadeu, A. and Almeida, R. (2016). Advanced glass materials for energy-efficient building renovation. *Journal of Architectural Engineering*, 22(4). https://doi.org/10.1061/(ASCE)AE.1943-5568.0000207

[22] Varvsstaden AB (2016). *Maskin- och Monteringshall 101 – Fönsteranalys*. Malmö: Varvsstaden AB.

[23] Varvsstaden AB (n.d.). Byggnader som bevaras. Available at: https://www.varvsstaden.se/byggnader-som-bevaras (Accessed: 21 August 2025).

[24] Wolf, A.T. (2005). *Facade engineering and building physics*. Basel: Birkhäuser.

[25] SMHI (2022). Atmosfäriskt tryck i Sverige – variationer och extrema värden. Available at: https://www.smhi.se/kunskapsbanken/meteorologi/atmosfariskt-tryck-variationer (Accessed: 10 November 2025).